

# **pH-BIASED ISOELECTRIC TRAPPING SEPARATIONS**

A Dissertation

by

EVAN ERIC SHAVE

Submitted to the Office of Graduate Studies of  
Texas A&M University  
in partial fulfillment of the requirements for the degree of

DOCTOR OF PHILOSOPHY

August 2005

Major Subject: Chemistry

# **pH-BIASED ISOELECTRIC TRAPPING SEPARATIONS**

A Dissertation

by

EVAN ERIC SHAVE

Submitted to the Office of Graduate Studies of  
Texas A&M University  
in partial fulfillment of the requirements for the degree of

DOCTOR OF PHILOSOPHY

Approved by:

Chair of Committee,  
Committee Members,

Head of Department,

Gyula Vigh  
Charles J. Glover  
Paul A. Lindahl  
Manuel P. Soriaga  
Emile A. Schweikert

August 2005

Major Subject: Chemistry

## ABSTRACT

pH-Biased Isoelectric Trapping Separations. (August 2005)

Evan Eric Shave, B.MedSc., University of Sydney

Chair of Advisory Committee: Dr. Gyula Vigh

The classical isoelectric trapping (IET) technique, using the multicompart ment electrolyzer (MCE), has been one of the most successful electrophoretic techniques in preparative-scale protein separations. IET is capable of achieving high resolution discrimination of proteins, by isolating proteins in between buffering membranes, in their isoelectric state. However, due to the inherent nature of the IET process, IET has suffered several shortcomings which have limited its applicability. During a classical IET separation, a protein gets closer and closer to its pI value, thus the charge of the protein gets closer and closer to zero. This increases the likelihood of protein precipitation and decreases the electrophoretic velocity of the protein, thus making the separation very long. Furthermore, the problems are aggravated by the fact that the instrumentation currently used for IET is not designed to maximize the efficiency of electrophoretic separations.

To address these problems, a new approach to IET has been developed, pH-biased IET. By controlling the solution pH throughout the separation, such that it is not the same as the protein's pI values, the problems of reduced solubility and low electrophoretic migration velocity are alleviated. The pH control comes from a novel use of isoelectric

buffers (also called auxiliary isoelectric agents or pH-biasers). The isoelectric buffers are added to the sample solution during IET and are chosen so that they maintain the pH at a value that is different from the pI value of the proteins of interest. Two new pieces of IET instrumentation have been developed, resulting in major improvements in protein separation rates and energy efficiency. A variety of separations, of both small molecules and proteins, have been successfully performed using the pH-biased IET principle together with the new instrumentation.

## ACKNOWLEDGMENTS

I would like to thank Prof. Gyula Vigh for educating me in the ways of a separations scientist. His enthusiasm and devotion to the task of understanding separations theory and putting it into practice are what makes him a great teacher and scientist. I have thoroughly enjoyed my research project and I thank Dr. Vigh for giving me the opportunity to pursue it.

I thank Margot for supporting me with love, encouragement and decent food, even when I have come home from the lab way too late, on way too many occasions. I thank Cleo for always being happy to see me, and for her creative filing system she has developed for my journal articles during the writing of this dissertation.

I have enjoyed working in the Separations Science Group and would like to thank all my fellow group members both past and present for their companionship, knowledge and support over the last four years. In particular, I want to thank Peniel for his fine machining skills, and Sanjiv and Nellie for supplying me with the many membranes I have needed. I thank Dr Scott Jaques and Malcolm Delovio for their help with the TSH project.

Lastly, I would like to acknowledge the generous financial support of Gradipore and Beckman Coulter, without which this work would not have been possible.

## TABLE OF CONTENTS

	Page
ABSTRACT.....	iii
ACKNOWLEDGMENTS.....	v
TABLE OF CONTENTS.....	vi
LIST OF FIGURES.....	x
LIST OF TABLES.....	xvi
NOMENCLATURE.....	xvii
1. INTRODUCTION.....	1
1.1 Isoelectric focusing.....	1
1.1.1 Fundamental principles.....	1
1.1.2 Types of pH gradients.....	2
1.2 Instrumentation for preparative-scale isoelectric focusing.....	5
1.2.1 General considerations for preparative-scale isoelectric focusing.....	5
1.2.2 Isoelectric focusing in anti-convective media.....	5
1.2.3 Zone-convection isoelectric focusing.....	7
1.2.4 Free-zone isoelectric focusing stabilized by rotation.....	8
1.2.5 Continuous free-flow isoelectric focusing.....	9
1.3 Classical isoelectric trapping.....	11
1.3.1 Fundamental principles.....	11
1.3.2 Instrumentation for isoelectric trapping separations.....	12
2. THE PROBLEMS WITH CLASSICAL ISOELECTRIC TRAPPING.....	17
2.1 The inherent problems of the classical isoelectric trapping principle....	17
2.2 The design flaws of existing isoelectric trapping instrumentation.....	18
3. SOLUTIONS TO THE PROBLEMS OF CLASSICAL ISOELECTRIC TRAPPING.....	19
3.1 The pH-biased isoelectric trapping principle.....	19
3.2 Improved instrumentation for isoelectric trapping separations.....	21

	Page
3.2.1 Development of the Twinflow.....	21
3.2.2 The Biflow.....	29
4. DESALTING DURING ISOELECTRIC TRAPPING.....	34
4.1 Initial desalting experiments on the Twinflow.....	34
4.1.1 Isoelectric trapping of ampholytes during desalting.....	34
4.1.1.1 Background and objective.....	34
4.1.1.2 Instrument set-up, materials, and method.....	35
4.1.1.3 Results and discussion.....	37
4.1.2 Concluding remarks.....	39
4.2 The pH-transient phenomenon.....	40
4.2.1 Ion mobility considerations.....	40
4.2.1.1 Background and objective.....	40
4.2.1.2 Instrument set-up, materials, and method.....	40
4.2.1.3 Results and discussion.....	41
4.2.2 Membrane pH considerations.....	46
4.2.2.1 Background and objective.....	46
4.2.2.2 Instrument set-up, materials, and method.....	46
4.2.2.3 Results and discussion.....	47
4.2.3 Control of the pH-transients during desalting.....	51
4.2.3.1 Background and objective.....	51
4.2.3.2 Instrument set-up, materials, and method.....	52
4.2.3.3 Results and discussion.....	52
4.2.4 Concluding remarks.....	54
5. SEPARATION OF SMALL ORGANIC MOLECULES BY ISOELECTRIC TRAPPING.....	56
5.1 Classical isoelectric trapping separations on the Twinflow.....	56
5.1.1 Separations in a hydro-organic solvent.....	56
5.1.1.1 Background and objective.....	56
5.1.1.2 Instrument set-up, materials, and method.....	56
5.1.1.3 Results and discussion.....	58
5.1.2 Separation of ampholytic enantiomers.....	62
5.1.2.1 Background and objective.....	62
5.1.2.2 Instrument set-up, materials, and method.....	63
5.1.2.3 Results and discussion.....	64
5.1.3 Separation of UV-absorbing carrier ampholytes.....	67
5.1.3.1 Background and objective.....	67

	Page
5.1.3.2 Instrument set-up, materials, and method.....	69
5.1.3.3 Results and discussion.....	70
5.1.4 Concluding remarks.....	74
5.2 pH biased isoelectric trapping separations on the Twinflow.....	74
5.2.1 Purification of a UV-absorbing pI marker.....	74
5.2.1.1 Background and objective.....	74
5.2.1.2 Instrument set-up, materials, and method.....	75
5.2.1.3 Results and discussion.....	76
5.2.2 Concluding remarks.....	78
5.3 pH-biased isoelectric trapping separations on the Biflow.....	78
5.3.1 Separation of UV-absorbing pI markers.....	78
5.3.1.1 Background and objective.....	78
5.3.1.2 Instrument set-up, materials, and method.....	79
5.3.1.3 Results and discussion.....	80
5.3.2 Concluding remarks.....	81
 6. PROTEIN SEPARATIONS BY ISOELECTRIC TRAPPING.....	 83
6.1 Classical isoelectric trapping separations on the Twinflow.....	83
6.1.1 Binary separations of chicken egg white proteins.....	83
6.1.1.1 Background and objective.....	83
6.1.1.2 Instrument set-up, materials, and method.....	83
6.1.1.3 Results and discussion.....	84
6.1.2 Concluding remarks.....	88
6.2 pH-biased isoelectric trapping separations on the Twinflow.....	89
6.2.1 A method for finding the optimum biaser concentration.....	89
6.2.1.1 Background and objective.....	89
6.2.1.2 Instrument set-up, materials, and method.....	91
6.2.1.3 Results and discussion.....	92
6.2.2 Concentration and fractionation of bovine serum proteins.....	99
6.2.2.1 Background and objective.....	99
6.2.2.2 Instrument set-up, materials, and method.....	100
6.2.2.3 Results and discussion.....	102
6.2.3 A comparison between two fractionation techniques: chromatofocusing versus pH-biased isoelectric trapping.....	 112
6.2.3.1 Background and objective.....	112
6.2.3.2 Instrument set-up, materials, and method.....	113
6.2.3.3 Results and discussion.....	114
6.2.4 Fractionation of recombinant thyroid stimulating hormone...	119
6.2.4.1 Background and objective.....	119



	Page
6.2.4.2 Instrument set-up, materials, and method.....	119
6.2.4.3 Results and discussion.....	121
6.2.5 Concluding remarks.....	123
6.3 pH-biased isoelectric trapping separations on the Biflow.....	124
6.3.1 Fractionation of egg white proteins.....	124
6.3.1.1 Background and objective.....	124
6.3.1.2 Instrument set-up, materials, and method.....	125
6.3.1.3 Results and discussion.....	126
6.3.2 Fractionation of bovine serum proteins.....	134
6.3.2.1 Background and objective.....	134
6.3.2.2 Instrument set-up, materials, and method.....	135
6.3.2.3 Results and discussion.....	136
6.3.3 Concluding remarks.....	141
7. CONCLUSIONS.....	142
7.1 Improved isoelectric trapping instrumentation.....	142
7.2 pH-biased isoelectric trapping.....	144
REFERENCES.....	146
VITA.....	151

## LIST OF FIGURES

FIGURE		Page
1	Charge vs. pH curve for a hypothetical protein containing the same amino acids residues as found in ovalbumin.....	21
2	Assembly view of the separation cartridge for the Gradiflow BF200.....	22
3	Exploded view of the separation cartridge between the two electrode compartments.....	23
4	Cross-sectional view of the Gradiflow BF200 separation unit.....	24
5	Schematic of the Twinflow IET instrument operating in pass-by-pass mode.....	27
6	Photograph of the Twinflow.....	28
7	An example of a generic two step binary separation on the Twinflow.....	30
8	Schematic of the Biflow.....	32
9	Photograph of the Biflow.....	33
10	Exploded view of the single-sample compartment cartridge used for desalting on the Twinflow.....	36
11	Schematic of the Twinflow in single-sample compartment desalting mode.....	37
12	Electropherograms of the samples taken during desalting a UV-absorbing salt from a mixture of three UV-absorbing ampholytes...	38
13	Potential, conductivity, and pH of the sample stream during IET desalting.....	39
14	IET desalting of mobility-matched ions.....	43

FIGURE	Page
15 IET desalting when the anion has a higher mobility than the cation.....	44
16 IET desalting when the cation has a higher mobility than the anion.....	45
17 IET desalting when the anodic and cathodic membranes are equidistant from pH 7 and the ions are mobility-matched.....	48
18 IET desalting when the anodic membrane is closer to pH 7 than the cathodic membrane and the ions are mobility-matched.....	49
19 IET desalting when the cathodic membrane is closer to pH 7 than the anodic membrane and the ions are mobility-matched.....	50
20 pH transients in the sample compartment during desalting and the influence of the pH value of the anodic membrane.....	54
21 CIEF analysis of the anodic and cathodic sample streams during IET of 3-PPA and MABA in the presence of 25% methanol in water.....	59
22 CIEF analysis of the purification of a technical grade, ampholytic dye (HMMB).....	60
23 CIEF analysis of the purification of an ampholytic fluoresceine derivative by single sample-compartment IET in 25% v/v methanol in water.....	61
24 CIEF analysis of Dns-Trp in 60 mM HP- $\beta$ -CD.....	64
25 Enantiomer composition in the anodic and cathodic sample reservoirs as a function of time during IET separation of the enantiomers of Dns-Trp.....	65
26 CIEF analysis of the cathodic and anodic sample streams after 540 minutes of electrophoresis.....	66
27 CIEF analysis comparing UV-transparent Pharmalytes to UV-absorbing Pharmalytes.....	70
28 CIEF analysis for the testing of the pH 8.0 separation membrane....	72

FIGURE		Page
29	CIEF analysis for the testing of the pH 7.0 separation membrane.....	73
30	CIEF analysis of the reaction mixture used in the synthesis of UV-absorbing pI markers.....	76
31	CIEF analysis of the purification of a pI marker from the raw reaction mixture.....	77
32	Schematic of the Biflow set-up for the separation of three UV-absorbing pI markers.....	80
33	CE of the sample streams during pH-biased IET of three UV-absorbing pI markers on the Biflow.....	81
34	CIEF analysis of the egg white sample feed before separation and after one pass through the separation compartments of the Twinflow during classical IET.....	86
35	CIEF analysis of the egg white sample after 11 passes and after 17 passes through the separation compartments of the Twinflow during classical IET.....	87
36	CIEF analysis of the major albumin isoforms isolated after two binary Twinflow separations using classical IET.....	88
37	Plot showing how pH changes affect the net charge on a hypothetical protein with the same amino acid residues as ovalbumin.....	90
38	pH and conductivity changes in the anodic and cathodic sample streams during pH-biased IET experiment for determining the optimum biaser concentration.....	93
39	CIEF analysis of the cathodic sample stream over 5 passes showing the transfer of ovalbumin when 2 mM CAR is used as biaser.....	94
40	CIEF analysis of the anodic sample stream over 5 passes showing the recovery of ovalbumin when 2 mM CAR is used as biaser in the cathodic sample stream.....	95

FIGURE	Page
41 Schematic of the Twinflow set-up for fractionation of proteins in bovine serum with pI values higher than 8.4.....	103
42 SDS-PAGE image of the samples analyzed from the anodic feed stream and the cathodic collection stream over passes 4 through the Twinflow during the high pI fractionation of bovine serum.....	104
43 Schematic of the Twinflow set-up for fractionation of proteins in bovine serum with pI values lower than 4.0.....	105
44 SDS-PAGE image of the samples analyzed from the cathodic feed stream and the anodic collection stream over passes 4 through the Twinflow during the low pI fractionation of bovine serum.....	106
45 IEF gel image showing the low pI fraction and the high pI fraction from whole bovine serum.....	107
46 2D gels of whole serum and the low pI fraction separated by the Twinflow.....	109
47 Chromatogram of the whole low pI fraction ( $2.0 < pI < 4.0$ ) from bovine serum analyzed by reversed phase HPLC.....	110
48 Chromatograms of the samples from the four sub-fractionations made on the low pI fraction analyzed by reversed phase HPLC.....	111
49 pH and UV-absorbance trace of bovine serum separated by the chromatofocusing column.....	115
50 Chromatograms for the reversed phase analysis comparing the whole serum, chromatofocusing high pI fraction and the Twinflow high pI fraction.....	116
51 Chromatograms for the reversed phase analysis comparing the whole serum, chromatofocusing low pI fraction and the Twinflow low pI fraction.....	118

FIGURE	Page
52	Plot of the TSH concentration, pH, and conductivity changes in the sample, and the corresponding voltage change during desalting on the Twinflow..... 122
53	Bar graph showing the amounts of TSH in each pI fraction..... 123
54	CIEF analysis of six pI markers and six pI markers with the egg white sample..... 125
55	Schematic of the Biflow set-up for the isolation of egg white proteins with pI values between 4.7 and 5.4..... 127
56	CIEF analysis showing the protein composition of the sample streams in the Biflow during the separation of egg white proteins with pI values between 4.7 and 5.4..... 128
57	2D gel images of unfractionated chicken egg white and the sample from the Biflow final product collection stream..... 129
58	CIEF analysis of egg white showing the two minor proteins that will be separated by pH-biased IET on the Biflow..... 131
59	CIEF analysis of the Biflow separation of the low pI minor protein target from egg white..... 132
60	CIEF analysis of the Biflow separation of the mid pI minor protein target from egg white..... 133
61	Schematic of the Biflow set-up for the separation of bovine serum proteins with pI values between 4.5 and 4.8..... 136
62	2D gels of whole bovine serum and the sample from the Biflow product collection stream..... 137
63	pH and UV-absorbance trace of bovine serum separated by the chromatofocusing column with extra detail of the pH 4.0 – 5.5 region..... 138
64	pH and UV-absorbance trace of the sample taken from the Biflow product collection stream during the fractionation and concentration of proteins with pI values in the 4.5-4.8 range..... 139

FIGURE	Page
65 Chromatograms of the reversed phase HPLC analysis comparing the samples containing proteins with pI values in the 4.5-4.8 range prefractionated on the Biflow and the serum sample that was not prefractionated.....	140

**LIST OF TABLES**

TABLE		Page
1	Effective mobility values for the strong electrolytes that were used in the desalting experiments.....	41
2	Comparison of the production rates and energy consumption for enantiomer separations on the Octopus, Isoprime, and Twinflow.....	67
3	Summary of the results showing the dependence of the pass number, required to complete the transfer of 24 mg of ovalbumin, on the concentration of CAR.....	97



## NOMENCLATURE

2DGE	Two dimensional gel electrophoresis
3PPA	3-(3-pyridyl)propionic acid
ASC	Anodic separation compartment
BSH	Benzenesulfonic acid
BzTMA <sup>+</sup>	Benzyltrimethylammonium ion
BzTMAOH	Benzyltrimethylammonium hydroxide
CAR	Carnosine
CIEF	Capillary isoelectric focusing
CSC	Cathodic separation compartment
DnsPhe	Dansyl-phenylalanine
Dns-Trp	Dansyl-tryptophan
DNS-GABA	Dansyl- $\gamma$ -aminobutyric acid
DOP	Dopamine
GLU	Glutamic acid
H <sup>+</sup>	Hydronium ion
HIS	Histidine
HMMB	4-hydroxy-3-(morpholinomethyl)benzoic acid
HP- $\beta$ -CD	Hydroxypropyl $\beta$ -cyclodextrin
IEF	Isoelectric focusing
IET	Isoelectric trapping

IgG	Immunoglobulin G
IPG	Immobilized pH gradient
LYS	Lysine
MABA	<i>meta</i> -aminobenzoic acid
MCE	Multi-compartment electrolyzer
MSA	Methanesulfonic acid
MW	Molecular weight
NaOH	Sodium hydroxide
OH <sup>-</sup>	Hydroxide ion
PET	poly(ethyleneterephthalate)
pI	Isoelectric point
PTSA <sup>-</sup>	<i>para</i> -toluenesulfonate
PVA	Poly(vinyl) alcohol
rTSH	Recombinant thyroid stimulating hormone
SDS-PAGE	Sodium dodecylsulfate-polyacrylamide gel electrophoresis
TERB	Terbutaline
TFA	Trifluoroacetic acid
TSH	Thyroid stimulating hormone
TYRA	Tyramine

# 1. INTRODUCTION

## 1.1 Isoelectric focusing

### 1.1.1 Fundamental principles

Isoelectric focusing (IEF) is a powerful electrophoretic method used for the separation of ampholytic substances, and has proven especially useful for the analysis of proteins [1].

Successful IEF depends on the generation of a stable pH gradient in which the pH increases from the anode to the cathode. If a protein is placed in this system, it will migrate with a velocity that is dependent on its electric charge and varies as a function of the pH. In this manner, the protein is moving or focusing towards a point in the pH gradient where its net charge and electrophoretic velocity are both zero; this pH value is known as the isoelectric point (pI). Each protein has a unique pI, determined by the amino acid composition of the protein and the acid dissociation constants ( $pK_a$ ) of the ionizable groups of the amino acid residues. IEF separation of proteins with different pIs is achieved because proteins focus at different places along the gradient. Provided the electric field and pH gradient are maintained, the system will reach a state of equilibrium where the proteins will remain focused in very sharp bands, constantly countering the effects of diffusion and convective mixing, if present.

---

This dissertation follows the style and format of *Electrophoresis*.

### 1.1.2 Types of pH gradients

The ideal pH gradient has a smooth slope that is shallow enough to resolve all the proteins of interest, and remains stable over the time of separation. These characteristics are strongly influenced by the chemicals that are used to form the gradient. Firstly, simple non-amphoteric buffers can be used to generate a pH gradient in an electric field [2]. The most successful buffer systems use a combination of the salt of a weak acid and weak base, chosen such that the difference between their  $pK_a$  values is less than 1 [3, 4]. Using this approach a smooth gradient will develop, however, one can only cover relatively narrow ranges of about 3 pH units. In addition, the effects of migration and diffusion of the buffering ions prevent the system from reaching an equilibrium point corresponding to a stable pH gradient. This problem can be overcome if the transport of buffering anions and cations is kept constant throughout the apparatus. This is called steady state rheoelectrolysis and was demonstrated in an apparatus where the anolyte and catholyte solutions were constantly inter-mixed at an appropriate flow rate [5]. This narrow pH gradient system is inexpensive and chemically well defined, although the practicalities of maintaining a stable gradient have made it an unattractive option for most IEF applications.

The second type of gradient is the amphoteric buffer-based pH gradient. It is formed by the isoelectric stacking of a large number of buffering species called carrier ampholytes [6]. Carrier ampholytes are complex mixtures of polyamino polycarboxylic acids, each of which is characterized by having a high buffering capacity and conductivity in the

vicinity of its unique pI [7]. To ensure the formation of a smooth and stepless pH gradient, the mixture must contain at least a minimum number of unique ampholytes per pH unit. Using ideal carrier ampholytes (where every ampholyte has an equal diffusion coefficient, mobility, relative concentration, and is evenly spaced from its neighbour), this number has been calculated to be at least 30 [8]. With this ideal carrier ampholyte mixture, the stability of the pH gradient should only be dependent on the application of a sufficient current to counter diffusion and sufficient cooling to counter thermally induced convective mixing. There are various synthetic routes available for the formation of carrier ampholytes with pIs ranging from 2.5 to 11, and within a single pH unit there may be as many as 1000 ampholytic species [7, 9-13]. Carrier ampholyte-based pH gradients have made IEF a successful technique for protein analysis.

Unfortunately, in practice, there are some issues that limit the utility of these pH gradients. Firstly, at the end of the IEF separation the carrier ampholytes will be present along with the separated analytes. If the analyte is needed in its pure form, or if it is to be analyzed by mass spectrometry, a further purification step is required to remove the carrier ampholytes. Secondly, the pH gradient formed by carrier ampholytes is not temporally stable. During electrophoresis, the gradient experiences time-dependent cathodic and anodic drift. The most acidic and most basic ampholytes in the pH gradient migrate out of the separating compartment into the anode and cathode compartment, respectively, and the pH gradient becomes flattened in the middle [14]. Thirdly, the focused carrier ampholyte pH gradient can have regions of uneven conductivity, causing uneven voltage drop across the gradient [1]. These problems did not really hinder the

development of analytical capillary IEF, however, together with the expense of carrier ampholytes, large scale IEF was never routinely implemented.

Buffer focusing is a hybrid technique used to make a pH gradient. A defined mixture of weak acids and bases, amino acids and ampholytes are used to form the gradient [15-17]. In this case the species align themselves from the anode to the cathode in order of increasing  $pK_a$  or  $pI$ . Buffer focusing is most useful for the generation of shallow pH gradients. As some of the components of the system are non-amphoteric species, the gradient stability will always be questionable.

The development of immobilized pH gradient (IPG) technology was a breakthrough for the field of IEF. In 1978, Righetti and his group were experimenting with immobilizing pre-focused commercial carrier ampholytes onto a Sephadex support [18]. To improve this technique and to avoid using the ill-defined carrier ampholytes, the pre-focusing step, and to make the gradient synthesis more flexible, a series of acrylamido buffers and titrants were synthesized (now commercially available as Immobilines) [19]. The Immobilines have a general structure of  $CH_2=CH-CO-NH-R$  (where R is either weakly acidic or basic), and can be co-polymerized with acrylamide and bisacrylamide to form a polyacrylamide gel. By using a density gradient mixer and the appropriate acrylamido buffers and titrant, the slope of the pH gradient can be tailor made for the particular application. The IPG technology solved the following problems which plagued the other types of pH gradients; temporal gradient instability, uneven buffering capacity and

conductivity, unknown chemical environment, cathodic and anodic drifts, low ionic strength and low sample capacity. In summary, IPGs have proven invaluable for analytical scale protein separations, particularly as the first step in two-dimensional gel electrophoresis.

## **1.2 Instrumentation for preparative-scale isoelectric focusing**

### 1.2.1 General considerations for preparative-scale isoelectric focusing

IEF was recognized early as a high resolution technique suitable for conducting preparative-scale separations of ampholytic substances. The biggest concerns for scaled-up IEF separations include, stabilizing the pH gradient, removal of Joule heat, load capacity and resolution, sample recovery, isoelectric precipitation, and cost. In addition, the benefits of continuous processing versus batch processing must be weighed up when considering the various instruments available for preparative-scale IEF.

### 1.2.2 Isoelectric focusing in anti-convective media

Using an anti-convective medium to stabilize the pH gradient for large scale IEF separations was a common approach for the early pioneers in this field. One of the first attempts used a density gradient column [20]. The density gradient, containing the sample and carrier ampholytes, is normally prepared with sucrose solutions. The density and pH gradients are formed along the length of the column between two electrodes. Short and thick columns have proven to be most effective, as this allows for a shorter electrode distance, thus higher field strength. For example, up to 1g of protein was

separated in about three hours in a 112 ml column [20]. If cooling was used, up to 20 W could be applied during focusing. However, as the column dimensions are increased it becomes more difficult to efficiently remove the Joule heat. If too great an axial and radial temperature gradient develops, thermally-induced convective mixing destroys the high resolution of IEF. The recovery of the focused bands also presents a problem as the scale increases. At the end of the separation, the column is drained from the bottom and this allows for remixing to occur, particularly for the bands furthest from the drain. Furthermore, the presence of sucrose can act as a sieving matrix. This can make interpretation of the IEF results confusing, particularly for proteins of similar pI but very different molecular weight.

As an alternative to sucrose density columns, a granulated gel slurry can be poured into a horizontal flat bed, typically 40 cm long x 20 cm wide and up to 5 mm deep [21]. In this situation, a suspension of Sephadex gel (in a 1-2% carrier ampholyte solution) is used as the anti-convective medium. The bottom of the flat bed is usually made of glass, and is placed on a cooling block during electrophoresis. The electrodes are at opposite ends of the bed and make contact with the gel through paper wicks soaked in the appropriate anolyte or catholyte. The protein sample can either be included in the Sephadex gel bed during mixing and casting, or applied directly to the gel once it is formed. At the end of the separation, the gel is divided into 30 horizontal fractions with a grid, and a spatula is used to collect each segment. This has been one of the most successful preparative IEF devices due to its ease of use and high sample load (up to 10g of protein) [22].



A third alternative for the anti-convective medium is the use of preparative-scale polyacrylamide or agarose gels. Both tube and horizontal slab gels have been used, however, the horizontal variety offers much better heat dissipation. The gel monomers are mixed with 2% carrier ampholytes, then poured into the gel casting tray [23]. The same sized tray used for the horizontal Sephadex beds can be used for gel casting. After focusing, the gel segments can be removed from the tray and the sample bands can be extracted by electrophoretic elution into an appropriate buffer. Sample loads of up to 1g of protein have been reported, although recovery is limited to around 70% [23].

### 1.2.3 Zone-convection isoelectric focusing

By constructing specially shaped separation chambers, one is able to mitigate the effects of convective mixing without the use of anti-convective media. The first instrument designed for zone convection IEF consisted of a lid with corrugations spaced 10mm apart and 10mm deep, and a corresponding base with similar corrugations [24]. The sample, in a solution of carrier ampholytes, is poured into the corrugations on the bottom plate. The lid is placed on top, such that the corrugations form inter-digitating projections creating a zig-zagged shaped separation channel. Platinum electrodes are inserted in either end, and while voltage is applied, the bottom plate is cooled. As proteins focus into a given region, a vertical density gradient develops because the more dense proteins concentrate against the bottom of the channel. Sample loads of up to 1g can be used; the time to finish such a separation can be more than two days.

Furthermore, achieving reproducible results with this instrument has proven difficult, because when the lid is lifted off to extract the separated sample, remixing can occur.

#### 1.2.4 Free-zone isoelectric focusing stabilized by rotation

Stabilization of the pH gradient formed by the carrier ampholytes can be achieved if a cylindrical separation tube is slowly rotated about its longitudinal axis during electrophoresis [25]. This idea was first used for zone electrophoresis, and then adopted for IEF. In the original design, the separation tube had an inner diameter of 3mm, and at either end polyacrylamide beads were packed in a short distance to prevent mixing of the carrier ampholytes with the anolyte and catholyte solutions [26]. In a non-rotating tube a focused band would sink downwards and spread out along the channel. By maintaining rotation, the proteins never get a chance to sink, thus preserving the sharp sample band. With this size instrument, sample loads of only 100 $\mu$ g could be separated. Stabilization by rotation has proven to be quite successful and several devices were made that can separate much higher protein loads than the original design. A massive rotating multi-compartment electrolyzer (MCE), 1 meter long with 46 compartments, held 7.6 L of solution and could separate several grams of protein [27]. The only commercial device based on this principle and currently available is the Rotofor. It is 15 cm long with twenty, 50 ml compartments, and is able to separate 1 g of protein in 4 to 6 hours [28]. The polyester screens that separate the compartments, are supposed to minimize mixing during harvesting when the chambers are drained.

A slightly different mode of rotation stabilization called vortex stabilized IEF was designed in the late 1980s [29]. The 30 cm long separation chamber is an annulus formed by the space created by placing a smaller diameter cylinder inside a larger diameter hollow cylinder. The inner cylinder is attached to a rotor, and has a grooved outer wall (forming the inner wall of the annulus). Similar grooves are on the inside wall of the non-rotating outer cylinder (forming the outer wall of the annulus). These grooves stabilize the vortex in the annulus, created by the rotating inner cylinder. This leads to improved axial heat and mass transfer, thus improving resolution. The pH gradient is formed along the  $z$  axis of the annulus from carrier ampholytes or non-amphoteric buffers. The electrode compartments at the top and bottom of the column are separated from the sample chamber by dialysis membranes to prevent bulk mixing. Typically, 10-20 kV can be applied across the separation chamber. At the end of the separation, fractions are sequentially withdrawn from the top down, using fifty-three sample ports along the length of the column. The present design takes a sample volume of 24 ml and is capable of fractionating batches of up to 100 mg of protein in about 5 hours [29]. The inventors claim that the cooled annulus design is suited for further scale-up as the cooling and vortices effectively control the extent of convective mixing.

#### 1.2.5 Continuous free-flow isoelectric focusing

The preparative methods discussed so far all use batch processing. In continuous free flow instruments the separation chamber volume does not limit the sample volume that can be processed. In addition, the sample recovery is high because there is no supporting

medium used. These IEF instruments are based on a design that was originally used for zone electrophoresis [30]. The separation channel is formed by two rectangular parallel glass plates that are spaced 0.3-0.5 mm apart. The electrode compartments run down along the two opposite sides of the plates, and are separated from the separation chamber by semi permeable membranes. The carrier ampholyte mixture is contained in an external reservoir and is continuously pumped in between the plates from the bottom. The pH gradient forms across the chamber as the solution moves perpendicularly to the electric field. After introducing a sample, different proteins will focus at different points in the horizontal plane. At the end of the glass plates, multiple tubes allow for sample collection across the entire pH gradient. The shallow separation chamber created between the two plates, and the continuous flow, eliminates the formation of vertical density gradients. At the same time, the problem of thermally-induced convective mixing is avoided, because extremely efficient heat removal can be achieved across the shallow chamber by cooling the glass plates. Several devices have been developed that use this general design. The main differences between them are the separation chamber dimensions, and the method of sample introduction and recovery. An apparatus using 50 cm wide x 44 cm long glass plates spaced 0.5 mm apart was made for larger scale IEF separations [31]. The typical residence time for this device is 150 minutes, and it is able to separate up to 500 mg protein/day. In another variation, called the Octopus [32], the anode-to-cathode distance is only 11 cm, and the plates are 55 cm long. The sample is collected at the end of the channel from 96 outlets which drip into a 96 well plate. This

large number of outlets retains more of the resolution from the pH gradient compared to other instruments with fewer outlets.

Rather than a single pass separation, the sample can be recycled for multiple passes through the separation chamber of some of these free flow instruments. This gives more freedom of choice for the sizes and concentrations of samples that can be separated on an instrument of a given size. In addition, it allows for more flexibility in the separation chamber dimensions. For example, the commercial instrument known as the RIEF has a reduced anode-to-cathode distance of just 3 cm, allowing for higher field strengths [33]. For large sample volumes, an appropriately sized external sample reservoir is used, and accordingly, the processing time is increased until a steady state is reached.

### **1.3 Classical isoelectric trapping**

#### 1.3.1 Fundamental principles

All of the instruments and methods outlined in section 1.2 rely on the use of carrier ampholytes or buffers in the sample to generate the pH gradient. In isoelectric trapping (IET), the pH gradient is defined by a series of buffering membranes that form a step-wise gradient, with the pH increasing from the anode to the cathode. These buffering membranes form the sample compartments in a device called a multi-compartment electrolyzer (MCE). The pore sizes of the hydrogel membranes are large enough to allow the majority of proteins (up to 1500 kDa) to pass, while still small enough to prevent convective mixing between adjacent compartments. The membranes contain

covalently bound buffering functionalities that define a single pH value throughout the membrane structure. Therefore, the shape and slope of the pH gradient is dependent upon the number of buffering membranes and the magnitude of the difference in pH between neighboring membranes. In addition, the membranes must have high conductivity and high buffering capacity. An ampholyte introduced into this system will migrate through the compartments and membranes until it reaches a compartment delimited by membranes with pH values encompassing the pI value of the ampholyte. At this point, the ampholyte is continuously titrated back to its isoelectric point, and becomes trapped as it migrates backwards and forwards between the two membranes. All strong electrolytes will migrate out of the sample chambers and accumulate in either the anode or cathode compartment. If the correct membranes are chosen for a given protein mixture, this system is able to trap a single, pure protein in solution, in its isoelectric form, rather than being contaminated by carrier ampholytes.

### 1.3.2 Instrumentation for isoelectric trapping separations

The birth of IET was in 1981 when Martin and Hampson patented the idea of using cloth-supported, isoelectric agarose gel membranes in an MCE [34]. For example, to create a membrane with a pH between 4.8 and 5.5, the agarose gel was carboxylated with chloroacetic acid and then amino alkylated with varying amounts of diethanolamine. In combination with the isoelectric membranes, monovalent buffering ions in solution were used to help generate the pH gradient. This technique never proved to be very successful as the membranes were not reproducible, it was difficult to

accurately predict the pH of the membrane, and the buffer chemistry could not cover the entire pH range.

The ingenious idea of IET suggested many new opportunities in the field of large scale IEF. Unfortunately, the technique would never be useful unless reliable buffering membranes could be made. In 1987, thanks to their work with the Immobilines for IPG strips, Righetti and co-workers came up with an answer [35]. By using the non-amphoteric acrylamido derivatives (the Immobilines), an isoelectric membrane with high buffering capacity, ionic strength, and conductivity can be made at any pH between 3 and 10. The Immobiline acrylamido derivatives are weak acids and bases, and two of them are strong electrolytes. Using the Henderson-Hasselbach equation, the correct ratio of acrylamido weak acid or base and titrant can be found for a desired pH [36]. With careful volumetric measurement one could cast two membranes with a difference of only 0.001 pH unit. The Immobilines are co-polymerized with acrylamide and N,N'-methylenebisacrylamide to form a 1mm thick gel cast onto a circular glass fiber filter paper with a 4.7 cm diameter [37]. The instrument which holds these membranes and is used to carry out the IET experiments is called the Isoprime [38]. The membranes form up to six chambers between the anodic and cathodic end compartments. Each sample compartment holds 5 ml and has an inter-membrane distance of 10 mm, making the total anode-to-cathode distance 10 cm. To process larger sample volumes, external reservoirs can be connected to each sample compartment and the system can be operated in

recycling mode. Overall, the Isoprime was a success, as it proved that the IET concept can be applied to larger scale protein separations (~100 mg).

Several other MCEs were made using the same basic idea as the Isoprime, but with some changes to the instrument design. For example, the Zoom is the smallest of the currently available commercial devices [39]. It has 7 compartments, each holding 640  $\mu$ l with an inter-membrane distance of 14 mm. This instrument targets the proteomics market, where it can be used to prefractionate up to 50 mg of protein before two-dimensional gel analysis. A larger alternative is the MCE in the IsoelectricQ2 instrument (IQ2). Up to 7 compartments can be used in the IQ2, each one with an inter-membrane distance of 22 mm and a volume of 5 ml [40]. The total anode-to-cathode distance is 22.2 cm. In the bottom of each compartment, stir bars keep the sample compartments mixed during electrophoresis. The MCE is placed on a cooling plate, which also has eight magnetic stirrers built into it. Suggested loads range from 50 – 500 mg, and the separation usually requires 12 - 24 hours of electrophoresis.

One of the major drawbacks of the IET technology is its dependence on the buffering membranes. The acrylamide-based membranes are mechanically fragile, they can become easily fouled, and they may exert a sieving effect on the larger proteins as the proteins move through the membranes. To get around this issue, a thin vertical bed of isoelectric beads can be used as a membrane substitute in an MCE [41]. The same Immobiline technology as used in the isoelectric membranes and IPG strips was utilized



for making the beads. Inverse emulsion polymerization was used to generate isoelectric polyacrylamide beads with an average diameter of 150  $\mu\text{m}$  [41]. The acrylamido buffers and titrants are mixed in with the neutral acrylamide and bisacrylamide monomers during the emulsion polymerization step to establish the desired pH. To create the isoelectric barrier, the slurry was poured between two glass fiber membranes coated with neutral polyacrylamide. Uncoated glass fiber membranes apparently possessed a large number of negative surface charges, because significant bulk flow from electroendosmosis was observed during IET. Only preliminary work has been published in this area, but the inventors claim that the beads will be more suitable for large scale MCE devices compared to membranes [41]. As a continuation of this work, another group has attempted to improve various physical and chemical characteristics of the beads [42]. Rather than the polyacrylamide beads, zirconium oxide beads are used with a thin polyacrylamide coating that incorporates the Immobilines. The hard ceramic zirconium oxide core of the beads does not allow transfer of proteins into the core of the bead, as was suggested to be occurring for the polyacrylamide beads. Also, to increase the surface area of the buffering coat, the diameter of the zirconium oxide beads was reduced to 60  $\mu\text{m}$ . A nylon net was used to hold the beads instead of the glass fiber filter to reduce the electroendosmotic flow observed in the original design. The nylon net had a mesh size of 20  $\mu\text{m}$  and the distance between the two nets was 1.5 cm. The authors found no difference in the fractionation of a protein mixture when the beads were used versus buffering membranes [43]. Although the beads are an attractive idea, they need to

be tested in a much larger preparative scale IET separation to substantiate the proposed advantages over buffering membranes.

Even though the isoelectric polyacrylamide chemistry used in the various approaches to IET has many advantages, it does have some drawbacks. The amide bond in polyacrylamide is prone to hydrolysis at low and high pH values, leading to several problems [44]. Firstly, substantial hydrolysis can cause a loss of buffering capacity and a change in the membrane pH. Also, the acrylic acid formed after hydrolysis can dissociate leaving fixed negative charges in the hydrogel, leading to electroendosmosis. Combined with the Joule heat effects during electrophoresis and the mechanical stress caused by the transport of macromolecules, the fragile polyacrylamide gel can start to come away from the support, leading to catastrophic leaks. Poly(vinyl) alcohol (PVA) can be used to form a more pH resistant hydrogel and has recently been used to make membranes for use in IET experiments [45-47]. Along with a new hydrogel polymer, a new chemistry was needed to make buffering membranes at different pH values.

Although not as flexible as the Immobiline chemistry, a variety of PVA-based isoelectric membranes have been manufactured ranging in pH from 1.7 to 13 [45-47]. They exhibit superior stability even in 1 M strong acid or base solutions, and have been used in IET experiments with power loads of up to 100 W for over 24 hours. Such sturdy membranes make the promise of IET on the industrial scale a more likely reality.

## **2. THE PROBLEMS WITH CLASSICAL ISOELECTRIC TRAPPING**

### **2.1 The inherent problems of the classical isoelectric trapping principle**

Preparative isoelectric trapping (IET) separations for the purification and fractionation of mixtures of proteins and other ampholytics, has proven to be an invaluable technique [48]. The technology has been found to be particularly useful as a lab-scale purification method for the separation of monoclonal antibody isoforms [49], and more recently as a prefractionation and concentration method for proteomics [50].

The governing principle of IET is to trap a target protein in its pure isoelectric state between two buffering membranes [37]. This feat is what makes IET such a powerful technique, but it is also the cause of its major limitations. As the IET separation progresses, the target protein approaches its isoelectric point, and its electrophoretic mobility decreases, making the separation times long. Another related complication is isoelectric precipitation. During IET, the strong electrolytes are removed from the sample solution and accumulate in the electrode compartments in an electro-desalting process. At the same time, the protein surface charge density decreases as the pH of the solution approaches the pI of the protein. Proteins in their isoelectric state and in a low ionic strength environment are prone to isoelectric precipitation. Long separation times, together with poor protein solubility make IET less attractive for preparative-scale IET.

## **2.2 The design flaws of existing isoelectric trapping instrumentation**

When IET is accomplished in a multi-compartment electrolyzer (MCE), the actual separation of the proteins occurs in the buffering membranes, not in the migration space that is between the membranes. In most MCEs, the distance between the buffering membranes is relatively large, in excess of 10 mm [38-40]. This leads to long separation times, because the proteins have to migrate to the membrane before any separation takes place. In addition, most MCEs have multiple compartments (up to 8), making the anode-to-cathode distance large. To achieve high field strengths, a relatively high voltage must be applied across the separation chambers. The voltage that can be applied, however, is limited by the apparatus's ability to remove Joule heat. Inconveniently, there is either no cooling system or a very inefficient one in most MCEs, so they must be operated at fairly low power loads. The large inter-membrane distance and the limited field strength that can be applied result in long separation times of up to 24 hours for the separation of 10 - 100 mg protein.

### 3. SOLUTIONS TO THE PROBLEMS OF CLASSICAL ISOELECTRIC TRAPPING

#### 3.1 The pH-biased isoelectric trapping principle

If a protein is maintained in either a cationic or anionic charge state over the entire time of an IET separation, the inherent problems of classical IET could be eliminated. To manipulate the charge state of a protein, the solution pH must be controlled. The typical weak electrolyte buffers would not be suitable for this task as they would be simply removed from the separation compartment during electrophoresis in a multi-compartment electrolyzer. The buffers need to be trapped, along with the protein, in between the buffering membranes. Therefore, such a buffer would have to possess an isoelectric point. Such buffers are referred to as auxiliary isoelectric agents or pH biasers [51]. Commonly used pH biasers include, aspartic acid (pI 2.7), glutamic acid (pI 3.2), histidine (pI 7.5), lysine (pI 9.9), and arginine (pI 10.7). In practice, isoelectric buffers are chosen such that they: will be trapped by the buffering membranes, have pI values different from the pIs of the target proteins, and, have high solubilities even in their isoelectric state. In addition, if the pH biaser satisfies the following condition;  $|pI - pK_a| < 1.5$ , then it will have high buffering capacity near its isoelectric point. These are considered the most effective pH biasing agents. For example, glutamic acid has a pI of 3.2, and the  $pK_a$  values of the two carboxylic acids are 2.2 and 4.2, thus  $|pI - pK_a| = 1$ . For the auxiliary isoelectric agent to be effective, it must be used at high enough

concentrations to move the solution pH away from the pI of the target protein, thus maintaining the target proteins in a non-isoelectric charge state.

The dependence of a protein's charge on the pH can be visualized by plotting a charge vs. pH graph. As a demonstration, the 385 amino acid sequence of the protein ovalbumin was used to construct such a plot. There are 14 aspartic acid, 33 glutamic acid, 4 cysteine, 10 tyrosine, 20 lysine and 15 arginine residues in ovalbumin [52]. Literature reports  $pK_a = 4.0$  for the  $\beta$ - and  $\gamma$ -carboxylic acid groups,  $pK_a = 5.0$  for the thiol groups,  $pK_a = 6.2$  for the imidazole groups,  $pK_a = 9.6$  for the phenolic groups,  $pK_a = 9.2$  for the  $\epsilon$ -amino groups, and  $pK_a = 11.0$  for the guanidino groups in bovine serum albumin [53]. Using these two sets of values [52, 53], the protein charge vs. pH curve was calculated for a hypothetical protein whose protonation behavior is similar to that of ovalbumin (Figure 1). The net charge on the protein increases very rapidly from zero to more than 10 as the pH of the solution is changed from  $pH = pI$  to  $pH = pI \pm 1$ . Under such conditions, the solubility and mobility of the protein ought to remain high.

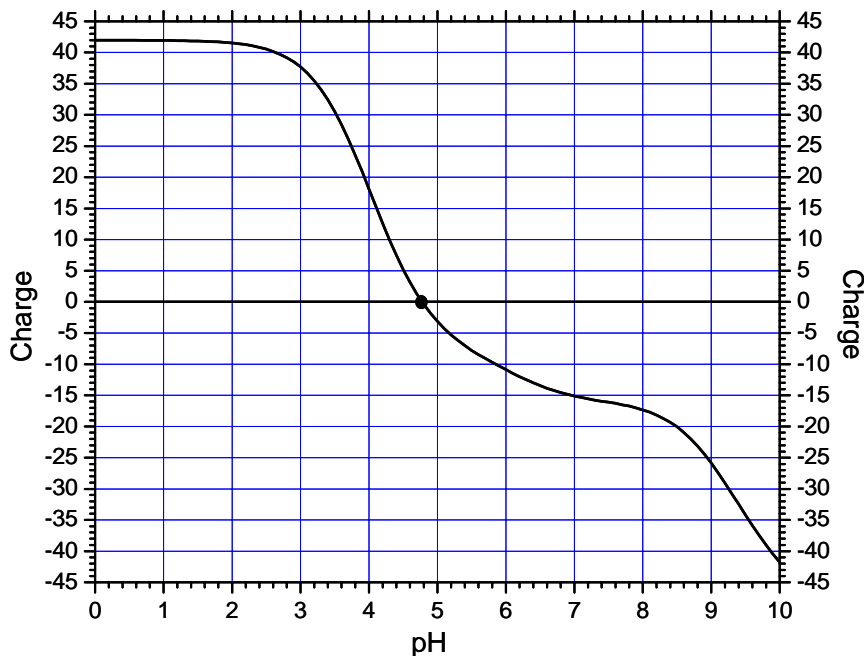


**Figure 1.** Charge vs. pH curve for a hypothetical protein containing the same amino acids residues as found in ovalbumin. When  $\text{pH} = \text{pI}$ , the net charge of the protein is zero.

### 3.2 Improved instrumentation for isoelectric trapping separations

#### 3.2.1 Development of the Twinflow

The modification of existing instrumentation, originally designed for zone electrophoresis, has been a popular approach for the development of new preparative IEF devices. In accordance with this trend, a new device has been designed for improved IET separations, using an existing instrument called the Gradiflow BF200 [54-65]. The Gradiflow BF200 was originally developed for size-based and charge-sign-based binary protein separations. In the Gradiflow, the sample is recirculated, orthogonally to the

electric field, through two shallow separation compartments formed by three polyacrylamide hydrogel membranes. The hydrogel is cast onto a poly(ethylene terephthalate) (PET) substrate for mechanical support. By changing the pore size of the middle polyacrylamide membrane (the separation membrane), size-based separations are achieved. The outer anode and cathode restriction membranes are made with a much smaller pore size (typically the nominal size cut-off is 5kDa) to prevent proteins from leaving the separation compartment. To perform a charge-sign-based separation the pH of the background is chosen to make proteins of a certain pI cationic or anionic and permit their passage through a large-pore separation membrane. The anolyte and catholyte streams are recirculated at 2 L/minute through electrode compartments adjacent to the two separation compartments and returned to the same external reservoir. The three hydrogel membranes are assembled in a disposable cartridge (Figure 2), and placed between the electrode compartments, shown in an exploded view in Figure 3.

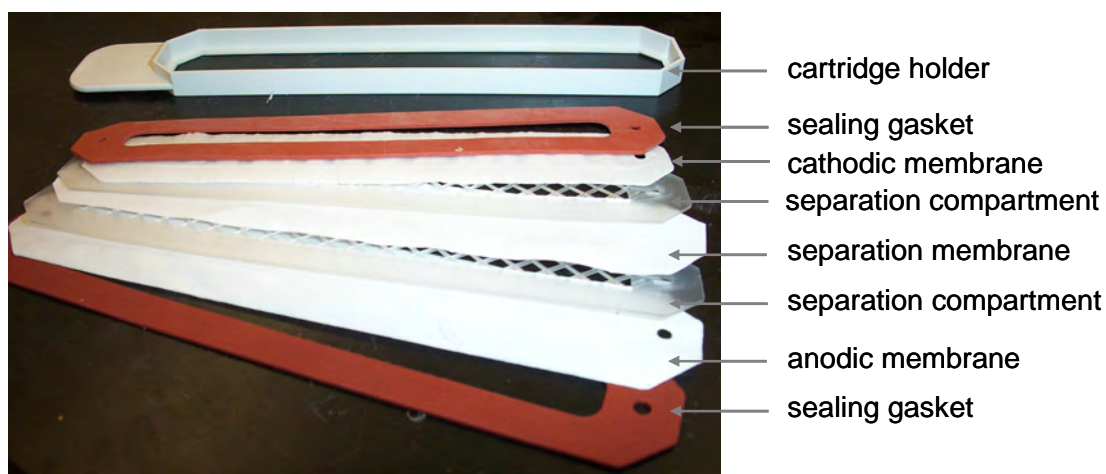


**Figure 2.** Assembly view of the separation cartridge for the Gradiflow BF200.



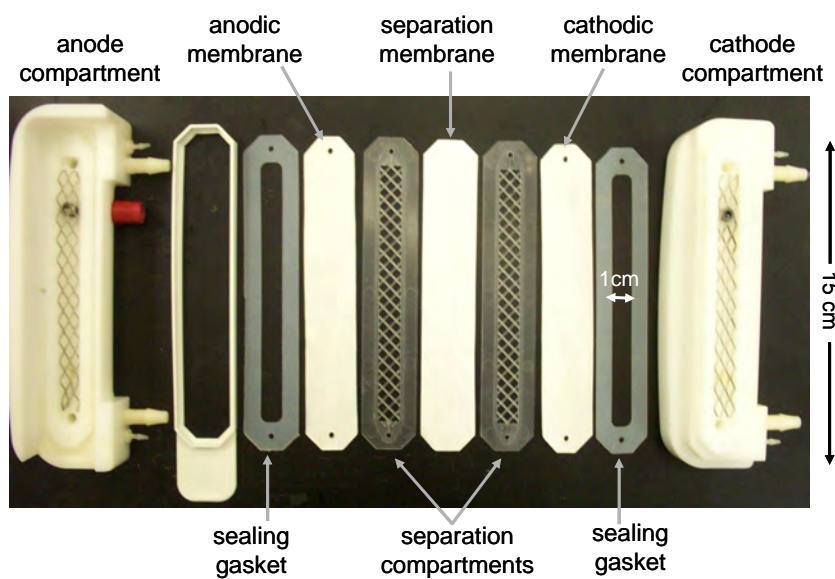


**Figure 3.** Exploded view of the separation cartridge between the two electrode compartments.

The 1mm thick grids between each membrane define the depth of the separation chambers and the gaskets form a seal. The platinum-coated titanium electrodes are in the movable head of the BF200 unit. Once the cartridge is placed between the heads, the heads can be compressed to form a seal between all four compartments. The active membrane surface area is  $15 \text{ cm}^2$ , and the distance from anode-to-cathode is 8 mm. Although each separation channel only holds 1.5 ml, large volume samples can be separated because an external reservoir of any size can be connected to the device and liquid can be recirculated through the separation unit. The cross-sectional view of the BF200 separation unit can be seen in Figure 4.

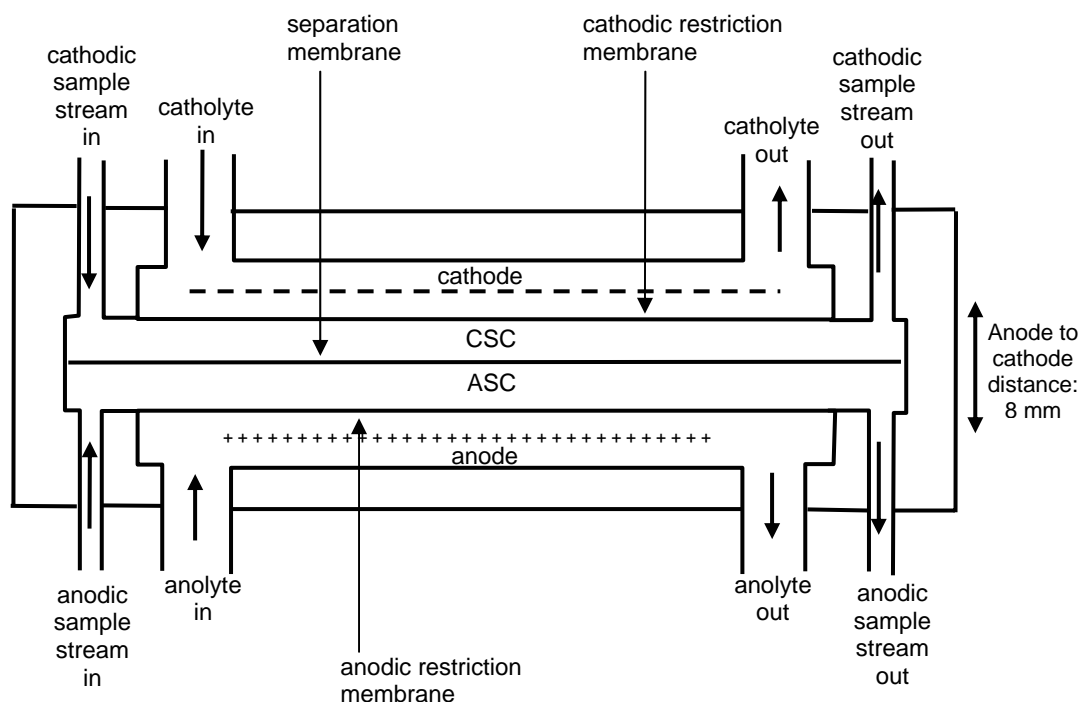


**Figure 4.** Cross-sectional view of the Gradiflow BF200 separation unit. ASC: anodic separation compartment, CSC: cathodic separation compartment.

The features of the Gradiflow, that made it appealing for modification into an IET device, were the small inter-membrane distances, and the small anode-to-cathode total distance (8 mm). These two features already gave it advantages over other multi-compartment electrolyzers. However, several other major modifications were needed to further improve the instrument and make it suitable for IET separations. Firstly, the single electrolyte reservoir of the Gradiflow needed to be split into separate anolyte and catholyte reservoirs, to be able to perform separations based on the IEF principle [66]. Separate electrolyte reservoirs would also enable more efficient removal of salt from a

sample. In the original BF200 design any salt present in the sample was removed, but returned again, albeit diluted, by the recombined electrolyte streams.

A design flaw in the original instrument was the inefficient removal of the Joule heat formed during electrophoresis. The sample streams were not cooled directly, instead they passed through a stainless steel heat exchanger in the cooled electrolyte reservoir after heating up in the separation chamber. To improve the cooling design, four new reservoirs with cooling jackets were made from glass. By recirculating a stream of ethylene glycol through a thermostatically controlled chiller and then through the glass jackets of each reservoir, the sample streams and the electrode streams could be kept at a low temperature. Typically, the streams were chilled to between 5 and 10 °C. Not only does this keep heat labile proteins stable, but it also controls the temperature inside the isoelectric membranes. This is important, because the  $pK_a$  values of the acrylamido buffers change with temperature. In turn, the operating pH inside the membrane will change during electrophoresis, affecting the outcome and / or the reproducibility of a separation.

The third design issue was the diameter of the outlet ports for the sample channels and the anolyte and catholyte. The original design had sample stream outlet diameters of 1 mm and the anode and cathode compartment outlets were 4 mm. Significant back pressure results inside the separation cartridge due to these restrictions when the streams are recirculating at their respective flow rates. A pressure gradient will be set up across

the membranes resulting in bulk liquid transport across the membranes from the compartment experiencing a higher back pressure to one of a lower pressure. Such a bulk flow can be particularly damaging for the separation of proteins with very close pI values. Significant reductions in the back pressure can be achieved by increasing the diameter of the outlet ports because reductions in the pressure drop scale with the 4<sup>th</sup> power of the diameter (at constant flow rate). Therefore, the sample outlet diameter was widened to 2.5 mm (the largest possible due to wall thickness limitations) and the anolyte and catholyte outlets to 12 mm.

The modified system is known as the Twinflow. The Twinflow uses the same kind of disposable membrane cartridge as the Gradiflow (Figure 2 and 3), however, rather than neutral polyacrylamide membranes, isoelectric buffering membranes are used. The Twinflow instrument, with two sample compartments, is capable of producing only binary separations [66]. For example, a binary separation on a mixture of proteins can be made so that the proteins with pI values greater than the pH of the separation membrane will accumulate in the cathodic separation compartment and the proteins with lower pI values will accumulate in the anodic separation compartment. There are two modes of operation for the Twinflow. It can be operated in recirculation mode, where the sample is continuously pumped through the separation unit and returned back to the same external reservoir. Alternatively, the Twinflow can be operated in pass-by-pass mode where the entire sample volume in the feed reservoirs is pumped through the unit and collected in a different external reservoir. The Twinflow instrument is depicted

schematically in Figure 5, operating in pass-by-pass mode. After the entire volume has been through the unit, a sample can be taken and that is designated as a single pass. The process is repeated until the separation is complete. This allows the user to monitor how the sample composition is changing as a function of the number of passes, but compared to the recirculation mode, it requires the constant attention of the operator.

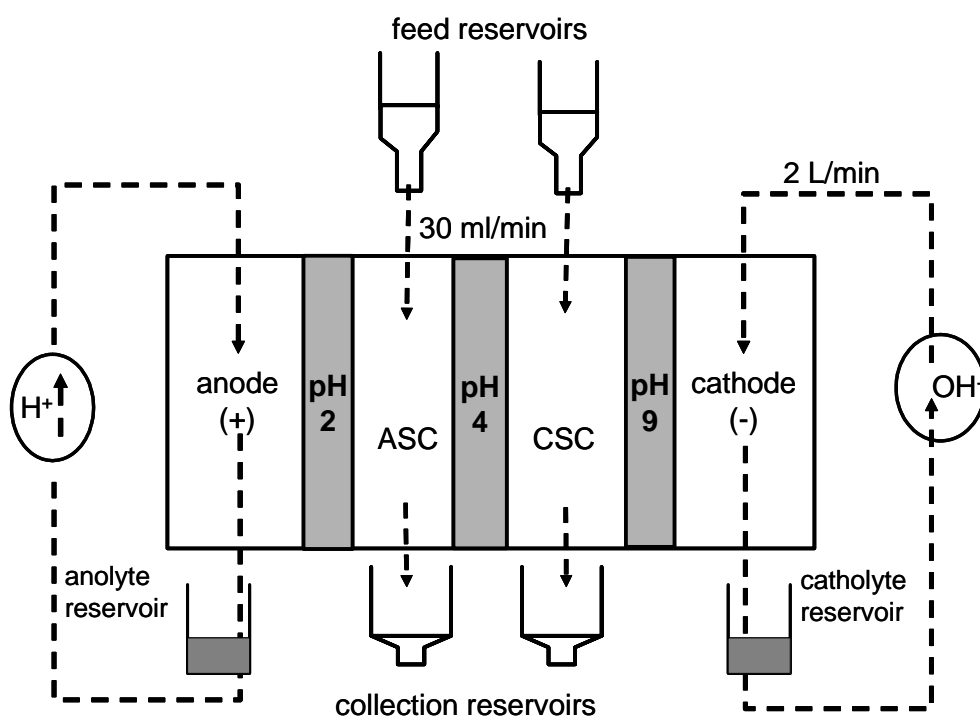


**Figure 5.** Schematic of the Twinflow IET instrument operating in pass-by-pass mode. ASC: anodic separation compartment, CSC: cathodic separation compartment.

A photograph of the front view of the Twinflow is shown in Figure 6. The cooling jackets around the sample reservoir and the modified outlets can be seen in the photograph. With the minimized anode-to-cathode length, field strengths of up to 1000

V/cm can be generated easily in this system, representing a fifty-fold increase compared to the Isoprime multicompartiment electrolyzer [66]. High field strengths, small inter-membrane distances, and effective cooling, are the results of the instrumental improvements that make the Twinflow a highly efficient IET device.

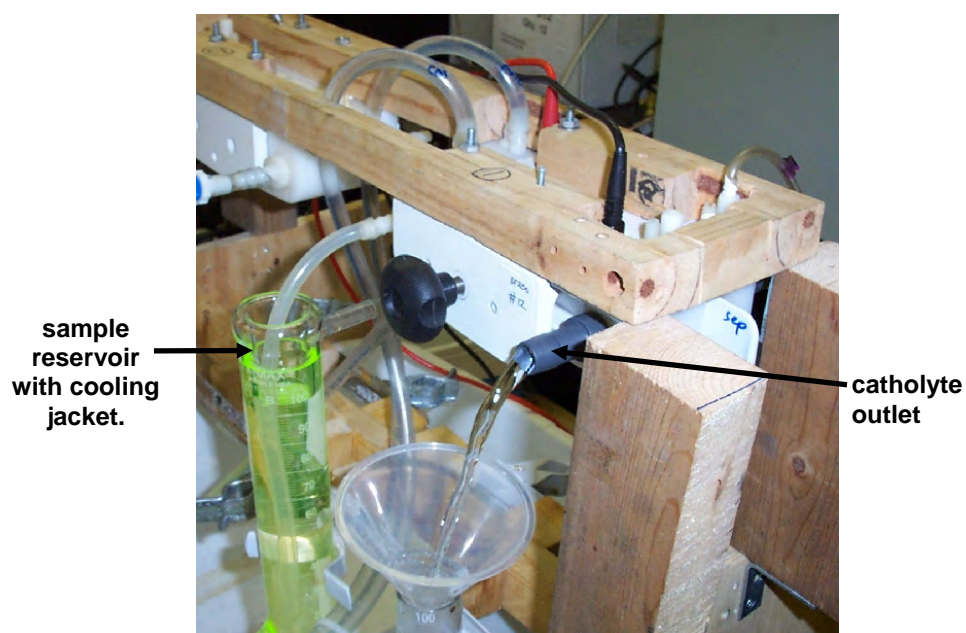


**Figure 6.** Photograph of the Twinflow. The modified separation head is mounted on a plywood frame above the external reservoirs. The leads from the high voltage power supply, and the tubing leading to the pumps can be seen connecting to the top of the unit. The cathodic sample reservoir cooling jacket and modified catholyte outlet are visible. The anodic sample reservoir and anolyte outlet are on the opposite side of the instrument and cannot be seen in this photograph.

### 3.2.2 The Biflow

To make a “pH cut” on a sample which has additional proteins with pI values above and below the pI value of the target, one of the sample streams from a Twinflow binary separation would have to be re-run through the Twinflow a second time, with a separation membrane having a slightly different pH. For example, a binary separation could be first done at pH 6.0, and then the proteins from the anodic sample compartment (i.e., proteins with  $pI < 6.0$ ) could be re-run with a separation membrane of pH 5.0. Thus, only proteins from the starting sample, with pI values between 5.0 and 6.0 would be in the cathodic separation compartment after the second separation. Figure 7 shows how such a separation would be performed in a two compartment device such as the Twinflow. In Figure 7, the rectangular box represents the Twinflow separation head configured with three buffering membranes. The middle compartments are for the sample, and the outer compartments contain the electrodes and the electrolyte solutions. To reduce the detail of the figure, the pumps and pump tubings are not depicted, however, in actual operation the sample and electrode solutions would be circulated through the unit during electrophoresis.

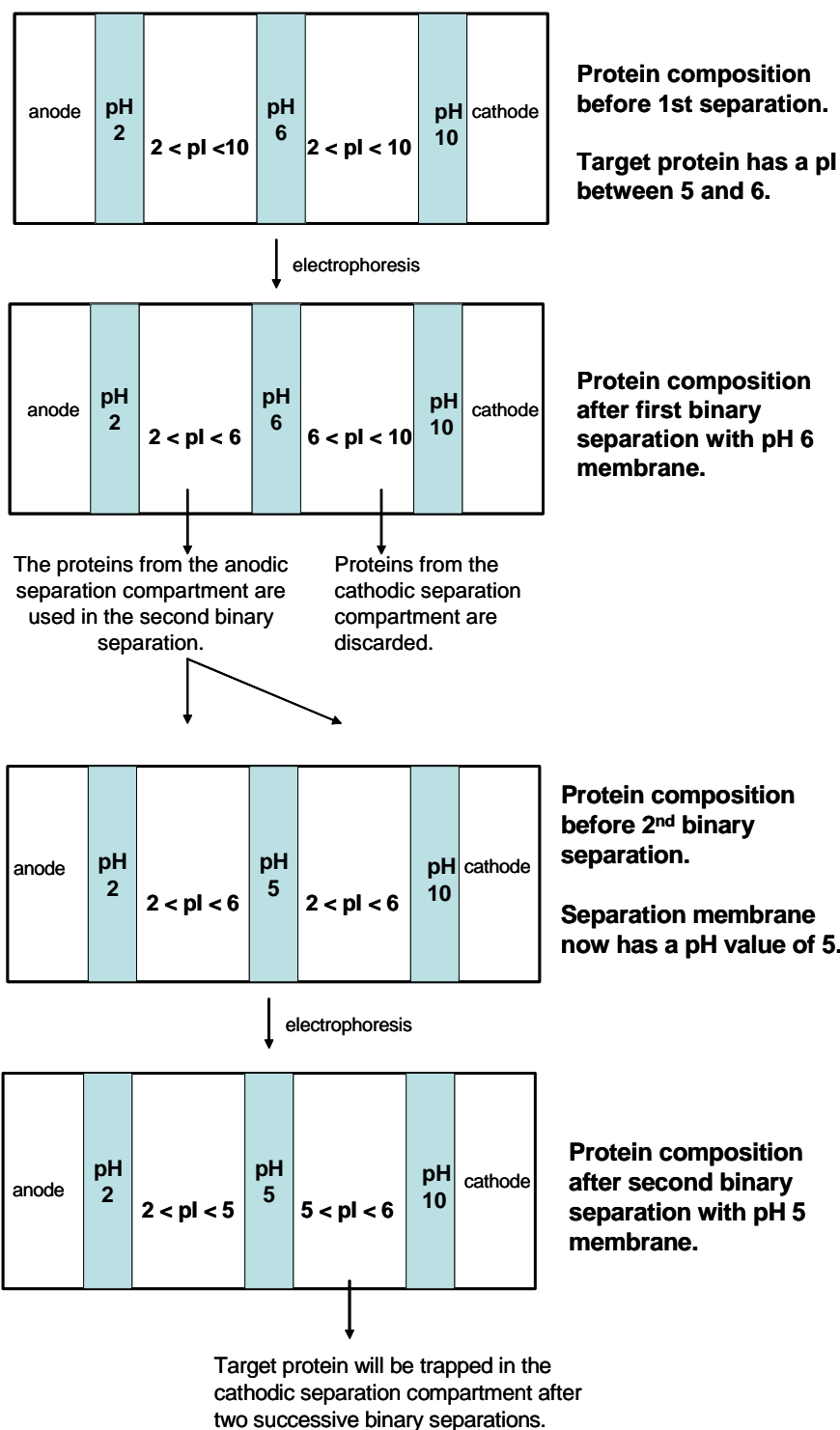


**Figure 7.** An example of a generic two-step binary separation on the Twinflow. The aim is to isolate the fraction of proteins with pI values between 5 and 6.



Ideally, narrow pH fractions from a complex protein mixture should be obtained in a single step. An instrument such as the Twinflow, but with multiple channels, could be envisaged to perform this separation. However, the gains made in separation efficiency, with the high field strength from the reduced anode-to-cathode distance, would be lost as more separation channels are added. A better solution is to serially connect two Twinflow units through a sample transfer loop, thus retaining the high field strengths. This instrument is known as the Biflow (Figures 8 and 9), and has three sample-related streams; feed, transfer loop, and product. The pH values of the separation membranes in the two units are chosen such that one is below and the other is above the pI of the target protein. In the example in Figure 8, the feed stream containing the protein mixture is fed into the cathodic sample compartment of the first unit. However, depending on the sample, either the cathodic or anodic sample stream could be used for the feed. The proteins (including the target) with pI values lower than the pH of the first separation membrane will move into the anodic sample compartment of the first unit. From there, they enter the transfer loop, that delivers them to an external reservoir, and then to the anodic sample compartment of the second unit. The membrane in the second unit has a pH lower than the first and lower than the pI of the target protein, so that the target protein will move through the membrane and into the product stream. In this way, a narrow pI cut is obtained where the proteins in the product reservoir of the second unit will have pI values less than the pH of the first separation membrane, but greater than the pH of the second separation membrane. The narrowness of the fraction obtained in the product stream is dependent on the difference in pH between the two separation

membranes. In the example in Figure 8, proteins with pI values below 6.0 would move over to the transfer loop stream in the first unit and get shuttled to the second unit. In the second unit, the separation membrane has a pH value of 5.0. Only the proteins in the transfer loop stream, with pI values above 5.0 will move into the product stream of the second unit. In this way, the Biflow has trapped proteins with pI values between 5.0 and 6.0 from the original feed mixture. Another advantage of this system is that there is always positive transport of the target protein, ensuring the highest level of purity in the product stream. Finally, the system can be configured to concentrate a target protein or specific fraction of proteins by having a large feed volume and a comparatively smaller transfer and product stream volume.

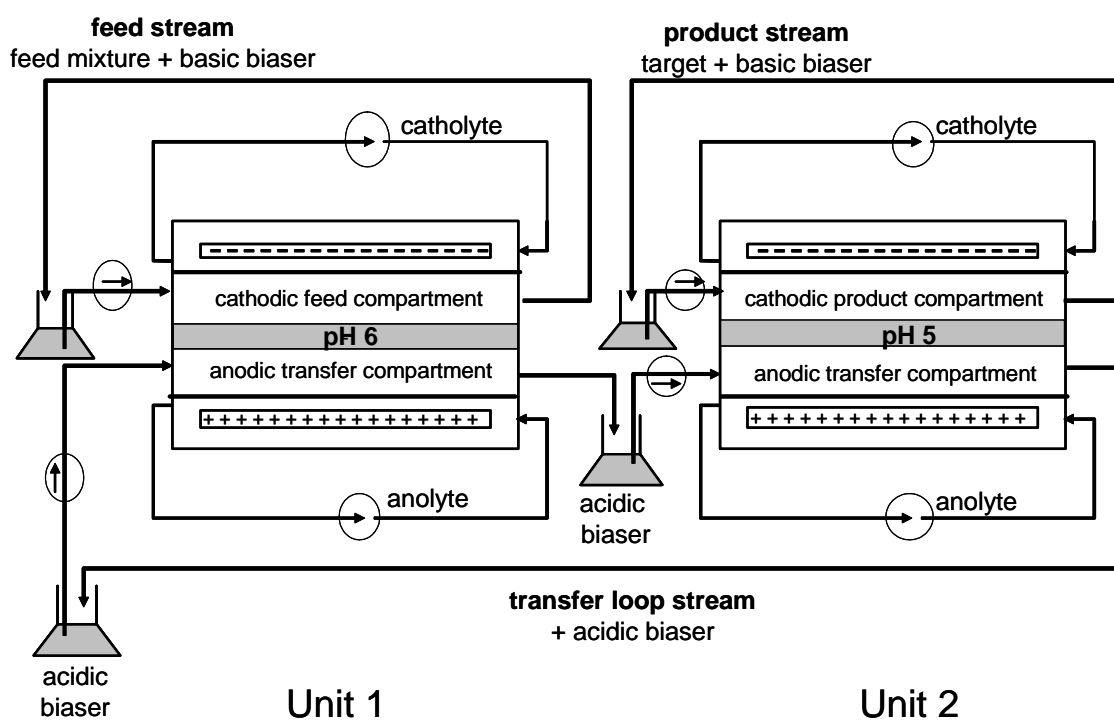


**Figure 8.** Schematic of the Biflow.

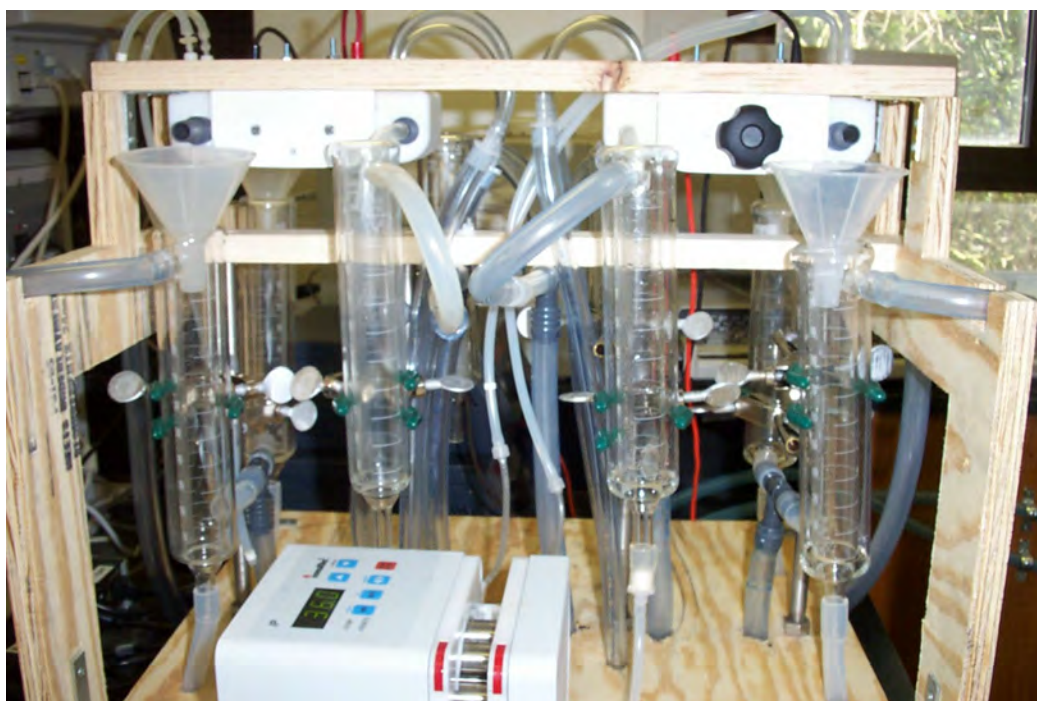


**Figure 9.** Photograph of the Biflow.

## 4. DESALTING DURING ISOELECTRIC TRAPPING

### 4.1 Initial desalting experiments on the Twinflow

#### 4.1.1 Isoelectric trapping of ampholytes during desalting

##### 4.1.1.1 Background and objective

The removal of salts, from protein samples derived from biological sources, is a major concern during the sample preparation steps prior to many downstream separations. Several desalting methods exist including, passive dialysis, electro dialysis, pressure-mediated tangential flow using hollow fibers or dialysis membranes, and centrifugal-force assisted dialysis. Many of these classical desalting approaches attempt to force a salty solution through a membrane of a particular pore size, small enough so that most of the proteins cannot pass through. A commonly used membrane would have a 10 000 molecular weight (MW) nominal cut-off. This has two consequences. Firstly, the larger proteins can be pushed up onto the membrane and adsorb there permanently. Secondly, the proteins and peptides with a molecular weight smaller than 10 000 would be lost with the salt. This is particularly undesirable in proteomics based projects where ideally the entire protein complement is to be characterized. Other problems with these classical desalting methods include, long desalting times, and incompatibility (for some) with large volumes of sample.

The IET process can be considered to take place in two phases, the first is the removal of salts (non-ampholytes) from the sample compartment, followed by the focusing of the

ampholytic components. Although the two phases are not completely exclusive, the strong electrolytes carry the majority of current at the start of the IET separation. The charge on a strong electrolyte is not affected by pH, so the buffering membranes will not trap them, and the permanent anions and cations will migrate out of the separation channel and accumulate in the anode and cathode compartments, respectively. Removal of the strong electrolytes is an unavoidable consequence of IET, and could lead to a good alternative to the classical desalting methods listed above. To investigate the desalting capabilities of the Twinflow, UV-absorbing salts and UV-absorbing ampholytes (as substitute proteins) were used to monitor the desalting process. The objective was to completely remove the salts without losing any of the ampholytes.

#### 4.1.1.2 Instrument set-up, materials, and method

The Twinflow was used for all the desalting experiments described in this section. It was set up in single-channel configuration, where there was no separation membrane, only the cathodic and anodic membranes with a single 1 mm separation compartment between them (Figure 10). The UV-absorbing salt was prepared by titration of a 10 mM solution of benzyltrimethylammonium hydroxide (BzTMAOH) with benzenesulfonic acid (BSH), until the pH of the solution was 7.0. The UV-absorbing ampholytes used were, *meta*-aminobenzoic acid (MABA, pI 3.9), histidine (HIS, pI 7.5), and tyramine (TYRA, pI 10.0). The 50 ml sample loaded into the Twinflow contained the 10 mM UV-absorbing salt solution with 2 mM TYRA and MABA, and 6 mM HIS. The catholyte was a 200 mM sodium hydroxide solution and the anolyte was a 30 mM

methanesulfonic acid solution. The anodic and cathodic membranes used were, pH 2.0 and pH 11.0 PVA-based membranes, respectively. The separation was run with a constant current of 500 mA, in recirculation mode, and aliquots were taken every 3 minutes. The aliquots were analyzed by capillary electrophoresis (CE) with the UV-detector set at a wavelength of 214 nm. The schematic of the Twinflow desalting set-up can be seen in Figure 11.

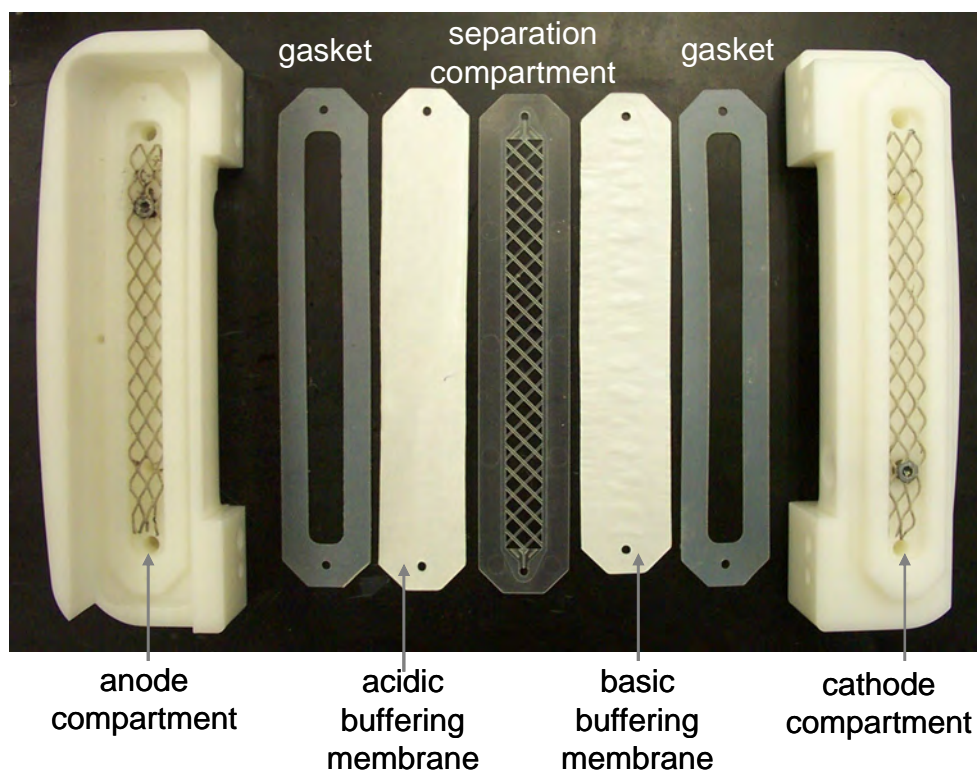


**Figure 10.** Exploded view of the single-sample compartment cartridge used for desalting on the Twinflow.

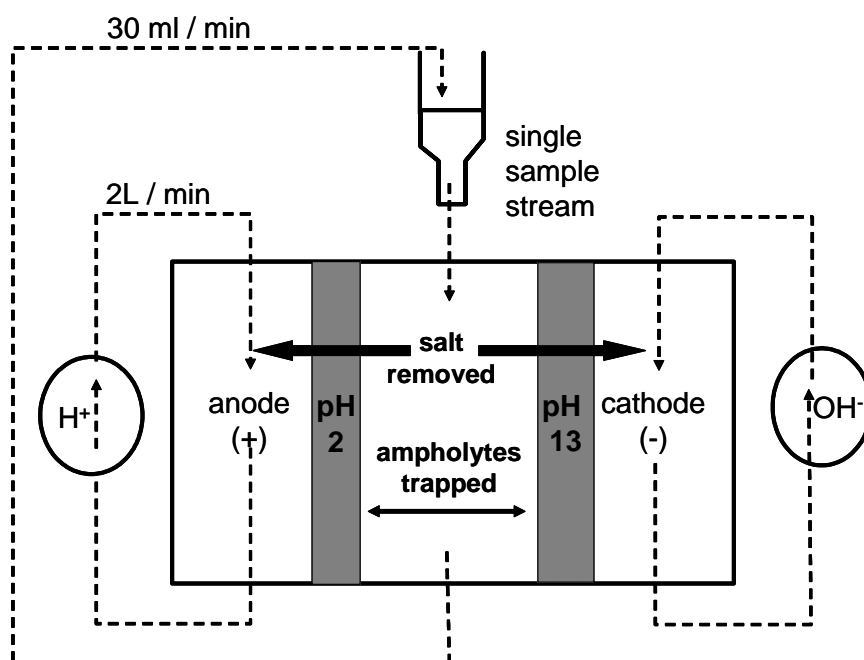


**Figure 11.** Schematic of the Twinflow in single-sample compartment desalting mode.

#### 4.1.1.3 Results and discussion

The CE electropherograms in Figure 12 show the changing sample composition over the desalting period during IET. The top panel shows the electropherogram for the initial sample (feed), the middle panel for the aliquot taken after 15 minutes, and the bottom panel for the aliquot taken after 30 minutes. Clearly, the benzyltrimethylammonium ion ( $\text{BzTMA}^+$ ) and the benzene sulfonate ion ( $\text{BS}^-$ ) are removed from the sample in 30 minutes. Importantly, no loss of the ampholytes is evident during the desalting process. The pH, conductivity, voltage and current are plotted in Figure 13. By 30 minutes, the potential and conductivity have leveled off, indicating that the majority of desalting has been accomplished and the current across the separation compartment is mainly being carried by the trapped ampholytes. The removal of the  $\text{BzTMA}^+$  ion and the  $\text{BS}^-$  ion was

selected to model the desalting behavior for the monovalent salt ions such as sodium and chloride, which are commonly found in protein samples.

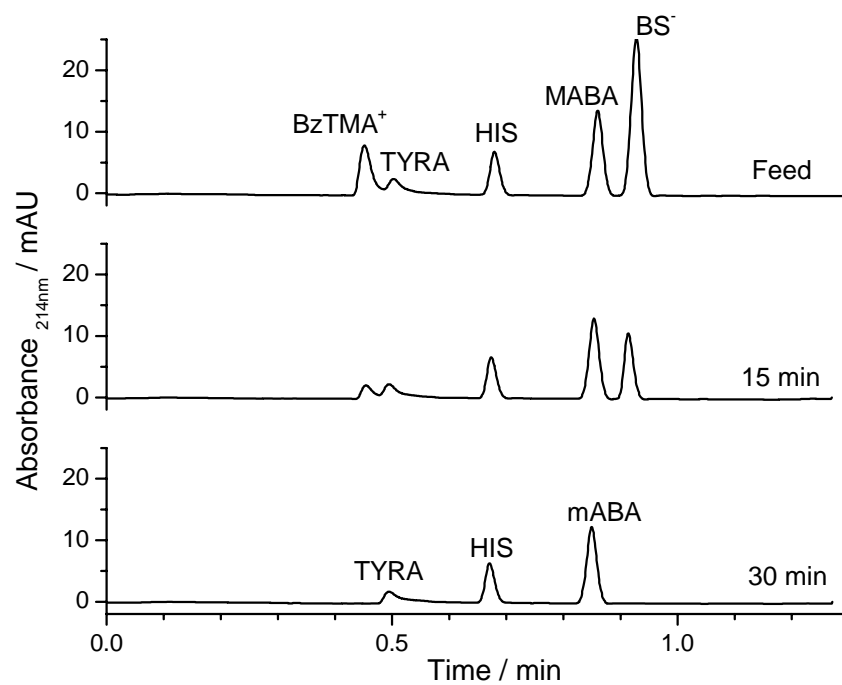


**Figure 12.** Electropherograms of the samples taken during desalting a UV-absorbing salt from a mixture of three UV-absorbing ampholytes. The three ampholytes remained trapped while the strong electrolytes are removed.



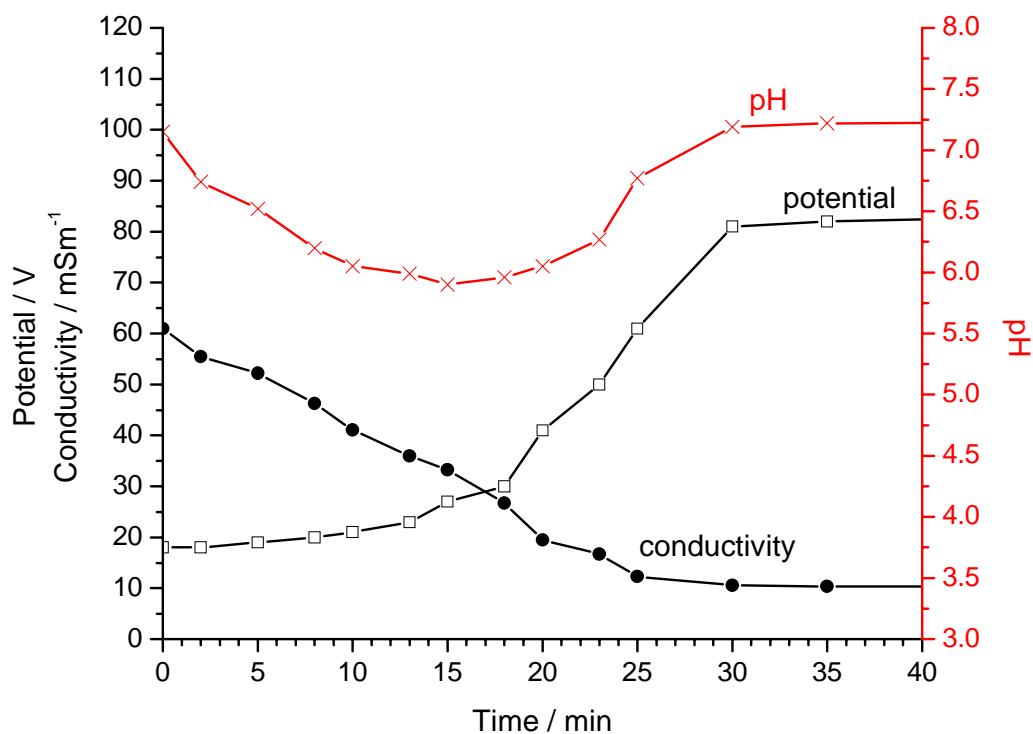


**Figure 13.** Potential, conductivity, and pH of the sample stream during IET desalting.

#### 4.1.2 Concluding remarks

The buffering membranes used in IET are able to completely trap ampholytes, and at the same time allow for the passage of strong electrolyte ions out to the electrode compartments. The high field strengths that can be generated on the Twinflow, together with its capacity for processing large sample volumes, make it a particularly useful instrument for the desalting of protein samples. In addition, the problem of losing low molecular weight proteins and peptides, which plagues classical desalting techniques, is avoided using the IET desalting method. As long as all the proteins have

pI values between the pH values of the two buffering electrode membranes, none should be lost. To further improve the desalting process for a given sample the current, flow rates, and cooling would have to be optimized to reach maximum salt removal rates.

## **4.2 The pH-transient phenomenon**

### 4.2.1 Ion mobility considerations

#### 4.2.1.1 Background and objective

During the investigation into IET and desalting, pH transients were occasionally observed in the sample solution. These pH transients could be either acidic or basic, but the pH would always return to the expected value by the end of the desalting process (as monitored by a leveling off of the current and confirmed by capillary electrophoresis analysis). Therefore, it was hypothesized that pH-transients were caused by an unequal removal rate between the cation and anion of the salt. From the literature, it was known that a difference in electrophoretic mobility between a cation and an anion will certainly affect the relative rates at which they are desalted in an IET experiment [67]. The cause of pH transients needs to be understood because changes in pH during an IET separation can denature certain proteins, and if the change is extreme, it can hydrolyze the polyacrylamide buffering membranes.

#### 4.2.1.2 Instrument set-up, materials, and method

Firstly, to examine the effects of mismatched ion mobilities for a given salt, a single separation compartment cartridge was assembled where the pH of the anodic and

cathodic membranes were equidistant from pH 7. The anodic membrane was pH 4, and the cathodic membrane was pH 10. Three different salts were tested, where the ions were either matched in mobility, or mismatched so that either the anion or cation was faster. The individual ions in the salts were BzTMA<sup>+</sup>, Na<sup>+</sup>, *para*-toluene sulfonate (PTSA<sup>-</sup>), and Br<sup>-</sup>. The effective mobilities of each are listed in Table 1. To the 10 mM salt solutions, 2 mM histidine (HIS) was also added as an ampholytic component. The anolyte was 25 mM glutamic acid, and the catholyte was 25 mM arginine. A constant current of 50 mA was used and the voltage varied from 150 to 200 V. The Twinflow was run in recirculation mode and multiple samples were taken over a time-course of 30 minutes. After the pH was recorded, the relative concentrations of the cations and anions were determined using capillary electrophoresis.

**Table 1.** Effective mobility values for the strong electrolytes that were used in the desalting experiments.

Ion	Mobility ( $\times 10^{-5} \text{ cm}^2/\text{Vs}$ )
BzTMA <sup>+</sup>	30
Na <sup>+</sup>	52
PTSA <sup>-</sup>	-31
Br <sup>-</sup>	-79

#### 4.2.1.3 Results and discussion

It was confirmed that differences in the ion mobilities of strong electrolytes contributed to the pH transients observed during desalting by IET. When a salt, made up of cations

and anions with very similar mobilities, was desalted, there was very little pH deviation (Figure 14). This indicated that the cation and anion were desalted at approximately the same rates. In the case of the  $\text{BzTMA}^+ / \text{Br}^-$  salt,  $\text{Br}^-$  has a much higher mobility than  $\text{BzTMA}^+$  ( $79 \times 10^{-5} \text{ cm}^2/\text{Vs}$  compared to  $30 \times 10^{-5} \text{ cm}^2/\text{Vs}$ ). As a result, the  $\text{Br}^-$  concentration decreased faster than that of  $\text{BzTMA}^+$  (Figure 15). The pH transient moves in the basic direction, reaching a maximum of pH 9 and then returns to approximately pH 7.5. Before desalting had begun, the  $\text{BzTMA}^+$  was equally balanced by the  $\text{Br}^-$ . As the  $\text{Br}^-$  starts to be desalted faster than  $\text{BzTMA}^+$ , hydroxide ions ( $\text{OH}^-$ ) from the catholyte migrate into the sample compartment to act as a replacement counter-ion for the  $\text{BzTMA}^+$ . The increased  $\text{OH}^-$  concentration in the separation compartment resulted in the basic pH transient. By the 15<sup>th</sup> minute,  $\text{BzTMA}^+$  was completely desalted, along with the  $\text{OH}^-$  counter-ion, and the solution pH was determined by the ampholytic histidine (pI 7.5) that remained trapped in the sample compartment. In the third case, the positively charged  $\text{Na}^+$  has a faster mobility than its counter ion,  $\text{PTSA}^-$  (Figure 16).  $\text{Na}^+$  departs faster, leaving  $\text{PTSA}^-$  to be balanced with the incoming hydronium ions, resulting in an acidic pH. Again, at the end of the experiment the pH returns to the pH determined by a solution of pure histidine (HIS). In all these experiments, the relative difference in the desalting rate for a monovalent anion versus cation can be considered in terms of transference number. If the ion mobilities and the concentrations of all the salt ions present in the sample are known, one can calculate the transference number for each, and predict which ions will linger in the sample stream and lead to what kind of pH transient.

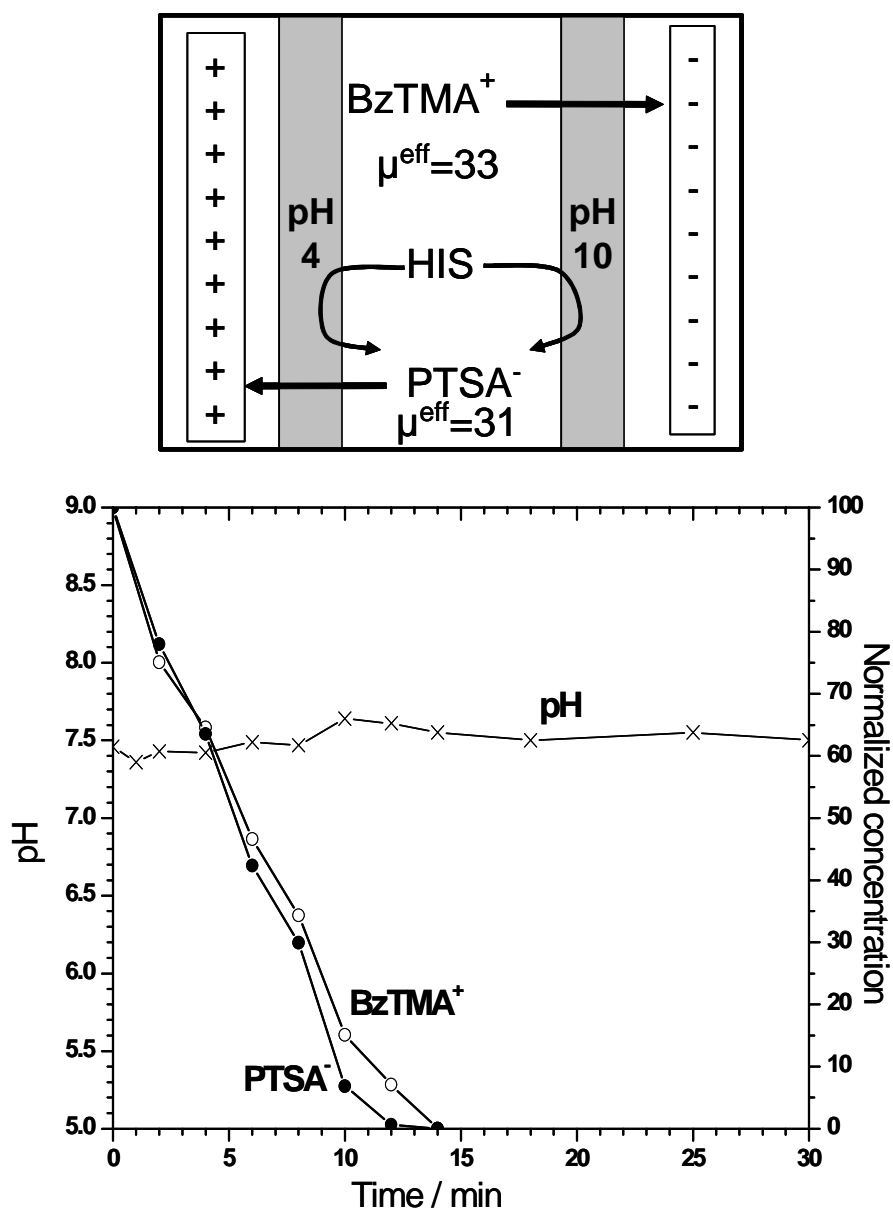


**Figure 14.** IET desalting of mobility-matched ions. The top panel is a visual representation of the desalting process inside the separation compartment. The bottom panel shows the pH and concentration changes in the sample compartment during the desalting of BzTMA<sup>+</sup> and PTSA<sup>-</sup>.

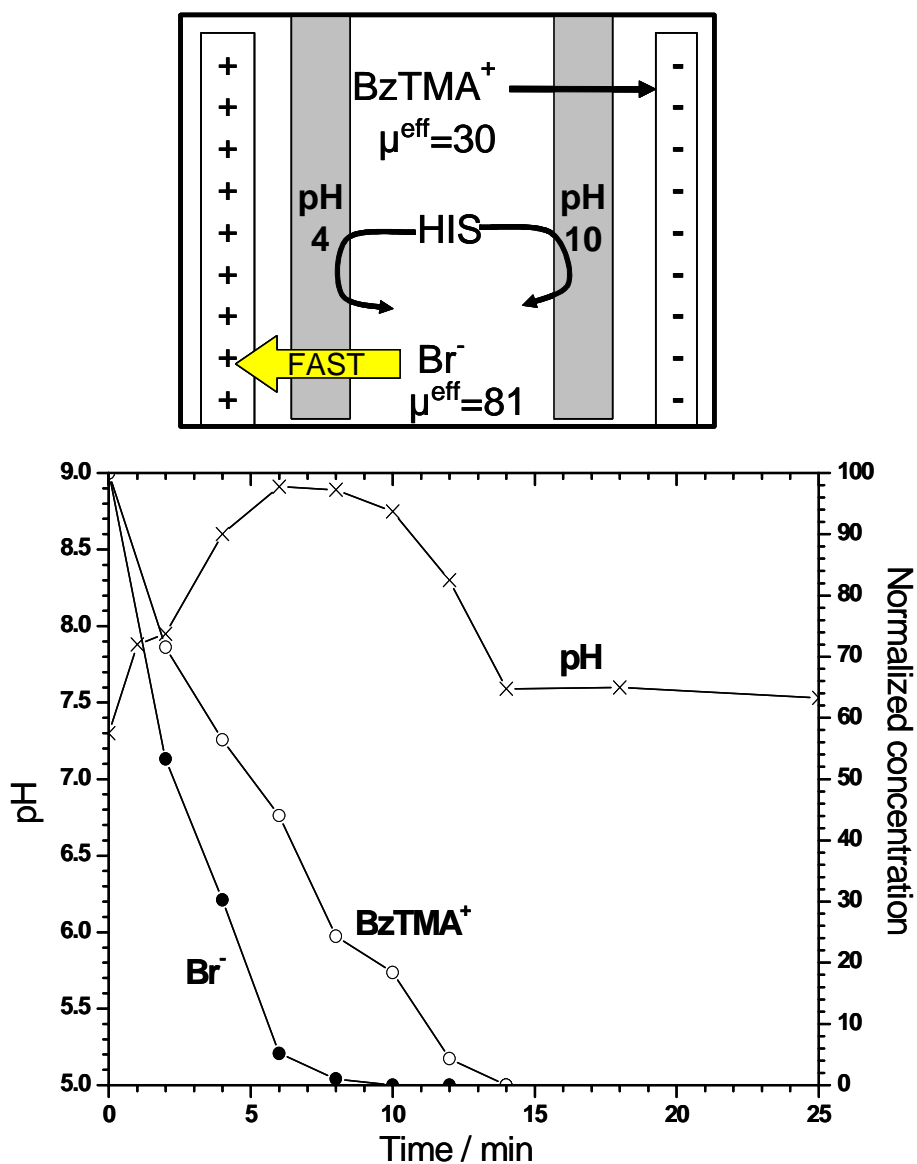


**Figure 15.** IET desalting when the anion has a higher mobility than the cation. The top panel is a visual representation of the desalting process inside the separation compartment. The bottom panel shows the pH and concentration changes in the sample compartment during the desalting of BzTMA<sup>+</sup> and Br<sup>-</sup>.

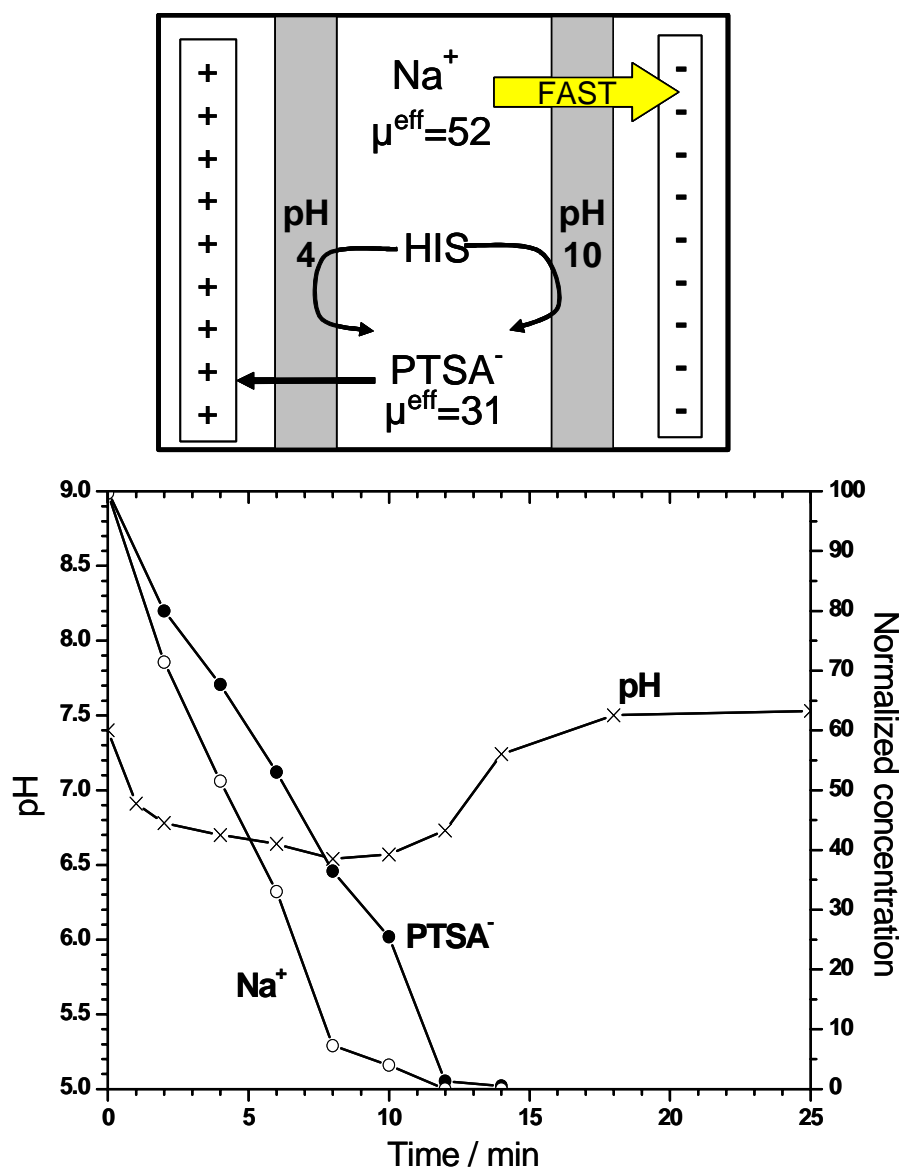


**Figure 16.** IET desalting when the cation has a higher mobility than the anion. The top panel is a visual representation of the desalting process inside the separation compartment. The bottom panel shows the pH and concentration changes in the sample compartment during the desalting of  $\text{Na}^+$  and  $\text{PTSA}^-$ .

## 4.2.2 Membrane pH considerations

### 4.2.2.1 Background and objective

To further investigate the origin of the pH transient phenomenon, another variable was also considered; the pH of the buffering membranes used in the single sample compartment configuration of the Twinflow. In this study, strong electrolytes were the molecules being desalted. The charge on a strong electrolyte is not governed by the pH, as would be the case for a weak electrolyte, so the expectation was that the pH of the buffering membranes should have no effect on the migration of the strong electrolytes out of the sample compartment. By matching the ion mobilities of a salt, the mismatched ion mobility effects described in Section 4.2 could be considered negligible. The objective here was to examine what effect the difference between the pH of the cathodic buffering membrane and pH 7 and the pH of the anodic buffering membrane and pH 7 had on the pH transients.

### 4.2.2.2 Instrument set-up, materials, and method

The mobility-matched strong electrolytes were  $\text{BzTMA}^+$  and  $\text{PTSA}^-$ . To investigate the membrane pH effects, this salt solution was used while the pH values of the membrane were varied. The symmetrical scenario was considered first where the pH of each membrane was equidistant from pH 7; the anodic buffering membrane was pH 4 and the cathodic buffering membrane was pH 10. Then, the pH of the anodic membrane was changed to pH 6 to be closer to pH 7 than the cathodic, pH 10 membrane. Conversely, in the final test the cathodic membrane was changed to pH 8 to be closer to pH 7 than the



pH of the anodic membrane at pH 4. In each scenario, a 30 ml sample of the salt, 10 mM BzTMA<sup>+</sup> and PTSA<sup>-</sup>, was mixed with 2 mM histidine (HIS). The same electrolyte solutions, Twinflow running mode, power supply settings, and sample analysis described in Section 4.2.1.2, were used for this set of experiments.

#### 4.2.2.3 Results and discussion

Using the pH 4 anodic membrane, and pH 10 cathodic membrane, where both membranes are 3 units from pH 7, no pH transient was observed (Figure 17). However, when the pH of the anodic membrane was changed to pH 6, only one unit away from pH 7, while the pH of the cathodic membrane remained 3 units away, a basic pH transient was recorded (Figure 18). This suggested that the pH transient was caused by the cation lingering in the sample compartment and pairing up with the OH<sup>-</sup> counter-ion. In the same way, when the pH of the cathodic membrane was brought down to pH 8, and the anodic membrane was at pH 4.0, the anion removal rate was decreased, creating an acidic pH transient (Figure 19).

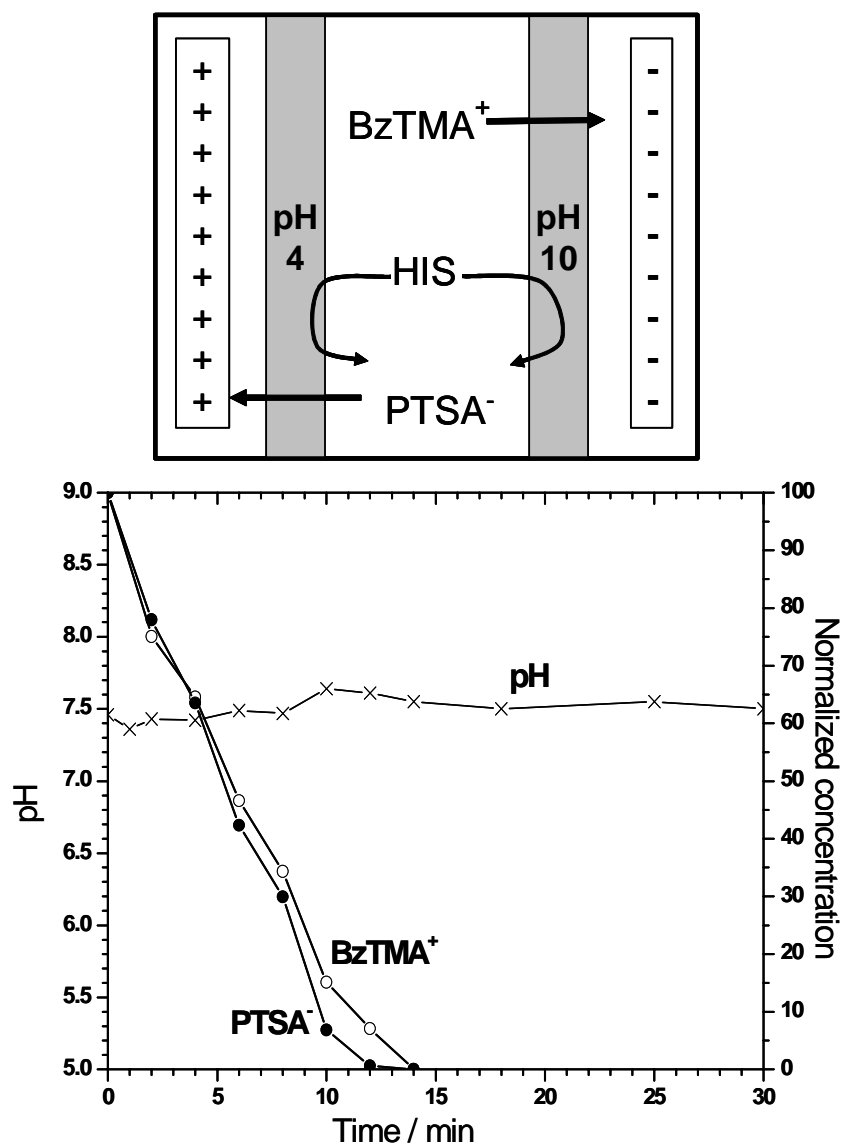


**Figure 17.** IET desalting when the anodic and cathodic membranes are equidistant from pH 7 and the ions are mobility-matched. The top panel is a visual representation of the desalting process. The bottom panel shows the pH and concentration changes in the sample compartment during the desalting of BzTMA<sup>+</sup> and PTSA<sup>-</sup>.

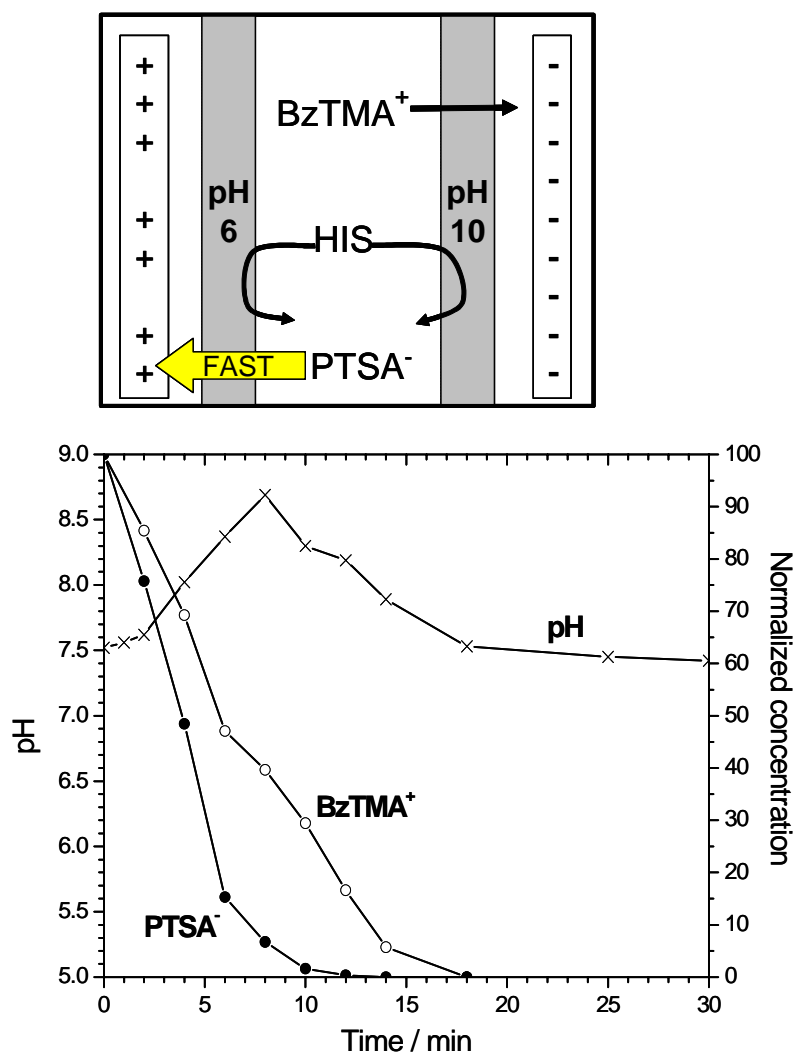


**Figure 18.** IET desalting when the anodic membrane is closer to pH 7 than the cathodic membrane and the ions are mobility-matched. The top panel is a visual representation of the desalting process. The bottom panel shows the pH and concentration changes in the sample compartment during the desalting of BzTMA<sup>+</sup> and PTSA<sup>-</sup>.

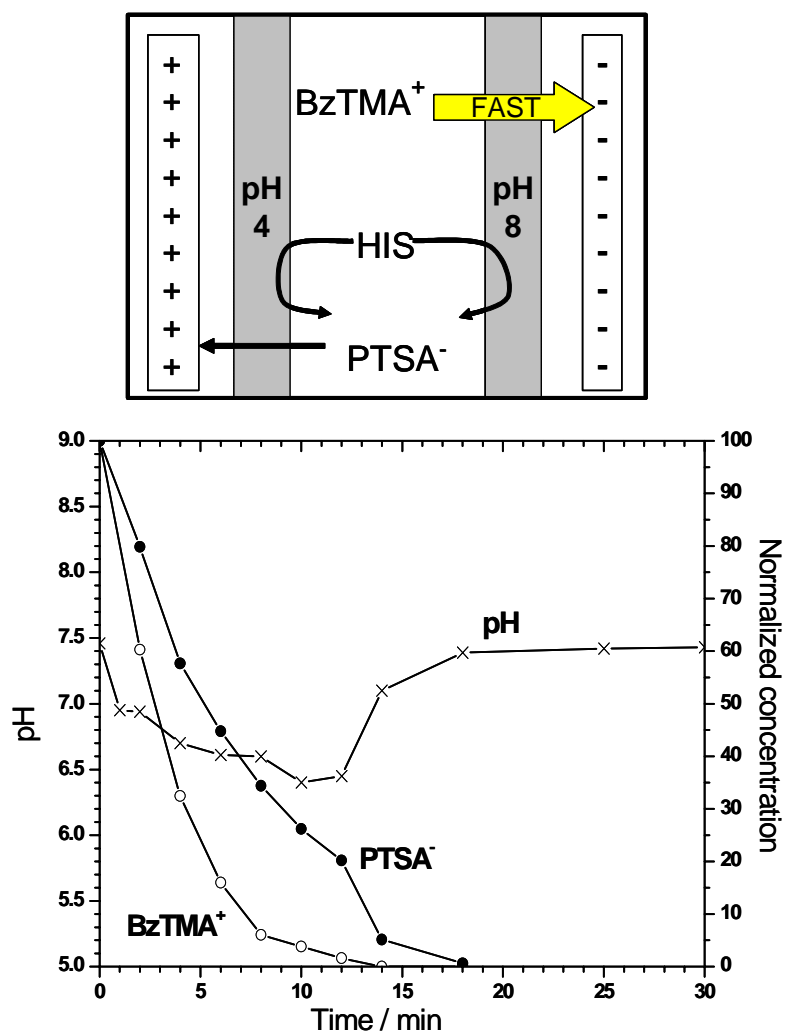


**Figure 19.** IET desalting when the cathodic membrane is closer to pH 7 than the anodic membrane and the ions are mobility-matched. The top panel is a visual representation of the desalting process. The bottom panel shows the pH and concentration changes in the sample compartment during the desalting of BzTMA<sup>+</sup> and PTSA<sup>-</sup>.

From the observations, the following rules can be used to predict the direction of pH transients generated during desalting:

If,  $|7 - \text{pH}^{\text{anodic membrane}}| < |7 - \text{pH}^{\text{cathodic membrane}}|$  then a basic transient will result;

and if,  $|7 - \text{pH}^{\text{anodic membrane}}| > |7 - \text{pH}^{\text{cathodic membrane}}|$  then an acidic transient will result.

These results suggest that there is an electric repulsion in the membrane that retards ion migration. For example, as the pH of a cathodic buffering membrane becomes more basic, the concentration of OH<sup>-</sup> in the membrane pores increases. Correspondingly, the concentration of the positively charged counter-ions, from the weakly basic buffering groups attached to the hydrogel, must also increase. These fixed positive charges may be creating a Donnan potential and causing the repulsion felt by a cation trying to migrate out towards the cathode. In an acidic buffering membrane, the fixed negative charges from the weakly acidic buffering groups would also be generating a Donnan potential, causing the repulsion of anions. Therefore, it is proposed that the unequal desalting rates for a mobility-matched anion and cation, and the subsequent pH transients, are caused by the unequal Donnan potentials in the anodic and cathodic buffering membranes.

#### 4.2.3 Control of the pH transient during desalting

##### 4.2.3.1 Background and objective

Being able to predict and control the pH transients during desalting, would be a powerful operating variable for IET, and would allow for the protection of proteins and membranes from extreme pH values. The only other reported study on the pH transients,

recommended the use of an external pH control system [67]. External pH control (a pH-stat) is counter-productive for a desalting process because it involves the introduction of more salt. After observing the membrane effects described in Section 4.2.2, the next step was to see if the pH transients could be manipulated by choosing different membrane pH values for the desalting of a given salt made from ions of mismatched mobilities. By selectively moving the pH of a membrane further from or closer to pH 7, the Donnan potential inside the membrane can be increased or decreased to make it more or less repulsive to the ion trying to exit.

#### 4.2.3.2 Instrument set-up, materials, and method

The salt chosen for this study was benzyltrimethylammonium bromide ( $\text{BzTMA}^+ / \text{Br}^-$ ). Four different single compartment membrane configurations were tested. In every case the cathodic buffering membrane was pH 10.0, and four different anodic membranes were tested, pH 2.0, 3.0, 3.5, and 4.0. The catholyte was 25 mM arginine and the anolyte was 10 mM MSA. The same Twinflow running mode, power supply settings, and sample analysis described in Section 4.2.1.2, were used for this set of experiments.

#### 4.2.3.3 Results and discussion

The selection of the pH of the buffering membranes certainly can influence the desalting rates of strong electrolytes. Figure 20 shows the pH data collected for each of the four membrane configurations, the pH values next to each trace indicate the pH of the anodic membrane used for that particular run. The pH 4.0 anodic membrane is 3 pH units from

pH 7, as is the cathodic membrane with a pH of 10. They are both equidistant from pH 7, and the expected basic transient, as determined by the ion mobilities, was observed. Thus, the BzTMA<sup>+</sup> ion lingers in the compartment, while Br<sup>-</sup> is removed quickly. To slow down the removal rate of Br<sup>-</sup>, the Donnan potential in the anodic membrane must be increased by decreasing the pH of the membrane. The lowest anodic membrane tested was pH 2.0, and the resulting pH transient was acidic. Under these conditions, Br<sup>-</sup> was repelled so greatly, that the BzTMA<sup>+</sup> actually desalted faster, leaving behind the excess anion that paired up with H<sup>+</sup>, causing acidification. By increasing the pH of the anodic membrane slightly to pH 3.0, the acidic transient was less severe, but still it was present. Finally, by using the pH 3.5 anodic membrane, the pH transient was eliminated almost altogether. This configuration represents the situation where the higher Donnan potential in the anodic membrane has decreased the anion removal rate to almost equal to that of the less mobile cation. As the relative concentrations of both strong electrolytes remained equal in the solution, no extra OH<sup>-</sup> or H<sup>+</sup> was needed to balance the charges, and the pH of the solution in the separation compartment remained relatively steady.

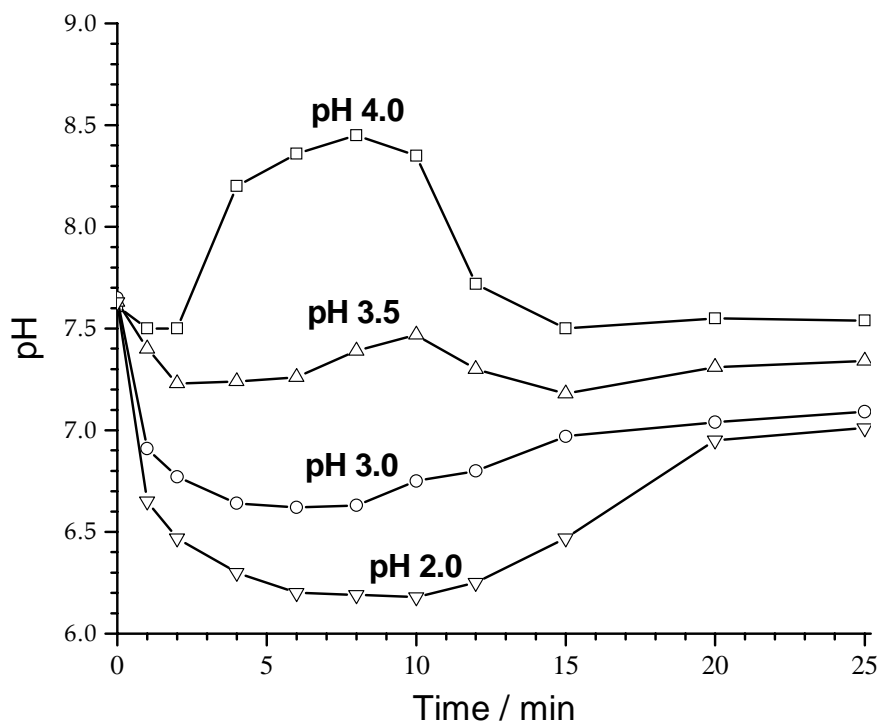


**Figure 20.** pH transients in the sample compartment during desalting and the influence of the pH value of the anodic membrane. The number next to each trace is the pH value of the anodic membrane. The pH of the cathodic membrane was 10.0.

#### 4.2.4 Concluding remarks

The unexpected result that the pH of the buffering membranes can affect the desalting rates of strong electrolytes is an interesting phenomenon, but it may also serve as a useful way to manipulate the direction and severity of the pH transients. This could be an attractive alternative to external pH control that was suggested for the elimination of pH transients. By altering the difference between the pH of each buffering membrane and pH 7, a limited amount of control could be gained over the direction and magnitude



of the pH transients during the desalting process, provided that the ion mobilities in a sample are known. Of course, in a real sample the flexibility of such an approach would be constrained by the pI values of the particular proteins that need to be trapped at the same time. Nonetheless, control of the pH of the buffering membranes represents a new approach which can be utilized for desalting applications, and one that is unique to IET.

## 5. SEPARATION OF SMALL ORGANIC MOLECULES BY ISOELECTRIC TRAPPING

### 5.1 Classical isoelectric trapping separations on the Twinflow

#### 5.1.1 Separations in a hydro-organic solvent

##### 5.1.1.1 Background and objective

Small organic molecules, which are also ampholytic, are not typically purified using electrophoresis. However, as these molecules have pI values, it should be possible to separate them using IET on the Twinflow. These small organic ampholytes are often hydrophobic, and their solubility in aqueous media is very low even in their non-isoelectric state, compared to their solubility in organic media. A hydro-organic solvent was used in the Twinflow, to see if the polyacrylamide buffering membranes could still operate as isoelectric barriers while separating small organic ampholytes.

##### 5.1.1.2 Instrument set-up, materials, and method

The Twinflow unit with a two sample-compartment configuration was used for all the preparative-scale IET separations. The buffering membranes were polyacrylamide-based and had a nominal thickness of 150  $\mu\text{m}$ . First, the stability of the membrane was tested at three different methanol-water concentrations: 25, 30, and 50% v/v methanol. A mixture of two hydrophobic ampholytic molecules, meta-aminobenzoic acid (MABA), pI 3.9, and 3-(3-pyridyl)propionic acid (3-PPA), pI 4.8, was prepared in the three methanol-

water solutions. The separation was attempted at each methanol-water concentration using an anodic membrane with pH 3.0 (in water), a separation membrane with pH 4.2 (in water), and a cathodic membrane with pH 7.8 (in water). To demonstrate a real-life example of an IET separation with a hydro-organic medium, the Twinflow was used to purify the hydrophobic, technical grade dye, 4-hydroxy-3-(morpholinomethyl)benzoic acid (HMMB). A 30 ml solution of 2mM HMMB was prepared in a 25% methanol-water solvent. The anodic, separation, and cathodic membranes had aqueous pH values of 4.2, 6.0, and 7.8. As a second demonstration, a hydrophobic fluorescent ampholyte derived from fluoresceine, was purified from the raw reaction mixture. The target had a pI of 5.76 and there were a variety of contaminants with lower and higher pI values. The reaction mixture has a low aqueous solubility: even in 25% (v/v) methanol-water only 0.1 mM concentration could be prepared. To accomplish the separation in one step, the Twinflow was operated in single sample-compartment mode with the anodic and cathodic buffering membranes chosen such that they were slightly lower (pH 5.6) and higher (pH 5.9) than the target pI value. In this way, the target should be retained in the separation compartment, while the contaminants will move out into the electrode solutions.

For each Twinflow run in this series of experiments, the anolyte was 15 mM glutamic acid (GLU), and the catholyte was 15 mM lysine (LYS), dissolved in the same methanol-water mixture as used for the sample. The sample was pumped through the separation compartments at 30 ml/min in recirculation mode, and 0.5 ml aliquots were

taken at the exit ports over the time-course of each experiment and analyzed by full column imaging capillary isoelectric focusing (CIEF), on an instrument called the iCE280 unit [68]. The iCE280 yields electropherograms in which absorbance is shown as a function of the position (expressed in pixels) of the focused analyte band in the separation capillary (2050 pixels correspond to 50 mm of capillary length). Since the pH gradient runs from 3 to 10 from one end of the capillary to the other, the pixel numbers can be correlated to pI. The pH gradient is calibrated using a series of standard ampholytes having high UV absorbance and known pI values. The separation cartridge in the iCE280 unit contained a 5 cm x 100  $\mu$ m internal diameter fluorocarbon-coated fused silica capillary. Separations were obtained at 3 kV, with a focusing time of 4.5 minutes.

#### 5.1.1.3 Results and discussion

The first membrane stability experiment, with 25% (v/v) methanol in water, was carried out in constant potential mode, at 950 V, for 1 hour. These conditions created an initial current of 25 mA and a final current of 11 mA. The results of the CIEF analysis of the original sample, and the aliquots collected after 60 minutes from the cathodic and anodic sample streams are shown in the top, middle, and bottom panels of Figure 21. MABA, with a pI of 3.9, was trapped between the pH 3.0 and 4.2 buffering membranes, and 3PPA, with a pI of 4.8, was trapped between the pH 4.2 and 7.8 buffering membranes. Clearly, IET separation has been achieved indicating that the polyacrylamide-based buffering membranes retain enough of their buffering capacities to function as effective

isoelectric barriers in the 25% (v/v) methanol-water solvent for at least 60 minutes. The same separation was done with 30% (v/v) methanol-water mixture and run at constant 950 V. The higher methanol concentration caused lower conductivities and resulted in lower electrophoretic currents. The separation was complete in 45 minutes, although the cathodic membrane began to leak slowly after about 30 minutes. Therefore, the membranes still functioned as isoelectric barriers, but the long term stability appears limited at 30% (v/v) methanol-water. The third methanol concentration tested was 50% (v/v) methanol in water, with the same hydrophobic ampholytes. All membranes began to leak after 10 minutes of electrophoresis. Visual inspection of the membranes after the run indicated that the polyacrylamide hydrogel layer had collapsed onto the PET substrate.

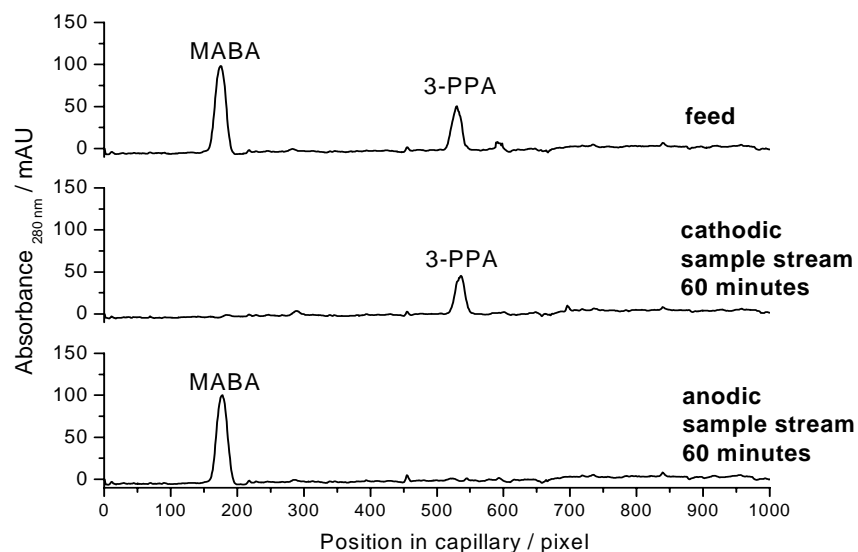


**Figure 21.** CIEF analysis of the anodic and cathodic sample streams during IET of 3-PPA and MABA in the presence of 25% methanol in water.

To prove the utility of the hydro-organic media, the technical grade dye, HMMB which is used as a pI marker for CIEF applications, was purified to homogeneity. Technical grade HMMB contains 90% active component and 10% contaminant, both of which are ampholytes. The active component has a pI of 5.8, while the contaminant has a pI of 6.2. The 2mM HMMB sample (in 25% v/v methanol) was recirculated through the anodic separation compartment until the minor contaminant had been removed to the cathodic separation compartment. The purity of the HMMB target in the anodic sample stream was greater than 99%, after 60 minutes of electrophoresis (Figure 22).

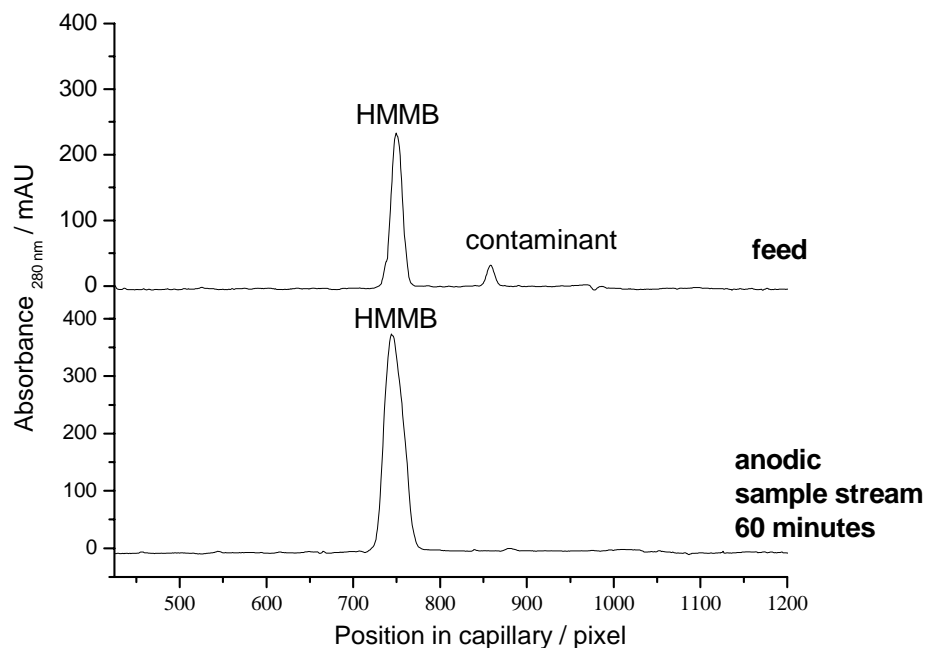


**Figure 22.** CIEF analysis of the purification of a technical grade, ampholytic dye (HMMB). The top panel is the starting feed in the anodic sample stream and the bottom panel is the anodic sample stream after 60 minutes of IET in the presences of 25% methanol in water.

In the second demonstration, the fluoresceine derivative was purified using the single separation compartment set-up in the Twinflow. CIEF analysis (Figure 23) shows that in just 20 minutes, the sample is cleared of both the major contaminant (unreacted fluoresceine) and the minor contaminants.

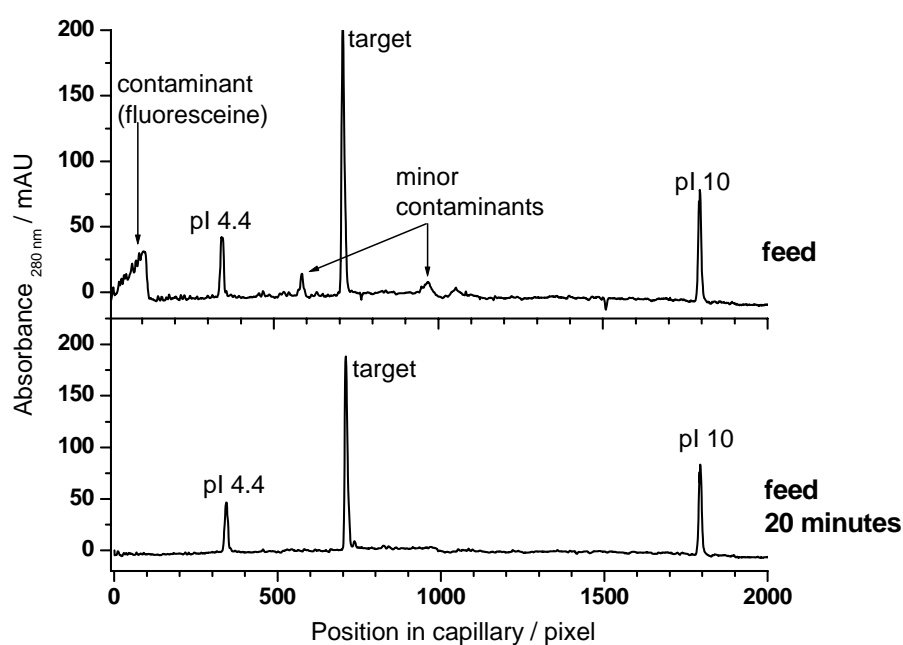


**Figure 23.** CIEF analysis of the purification of an amphoteric fluoresceine derivative by single sample-compartment IET in 25% v/v methanol in water.

This study has shown that PET supported, polyacrylamide-based buffering membranes could be successfully used in hydro-organic media containing up to 25% (v/v) methanol-water. The solubility of HMMB was sufficiently high (2mM) in 25% methanol to permit meaningful preparative-scale IET separations. A processing rate of 7 mg/hour and a

product purity of 99% could be achieved using the Twinflow. By using 25% (v/v) methanol in water, the fluoresceine derivative could be dissolved and IET was successfully performed on a sample that could not be purified using water as the solvent.

The presence of methanol probably alters the pI values of the ampholytes and the pH of the buffering membranes. When separating components with very close pI values (e.g.,  $\Delta pI < 0.1$ ), this uncertainty could prevent an accurate prediction of the right separation membrane to use. However, this does not appear to be a major impediment, because the appropriate separation membrane can still be selected in a few simple trial-and-error experiments by testing a series of separation membranes with closely spaced aqueous pH values in the hydro-organic solvent.

### 5.1.2 Separation of ampholytic enantiomers

#### 5.1.2.1 Background and objective

IEF separations of ampholytic enantiomers were first reported by Righetti et al. [69], who saturated a polyacrylamide slab gel with a mixture of  $\beta$ -cyclodextrin (CD) and carrier ampholytes. In 1999, Glukhovskiy and Vigh developed an analytical expression to predict the magnitude of the isoelectric point difference ( $\Delta pI$ ) that can be generated between the ampholytic enantiomers by a non-charged chiral resolving agent, such as a non-charged cyclodextrin CD:

$$\Delta pI'_{R,S} = \frac{1}{2} \log \frac{1 + K_{S-CD} [CD] \quad 1 + K_{H^+RHCD} [CD]}{1 + K_{R-CD} [CD] \quad 1 + K_{H^+SHCD} [CD]} \quad (1)$$



where  $K_{R-CD}$ ,  $K_{S-CD}$ ,  $K_{H^+RHCD}$ , and  $K_{H^+SHCD}$  are the equilibrium constants for the formation of the anionic complexes of the two enantiomers ( $R^-CD$  and  $S^-CD$ ) and the cationic complexes of the two enantiomers ( $H^+RHCD$  and  $H^+SHCD$ ), and  $[CD]$  is the species concentration of the free, uncharged cyclodextrin [70]. This relationship has also proved applicable to enantiomer separations using CIEF [71,72], preparative continuous free-flow IEF [70,72], and preparative IET with the multicompartiment electrolyzer known as the Isoprime [73]. The objective of this study was to show that preparative-scale IET separations of enantiomers can be performed on the Twinflow unit using hydroxypropyl  $\beta$ -cyclodextrin (HP- $\beta$ -CD) as the uncharged chiral resolving agent.

#### 5.1.2.2 Instrument set-up, materials, and method

The Twinflow was used in the recirculating, two sample-compartment mode. The anodic membrane was pH 3.0, the separation membrane was pH 3.7, and the cathodic membrane was pH 7.5. The sample was prepared by dissolving 0.75 mM of the piperidinium salt of racemic dansyl-tryptophan (Dns-Trp) in a 100 ml solution of 60 mM hydroxypropyl- $\beta$ -CD (HP- $\beta$ -CD). The 60 mM HP- $\beta$ -CD concentration was previously determined to give the maximum  $\Delta I$  between the Dns-Trp enantiomers [72]. 50 ml of the sample solution was added to both the anodic and cathodic sample compartment reservoirs. The anolyte was 2 mM phosphoric acid, and the catholyte was 2 mM ethanolamine. The power supply delivered a constant power of 10 W, and was maintained throughout the separation, until the enantiomeric purity reached at least 95%.

Aliquots taken from the Twinflow sample streams were analyzed by CIEF on the iCE280 device.

### 5.1.2.3 Results and discussion

The  $\Delta pI$  that is created between the two enantiomers in the presence of 60 mM HP- $\beta$ -CD was determined before the separation was started. The racemic mixture was analyzed by CIEF. By using the calibrated pH gradient, pI values of 3.6 and 3.9 were assigned to the two enantiomers, respectively (Figure 24). Based on this result, the pH 3.7 separation membrane ought to be a good choice to separate the two enantiomers.

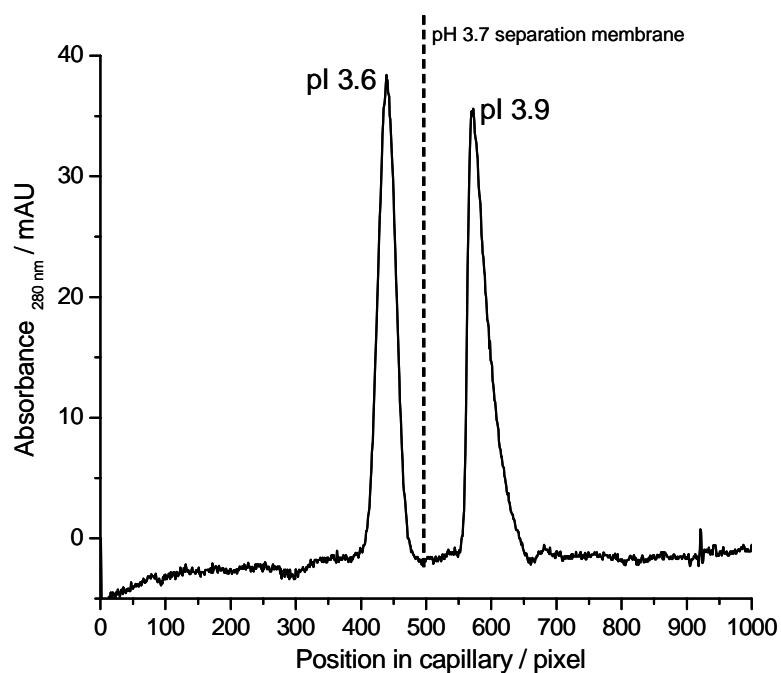


**Figure 24.** CIEF analysis of Dns-Trp in 60 mM HP- $\beta$ -CD. The dotted line represents the expected position at which the pH 3.7 separation membrane would separate the sample.

Over the first 15 minutes of the electrophoresis, a rapid rise in the potential was observed. This indicated that the piperidinium counter-ion of the racemic Dns-Trp was completely removed from the sample compartments within the first 15 minutes. The aliquots taken every 60 minutes were analyzed for enantiomeric purity (expressed as %, m/m) using the iCE280 unit (Figure 25). The enantiomeric purity increased in both reservoirs over time, and the rate slowed as the separation progressed.

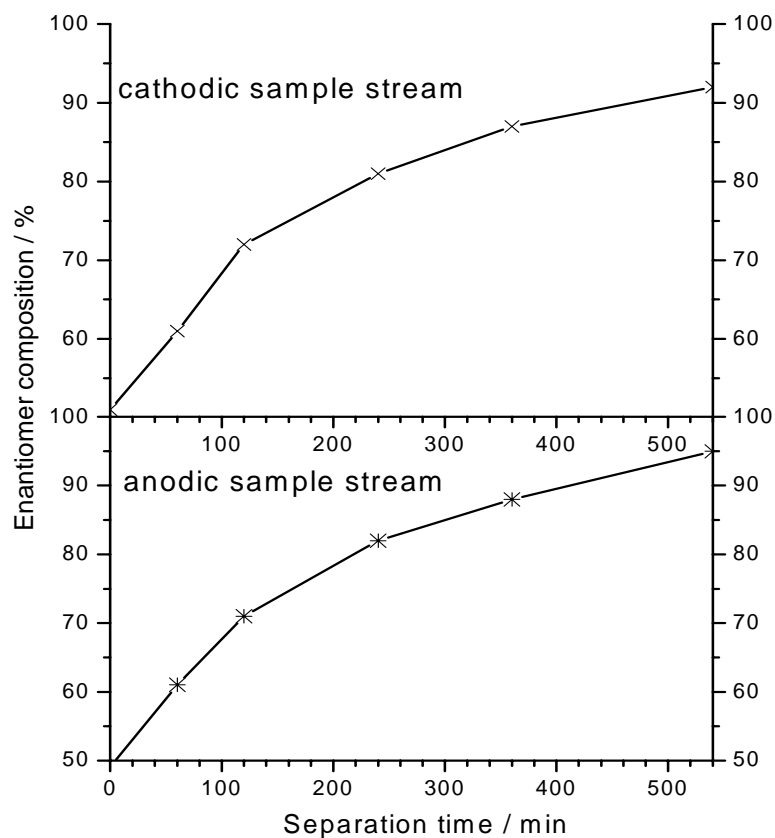


**Figure 25.** Enantiomer composition in the anodic and cathodic sample reservoirs as a function of time during IET separation of the enantiomers of Dns-Trp.

After 9 hours, the 95% purity level was reached, and the solutions from the sample streams were harvested. Figure 26 shows the full column imaging CIEF separation of the contents of the anodic and cathodic sample streams after 9 hours of electrophoresis.

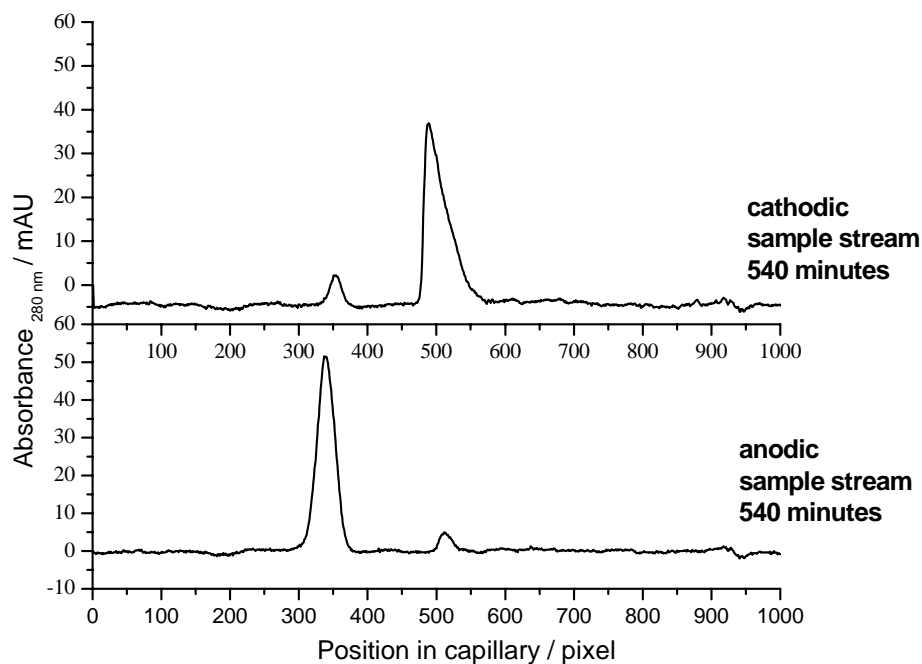


**Figure 26.** CIEF analysis of the cathodic and anodic sample streams after 540 minutes of electrophoresis.

Previously published data on enantiomer separations using the continuous free-flow IEF unit, called the Octopus [72], and the IET unit, called the Isoprime [73], were used to compare the production rates and energy consumption obtained on these instruments with the Twinflow (Table 2). The Twinflow was able to produce 1.8 mg / h of enantiomer, with an electrophoretic energy consumption of only 5.5 W h / mg. The

production rates and energy consumption values observed for the Twinflow were more favorable than those obtained with either the Octopus or the Isoprime. These figures of merit for the Twinflow are a reflection of the instrumental design modifications that make the unit more efficient than other instruments used for IET separations.

**Table 2.** Comparison of the production rates and energy consumption for enantiomer separations on the Octopus, Isoprime, and Twinflow. (These comparisons do not take into account the energy costs of cooling and pumping).

<b>Instrument</b>	<b>Production rate (mg / h)</b>	<b>Electrophoretic Energy Consumption (W h / mg)</b>
Octopus	0.1	120
Isoprime	1.2	70
Twinflow	1.8	5.5

### 5.1.3 Separation of UV-absorbing carrier ampholytes

#### 5.1.3.1 Background and objective

The pH of a buffering membrane can be readily calculated if the concentration and  $pK_a$  values of the buffering functionalities in the membrane are known. However, the operational pH in the membrane during an IET separation may actually be different from the calculated value for several reasons. Firstly, incomplete incorporation of the buffering groups into the membrane during membrane preparation can result in a lower concentration than expected. Secondly, during electrophoresis, the membrane can be exposed to an increased temperature due to Joule heat effects, which can shift the  $pK_a$

values and hence, the pH value of the membrane. Thirdly, the  $pK_a$  values of these groups may also change once they have been covalently attached onto the polymer backbone and are in the hydrogel environment. Lastly, the pH value of a buffering membrane may be affected by long storage times, for example the acrylamido groups may undergo hydrolysis causing a shift in the membrane pH [74]. Therefore, knowing the operational pH value of a buffering membrane is important for selecting the correct membrane for a given separation.

One approach to finding the operational pH in a membrane is to use a series of pI markers in the Twinflow during an IET separation. These pI markers have high UV absorbance and known pI values. After a separation, depending on whether the pI markers are in the cathodic or anodic sample compartment, the pH of the membrane can be estimated. There are, however, only a limited number (twelve) of these molecules available in the pH range of 2 to 11. Therefore, only a pH range can be found, limiting the utility of the method for finding an accurate pH value for a given membrane.

Commercial carrier ampholytes (such as Pharmalyte) consist of hundreds of species per pH unit. These can be derivatized with a chromophore to make them absorb UV light at 280 nm. Such a mixture could be separated on the Twinflow, in the two compartment mode, and then the individual sample streams could be analyzed by CIEF after diluting them in a mixture of non-UV absorbing carrier ampholytes. The anodic sample compartment will contain the UV-absorbing carrier ampholytes with pI values below the pH of the separation membrane, and the cathodic sample compartment will contain the

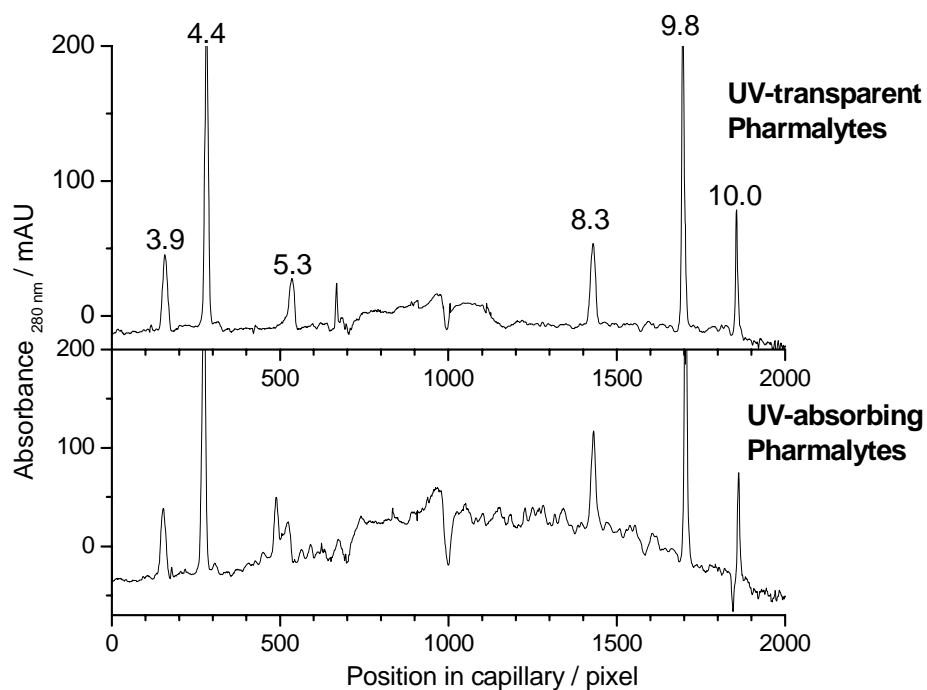
UV-absorbing carrier ampholytes with pI values above the pH of the separation membrane. Therefore, wherever there are UV-absorbing carrier ampholytes, a higher absorbance will be measured, compared to the background of non-UV absorbing carrier ampholytes. The point at which the step change in absorbance occurs would represent the operating pH of the separation membrane.

#### 5.1.3.2 Instrument set-up, materials, and method

The UV-absorbing carrier ampholytes were synthesized by a reaction of 40% solution of UV-transparent carrier ampholytes (Isolyte, ICN pI 3-10) with the chromophore, glycidyl 4-methoxyphenyl ether. To test a buffering membrane, the UV-absorbing carrier ampholytes were placed in the Twinflow sample compartments. The anodic membrane had a pH of 2, and the cathodic membrane had a pH of 12, the membrane being tested for its operational pH was used as the separation membrane. The two membranes tested had calculated nominal pH values of 7.0, and 8.0. The anolyte and catholyte were 30 mM methanesulfonic acid and 200 mM sodium hydroxide, respectively. The samples were recirculated through the Twinflow with an applied voltage of 300 V for 30 minutes. Samples were taken from the exit ports and analyzed by CIEF using the iCE 280. The aliquots were diluted four-fold in a 5% (v/v) solution of UV-transparent carrier ampholytes (pH 3-10 Pharmalyte). Added to each sample were the following pI markers to calibrate the pH gradient: meta-aminobenzoic acid, pI 3.9, dansyl- $\gamma$ -aminobutyric acid, pI 4.4, 4-(4-aminophenyl)butyric acid, pI 5.3, labetalol, pI 8.3, dopamine, pI 9.8, tyramine, pI 10.0.

### 5.1.3.3 Results and discussion

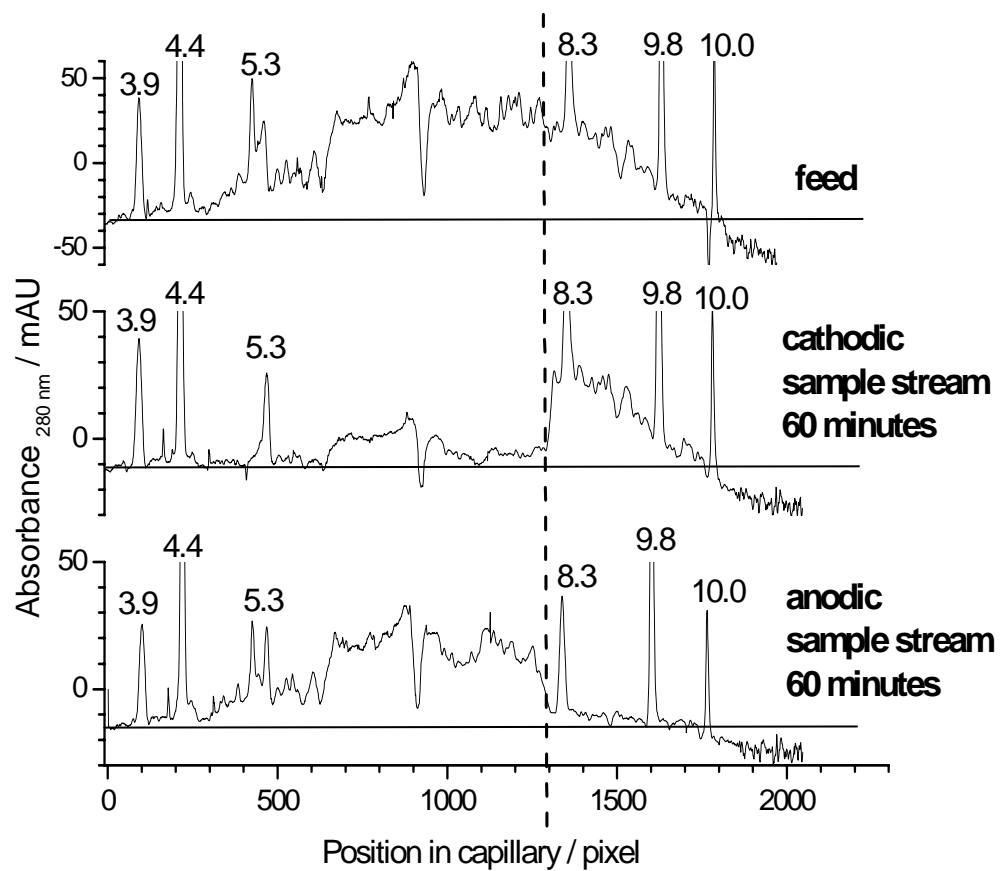
The top panel of Figure 27 shows the iCE280 electropherogram of a sample containing the pH 3-10 Pharmalyte (UV-transparent) and the six pI markers. The bottom panel contains the Pharmalyte and pI markers too, but it also contains the unfractionated UV-absorbing carrier ampholytes. The UV-absorbing Pharmalytes create a rise of approximately 50 mAU higher in the baseline compared to the baseline in the top panel. Using the pI markers to calibrate the pH gradient, the pI range of the derivatized carrier ampholytes was estimated to be  $6 < \text{pI} < 9$ .



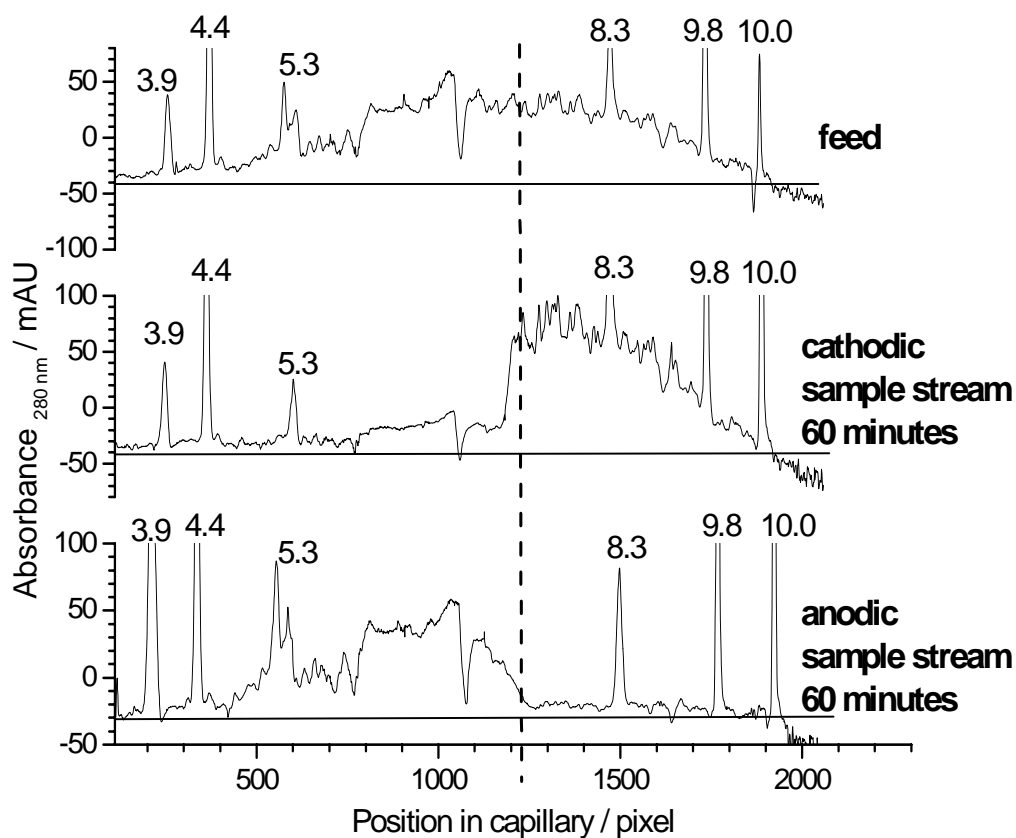
**Figure 27.** CIEF analysis comparing UV-transparent Pharmalytes to UV-absorbing Pharmalytes. Six pI markers are used to calibrate the pH gradient in the capillary.



Figure 28 shows the iCE280 electropherograms for the testing of the pH 8.0 separation membrane. The top panel is the starting sample (unfractionated UV-absorbing carrier ampholytes), the middle and bottom panels show the samples taken after 60 minutes of IET, from the cathodic and anodic sample compartments, respectively. A step change in absorbance is observed in both the middle and bottom electropherograms. The pixel number where the step occurs corresponds to a particular pI value (calculated with the help of the calibrating pI markers), and represents the operational pH value of the buffering membrane. In this example, the experimental pH value of 8.0 was the same as the nominal pH value of the membrane. The electropherograms for the second membrane tested are displayed in Figure 29. The measured membrane pH value was 7.6, compared to the nominal value of 7.0 that was calculated at the time of membrane manufacture.



**Figure 28.** CIEF analysis for the testing of the pH 8.0 separation membrane. The dotted line represents the experimental value for the operating pH value of the separation membrane (corresponding to pH 8.0).



**Figure 29.** CIEF analysis for the testing of the pH 7.0 separation membrane. The dotted line represents the experimental value for the operating pH value of the separation membrane (corresponding to pH 7.6).

This procedure demonstrates how the Twinflow can be used to fractionate carrier ampholytes, and shows how it could be used to characterize the operational pH value of a buffering membrane during actual IET operation. Using this method it was found that the nominal pH value calculated for a buffering membrane was not necessarily the same as the operational pH value. The accuracy of this procedure depends heavily on the CIEF analysis. Similarly, accurate CIEF analysis relies on the availability of a wide range of pI

markers with well characterized pI values, so that the pH gradient can be precisely calibrated across the capillary, even if it is non-linear in some regions. In addition, to make this method useful for all membranes, a wider range of UV-absorbing carrier ampholytes needs to be manufactured to cover the regions on the pH gradient below pH 6 and above pH 9. Being able to measure the operating pH value in a membrane is very important for planning a successful IET experiment, and could be used as a quality control method for the membranes.

#### 5.1.4 Concluding remarks

Several applications of classical IET using the Twinflow were explored, including the use of hydro-organic media to increase the solubility of hydrophobic organic ampholytes, the use of a neutral chiral resolving agent to separate ampholytic enantiomers, and finally, the separation of carrier ampholytes. The instrumental improvements in the Twinflow design have allowed for faster and more efficient classical IET separations compared to other IET instruments.

## **5.2 pH-biased isoelectric trapping separations on the Twinflow**

### 5.2.1 Purification of a UV-absorbing pI marker

#### 5.2.1.1 Background and objective

As discussed in Section 5.1.3, pI markers are needed for the calibration of pH gradients in IEF-based techniques. Currently, there is an insufficient number of pI markers in the mid pI range. To increase the range of markers available in this region, new isoelectric,

UV-absorbing molecules have been synthesized by derivatizing natural amino acids with a strongly UV-absorbing chromophore. Typically, such reactions yield a mixture of products, both ampholytic and non-ampholytic. These side products often have similar physical and chemical properties to each other and to the target, making purification of the target difficult. IET, however, is well suited to such separations. To demonstrate the utility of pH-biased IET for small molecule separations, the Twinflow has been used to purify and concentrate a single component from a complex reaction mixture.

#### 5.2.1.2 Instrument set-up, materials, and method

The reaction mixture was analyzed on the iCE280 instrument to characterize the complexity of the sample and the pI range of the components (Figure 30). The target in this case is the single peak at pixel number 730, just on the acidic side of the major contaminants. After calibrating the pH gradient, the target was found to have an estimated pI value of 5.3. To purify this component with a binary separation on the Twinflow, a separation membrane with a pH 6.1 was used. The anodic membrane had a pH of 3.0, and the cathodic membrane a pH of 11.0. The feed consisted of the reaction mixture with 10 mM lysine as the basic pH biase. 60 ml of this solution was added to the cathodic sample reservoir. The anodic sample reservoir contained 20 ml of 5 mM glutamic acid, acting as an acidic pH biase. While the Twinflow was operated in recirculating mode, the power supply delivered a constant current of 150 mA for 60 minutes. Aliquots taken from the sample compartment exit ports were analyzed by CIEF on the iCE280 unit.

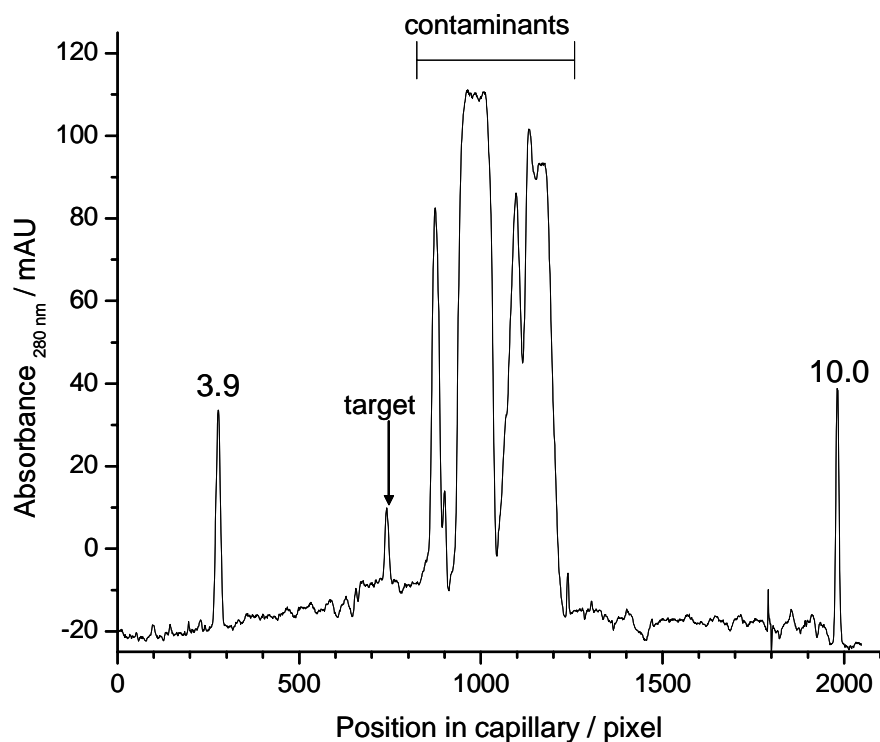


**Figure 30.** CIEF analysis of the reaction mixture used in the synthesis of UV-absorbing pI markers.

### 5.2.1.3 Results and discussion

The target in this example was the most acidic component in the reaction mixture.

Binary separations on the Twinflow are capable of purifying either the most acidic or most basic component from a mixture of ampholytes in a single step. The top panel in Figure 31 is the electropherogram of the starting feed mixture that was filled into the cathodic separation compartment. The middle and bottom panels show the composition of the solution in the sample compartments after 30 minutes of electrophoresis. Clearly,

the target has been moved completely into the anodic sample stream, leaving all the higher pI value contaminants in the cathodic sample stream. In addition, the peak area of the target in the anodic sample stream (the product stream) is approximately three times higher than the target peak area in the original feed solution. This concentration factor was achieved by having 60 ml in the anodic feed stream, but only 20 ml in the cathodic collection stream.

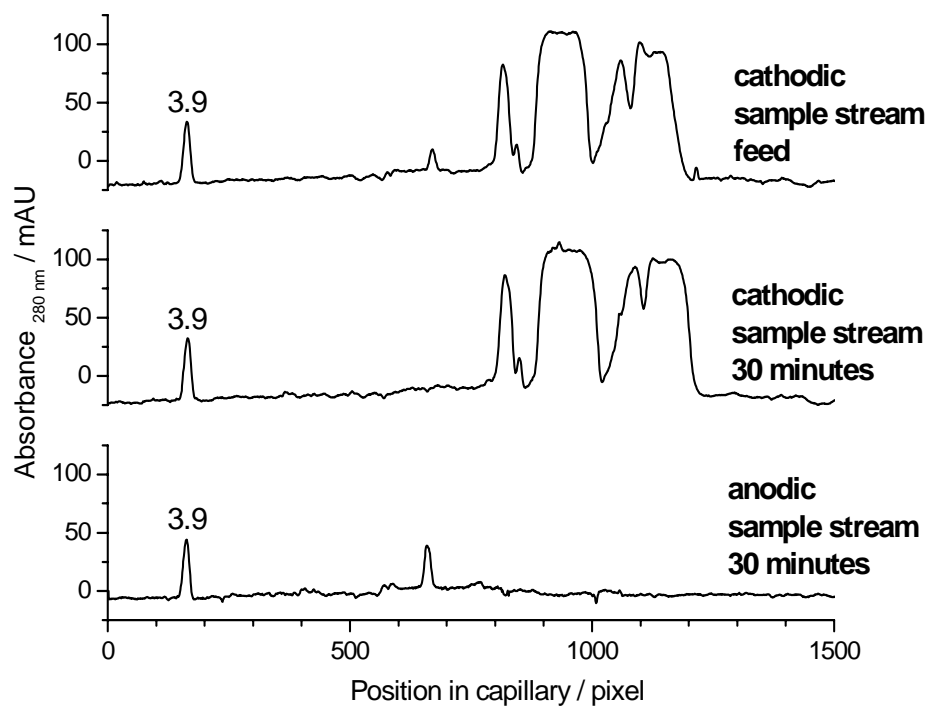


**Figure 31.** CIEF analysis of the purification of a pI marker from the raw reaction mixture. After 30 minutes, the target has been completely transferred to the anodic sample stream.

### 5.2.2 Concluding remarks

The purification of a UV-absorbing small ampholytic molecule has been successfully carried out on the Twinflow using pH biased IET. The addition of the pH biaser to the solutions in the anodic and cathodic separation compartments maintains the ampholytic components in a highly charged state, thus maintaining a high electrophoretic velocity throughout the separation. If it was desired to have the target in its pure isoelectric state, a second binary Twinflow separation, operated in classical, non-pH biased mode, could easily be performed to remove the target from the acidic pH biaser.

## **5.3 pH-biased isoelectric trapping separations on the Biflow**

### 5.3.1 Separation of UV-absorbing pI markers

#### 5.3.1.1 Background and objective

The utility of the binary Twinflow separation is limited when a mixture contains a target, together with contaminants with pI values both above and below the target pI. The separation is still possible on the Twinflow, but it would require processing of the solution twice, with two different membrane configurations. To obtain a purified product from this type of mixture, in a single step, the Biflow can be used. To demonstrate the effectiveness of the Biflow, a model separation of three UV-absorbing pI markers was performed.



### 5.3.1.2 Instrument set-up, materials, and method

The three ampholytes for the sample were *meta*-aminobenzoic acid (MABA, pI 3.9), carnosine (CAR, pI 8.2), and tyramine (TYRA, pI 10). The aim of the separation was to separate CAR, the mid pI component, from the other two. The cathodic sample compartment of the first unit was designated the sample feed stream. The anodic sample compartments of the first and second, made up the transfer stream. The cathodic sample compartment in the second unit formed the product collection stream. The anodic buffering membranes for both units had a pH of 2.0, and the cathodic buffering membranes for each unit had a pH of 11.0. The first unit's separation membrane had a pH of 8.4, and the second unit's separation membrane had a pH of 6.5. The setup of the two units, showing all the membrane pH values, is displayed in Figure 32. The feed stream contained 5 mM lysine (LYS), which was the basic pH biaser, together with 3 mM of each pI marker. The transfer loop stream had 5 mM of the acidic pH biaser, glutamic acid (GLU), and the product stream contained 5 mM of the basic biaser, LYS. The anolyte and catholyte solutions for both units were 30 mM MSA and 100 mM NaOH, respectively. Two separate power supplies delivered constant current of 100 mA to each separation unit. Sample aliquots were taken from all three sample streams and analyzed by capillary electrophoresis (CE) at 214 nm.

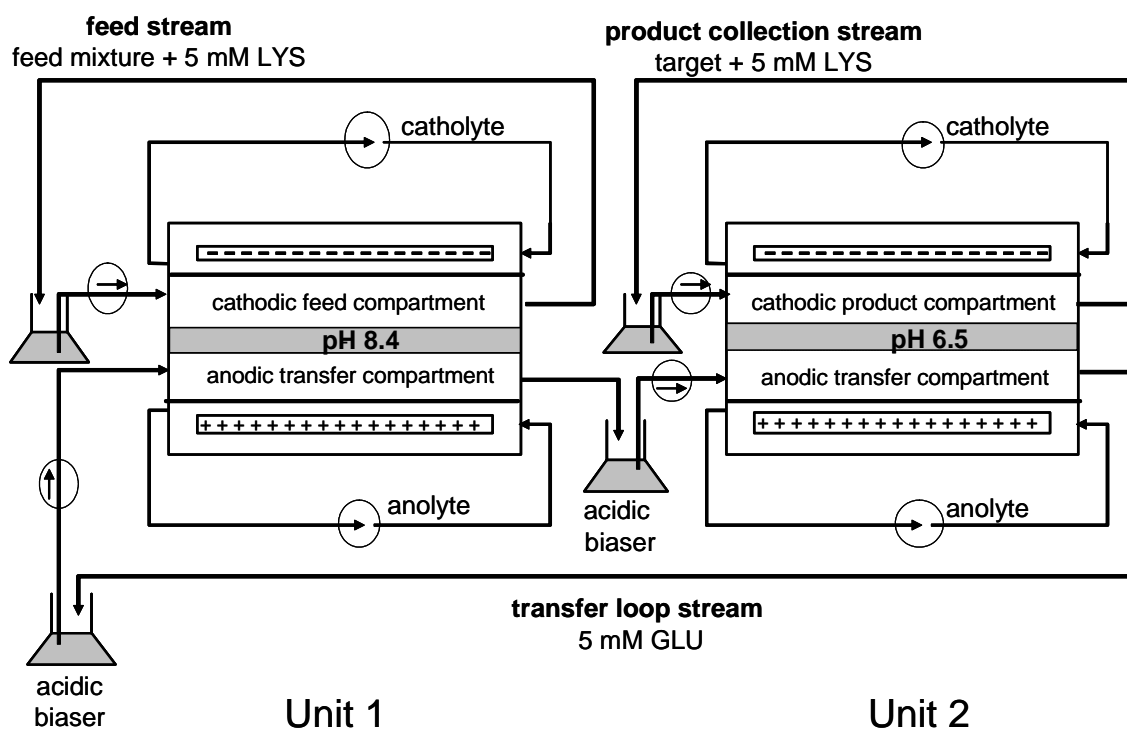


**Figure 32.** Schematic of the Biflow set-up for the separation of three UV-absorbing pI markers.

### 5.3.1.3 Results and discussion

The CE analysis of the samples taken from the Biflow over 45 minutes are displayed in Figure 33. The top panel shows the time-course of the samples taken from the feed stream. The highest pI marker, TYRA, remained trapped in the feed over the 45 minutes. The two lowest pI markers, MABA and CAR, were removed from the feed, through the pH 8.4 separation membrane, and into the transfer stream. MABA stays trapped in the transfer stream, while CAR, which has a pI value above the pH of the separation membrane in the second unit, was constantly depleted from the transfer loop stream and moved into the product collection stream (Figure 33, middle panel). The bottom panel in

Figure 33 shows the steady increase in the concentration of CAR as the separation progresses. At the end of the 45 minutes, the feed stream contains only TYRA, the transfer stream contains only MABA, and the product stream contains only CAR.

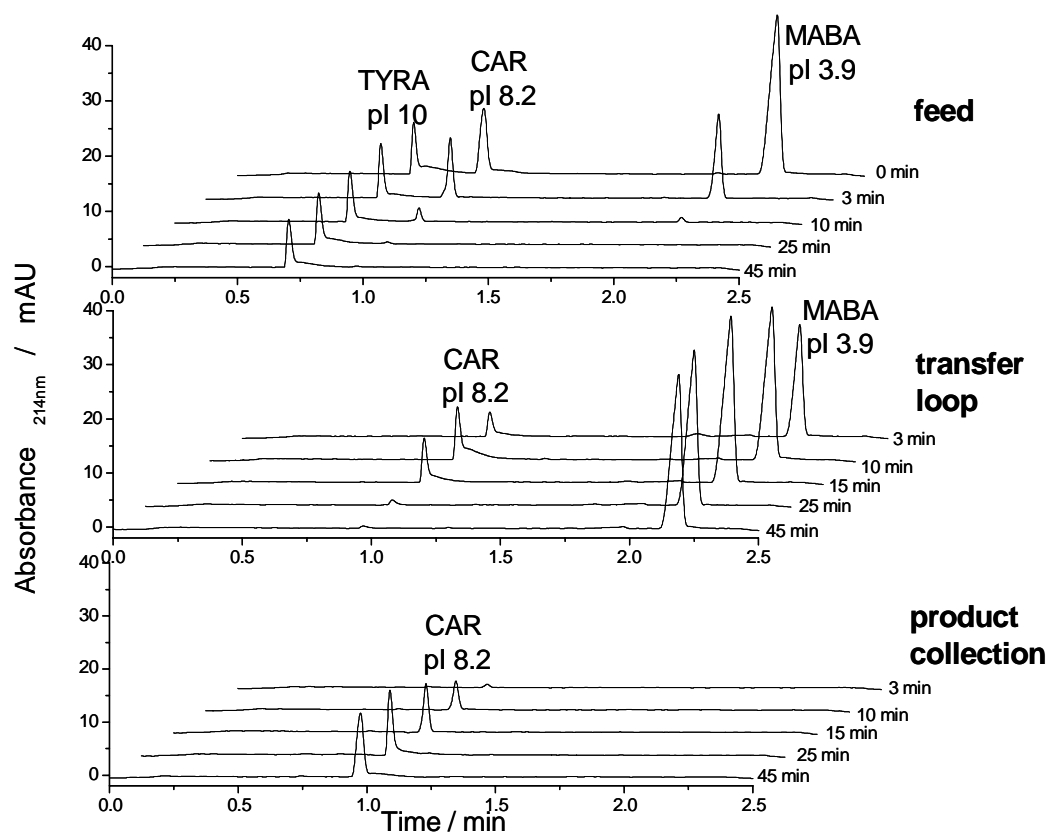


**Figure 33.** CE of the sample streams during pH-biased IET of three UV-absorbing pI markers on the Biflow.

### 5.3.2 Concluding remarks

Using the Biflow in pH-biased mode, the separation of three pI markers has been accomplished. In this particular example, the marker with the middle pI value (CAR)

was designated as the target and remained trapped in the product stream at the end of the separation. Similar separations on the Twinflow unit would require two successive separate operations. Once the Biflow is assembled, three individual fractions can be obtained in a single step without operator intervention.

## 6. PROTEIN SEPARATIONS BY ISOELECTRIC TRAPPING

### 6.1 Classical isoelectric trapping separations on the Twinflow

#### 6.1.1 Binary separations of chicken egg white proteins

##### 6.1.1.1 Background and objective

The high resolution separations achievable using IET technology are especially attractive for obtaining purified fractions of proteins. Chicken egg white is a complex sample containing proteins with a wide range of pI values, molecular masses, and concentrations. This sample was used to evaluate classical binary IET separations on the Twinflow. The most abundant protein in egg white is ovalbumin, making up about 60 % (m/m) of the total protein content [75]. The major isoform of ovalbumin is diphosphorylated, it has a relative molecular mass of approximately 45 000, and an approximate pI value of 4.8 [76]. There are also monophosphorylated (pI ~ 4.9) and unphosphorylated (pI ~ 5.0) forms of ovalbumin [76]. The second most abundant protein in egg white is ovotransferrin, with a relative molecular mass of 77 000 and pI value of 6.6 [77]. Two binary Twinflow separations were performed to fractionate the major ovalbumin isoforms from chicken egg white.

##### 6.1.1.2 Instrument set-up, materials, and method

The separation membrane for the first step had a pH of 4.9. The anodic and cathodic membranes had pH values of 3.0 and 7.0. The anolyte was 50 mM phosphoric acid, and the catholyte was 10 mM sodium hydroxide. 2 ml of chicken egg white was mixed with

48 ml of deionized water, and then filtered through a glass fiber filter membrane. 25 ml of the diluted egg white was added to both the anodic and cathodic sample reservoirs, and pumped through the separation unit at a flow rate of 20 ml/min using the pass-by-pass mode of operation. In the second part of this experiment, the separation membrane was changed to a pH 4.6 membrane, and the same anodic and cathodic membranes were used again. The proteins collected in the anodic sample stream after the first IET separation were run through the new set up in the recirculating mode. In both experiments, a constant potential of 250 V was used. Samples were taken at the end of each pass, and the protein composition was analyzed by CIEF using the iCE280 instrument.

#### 6.1.1.3 Results and discussion

The electropherogram of the unfractionated egg white sample, analyzed by CIEF, is displayed in the top panel of Figure 34. Each sample analyzed by the iCE280 contained two pI markers, dansyl-phenylalanine (DnsPhe, pI 3.5) and terbutaline (TERB, pI 9.6), which were used to calibrate the pH gradient. The major ovalbumin isoform (pI 4.8) is at pixel number 490, while ovotransferrin (pI 6.6) is at pixel number 1050. In addition, several minor proteins are seen in the region between ovalbumin and ovotransferrin. Based on their apparent pI values, these are likely to be ovoglobulins [76]. The electropherogram in the bottom panel of Figure 34 shows the protein composition of the aliquots taken from both sample reservoirs after one pass. All of ovotransferrin has moved from the anodic sample stream into the cathodic sample stream in a single pass,

the ovalbumin remains evenly split between the two sample streams. By the 11<sup>th</sup> pass (Figure 35 top panel), ovalbumin has clearly accumulated in the anodic sample stream, while ovotransferrin remains trapped in the cathodic sample stream. The bottom panel in Figure 35 shows that the separation has been completed after 17 passes. All the proteins with pI values less than pH 4.9 (the pH of the separation membrane) are collected in the anodic sample reservoir, while all those with higher pI values are collected in the cathodic sample reservoir. The anodic sample stream collected at the end of the first separation contained the ovalbumin isoforms, plus some even lower pI proteins (based on their pI value they were tentatively identified as ovomucoids [76]). A second IET separation was performed on this sample to remove the ovalbumin isoforms from the lower pI proteins, using a separation membrane with a pH value of 4.6. After 15 minutes of electrophoresis, the proteins with pI values above pH 4.6 have moved into the cathodic sample stream, including the major ovalbumin isoforms (Figure 36). By performing two binary IET separations, a narrow pI fraction of proteins was separated from the original egg white protein mixture.

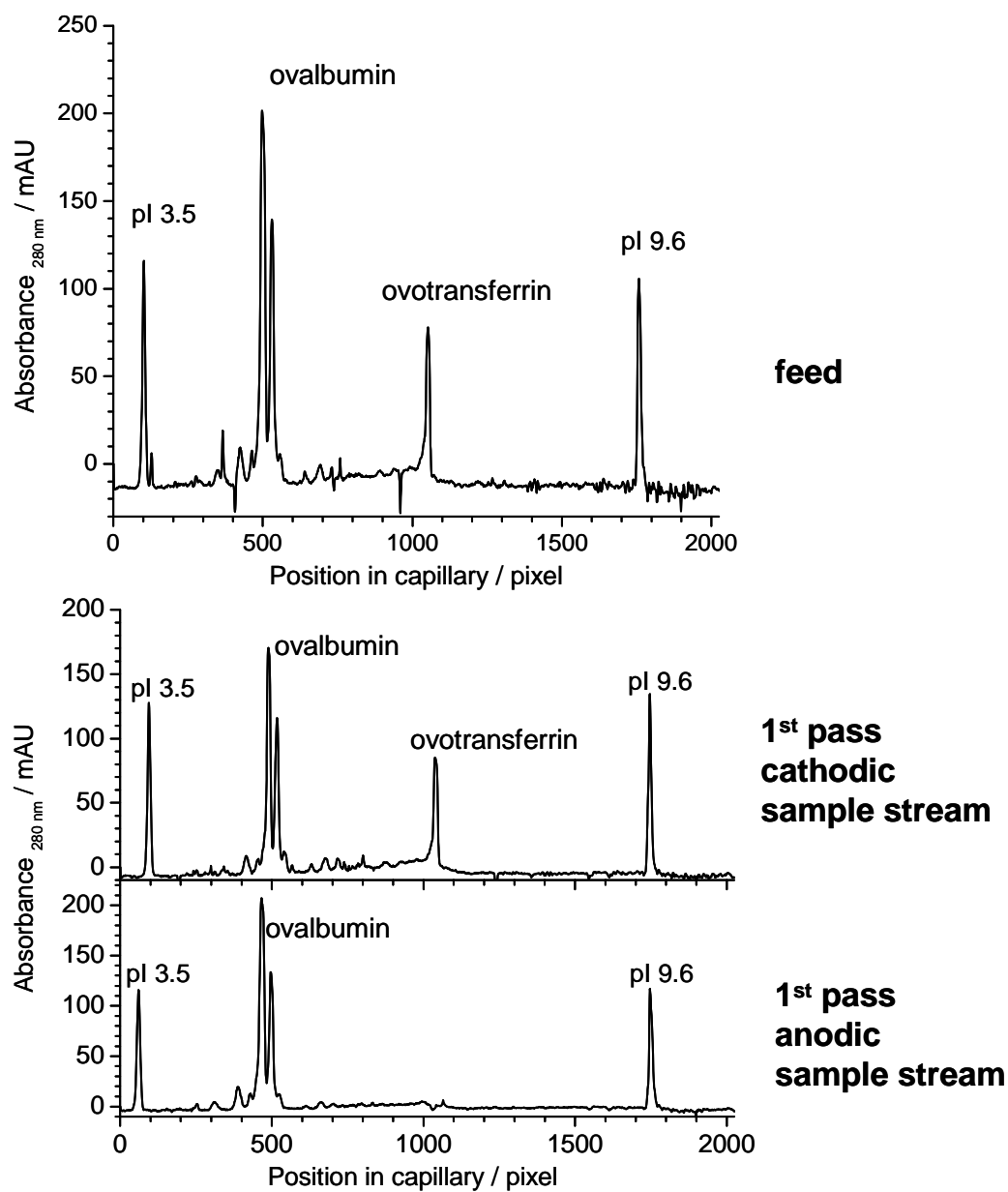


**Figure 34.** CIEF analysis of the egg white sample feed before separation (top panel) and after one pass through the separation compartments of the Twinflow during classical IET (bottom panel).



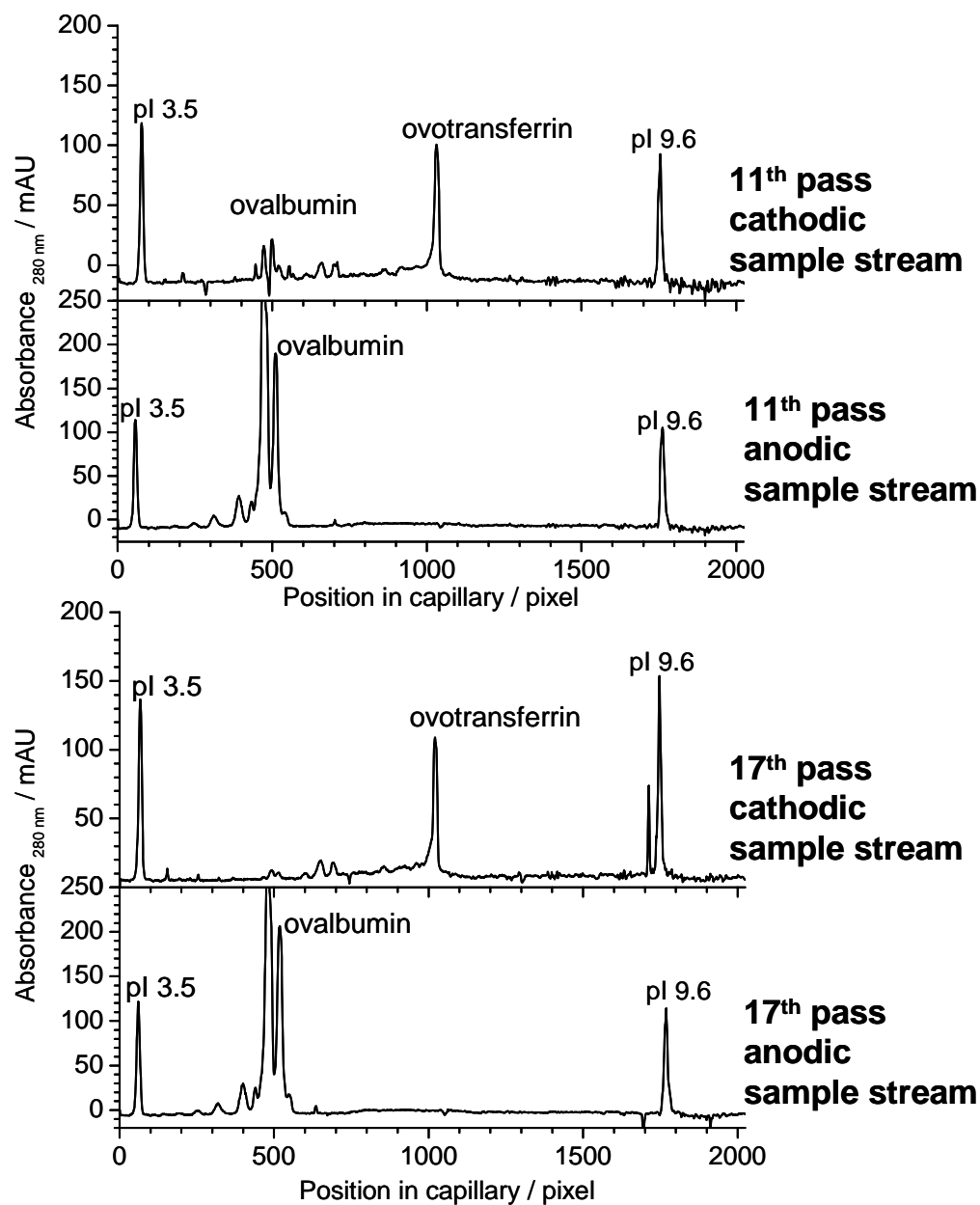


**Figure 35.** CIEF analysis of the egg white sample after 11 passes (top panel) and after 17 passes (bottom panel) through the separation compartments of the Twinflow during classical IET.

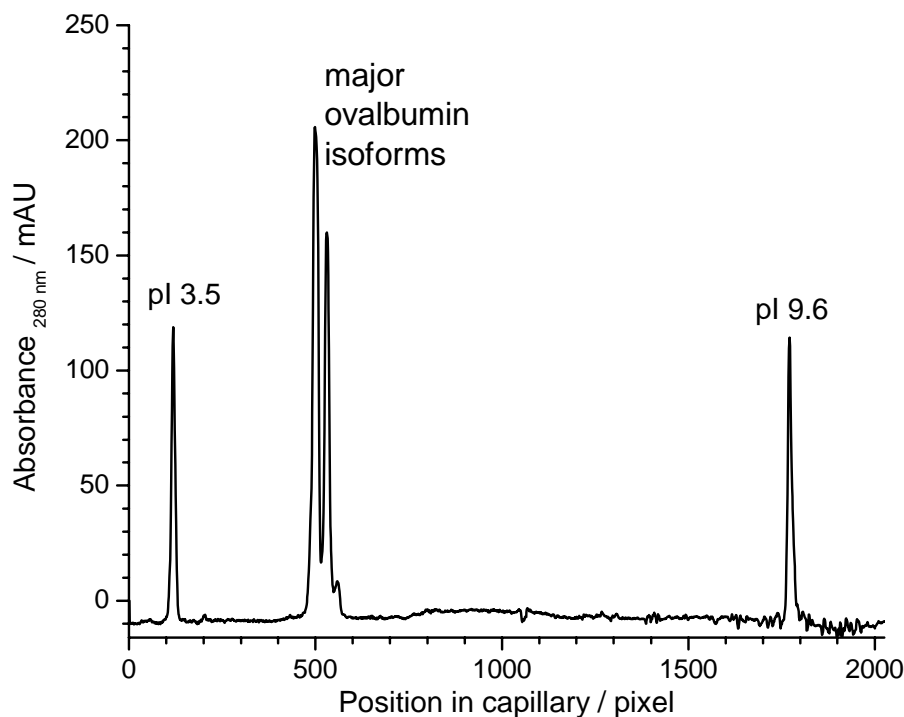


**Figure 36.** CIEF analysis of the major albumin isoforms isolated after two binary Twinflow separations using classical IET.

### 6.1.2 Concluding remarks

The Twinflow was successfully tested using the classical IET mode. The Twinflow, which boasts short electrophoretic distances and is capable of generating high field strengths (in this case, 500 V/cm), performed fast binary separations of the egg white proteins. In 17 passes through the Twinflow separation unit, approximately 120 mg of chicken egg white protein was separated, which is equivalent to a processing rate of about 300 mg protein / hour.

## **6.2 pH-biased isoelectric trapping separations on the Twinflow**

### 6.2.1 A method to find the optimum pH-biaser concentration

#### 6.2.1.1 Background and objective

In Section 3.1, the principle of pH-biased IET was introduced. The auxiliary isoelectric agent (the pH biaser) added to the sample is trapped between the buffering membranes, along with the proteins. The sample pH is controlled by the pH biaser, in a way that keeps the proteins in a charged state, maintaining their high electrophoretic velocity and reducing the risk of isoelectric precipitation. These additional isoelectric species will carry part of the IET current during a separation. This, in turn, would reduce the transference number for the target proteins, and increase the amount of energy required for the separation.

Thus, the real question becomes, what is the minimum concentration of the pH-biaser that is sufficient to effectively maintain this pH (the “pH bias”), but does not carry significant amounts of charge through the separation compartment. To investigate this question, binary separations of chicken egg white were performed in the absence and presence of varying concentrations of a pH biaser. Specifically, the transfer rate of ovalbumin from one separation compartment to the other was calculated to evaluate the effects of pH biaser on the separation. Before performing this experiment, a first order approximation of how pH affects the charge on the protein was obtained with the help of the Doctor pH program [36] and the charge vs. pH curve for ovalbumin (see Section 3.1). A convenient ovalbumin concentration in the feed solution is typically about 1

mg/mL, corresponding to approximately 22  $\mu\text{M}$ . The biaser in the feed stream for this experiment was carnosine (CAR) which has a pI of 8.2 ( $\text{pK}_{\text{a},1} = 2.51$ ,  $\text{pK}_{\text{a},2} = 6.76$  and  $\text{pK}_{\text{a},3} = 9.35$ ). Using the Doctor pH program [36], the pH values were calculated for 22  $\mu\text{M}$  solutions of ovalbumin, that contained increasingly higher concentrations of CAR. The results are: 0.5 mM, pH = 6.67; 1 mM, pH = 7.12; 2 mM, pH = 7.46; 5 mM, pH = 7.78; and 15 mM CAR, pH = 7.99. As the pH increases, the number of charges on ovalbumin increases (Figure 37). Thus, this approximation suggested that even a CAR concentration as low as 0.5 mM should significantly increase ovalbumin's net charge.

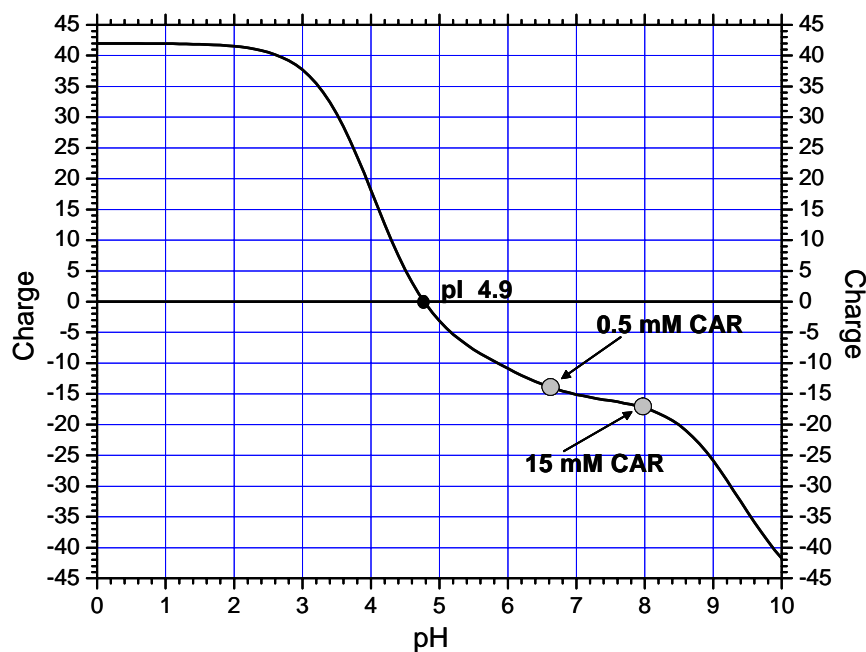


**Figure 37.** Plot showing how pH changes affect the net charge on a hypothetical protein with the same amino acid residues as ovalbumin. The pH obtained with 22  $\mu\text{M}$  ovalbumin and the lowest (0.5 mM) and highest (15 mM) CAR concentrations are labeled on the curve.

### 6.2.1.2 Instrument set-up, materials, and method

To test the first order approximation calculated in Section 6.2.1.1, six solutions of 1 mg/ml egg white were prepared with increasing concentrations of CAR (0 mM, 0.5 mM, 1 mM, 2 mM, 5 mM, 15 mM). Each 1 mg/ml egg white solution contained approximately 24 mg of ovalbumin; this was filtered, and filled into the reservoir connected to the cathodic separation compartment. The initial solution in the anodic separation compartment contained glutamic acid; its concentration was always equal to the concentration of CAR in the cathodic separation compartment. In addition, to investigate the scalability of these separations, an experiment was performed in which the egg white concentration was increased fourfold, and again the transfer rate of ovalbumin was monitored.

Lastly, to see if the separation could be improved by manipulating where the majority of the electric field dropped, the concentration of the acidic pH biaser (glutamic acid) in the anodic separation compartment was increased to 20 mM, and the biaser concentration in the cathodic separation compartment was kept at 2 mM CAR. By dropping more potential across the feed compartment, the transfer of the target protein ought to be faster.

For all the experiments, the anolyte was a mixture of 15 mM iminodiacetic acid and 15 mM aspartic acid, the catholyte was a mixture of 15 mM lysine and 15 mM arginine. The anodic isoelectric membrane had a pH of 3.0, the separation membrane a pH of 6.2,

and the cathodic membrane a pH of 9.0. The Twinflow was run in the pass-by-pass mode, and sample stream aliquots were taken at the end of each pass. The samples were analyzed by CIEF using the iCE280.

#### 6.2.1.3 Results and discussion

The aim of the separation was to move ovalbumin, and other proteins with pI values in the range of  $3.0 < \text{pI} < 6.2$ , through the separation membrane and trap them in the anodic separation compartment. The proteins (including ovotransferrin) with pI values higher than 6.2 (the pH of the separation membrane) will remain in the cathodic separation compartment. Each of the six egg white solutions containing varying amounts of CAR, were run on the Twinflow using the same conditions. The separations were started with the power supply in constant current mode, at 90 mA. As the separation proceeded, the potential increased until it reached the 1000 V limit of the power supply. From then on, the power supply was operated in constant potential mode, at 1000 V. The current decreased and the potential remained constant at 1000 V, as the separation progressed further. The pH (top panel) and the conductivity (bottom panel) values of the aliquots collected after each pass are shown in Figure 38 as a function of the pass number for the 2 mM CAR-biased separation. As the separation progresses, both the conductivity and the pH values level off, indicating that transfer of ovalbumin and the other proteins with pI values below 6.2, is almost complete.

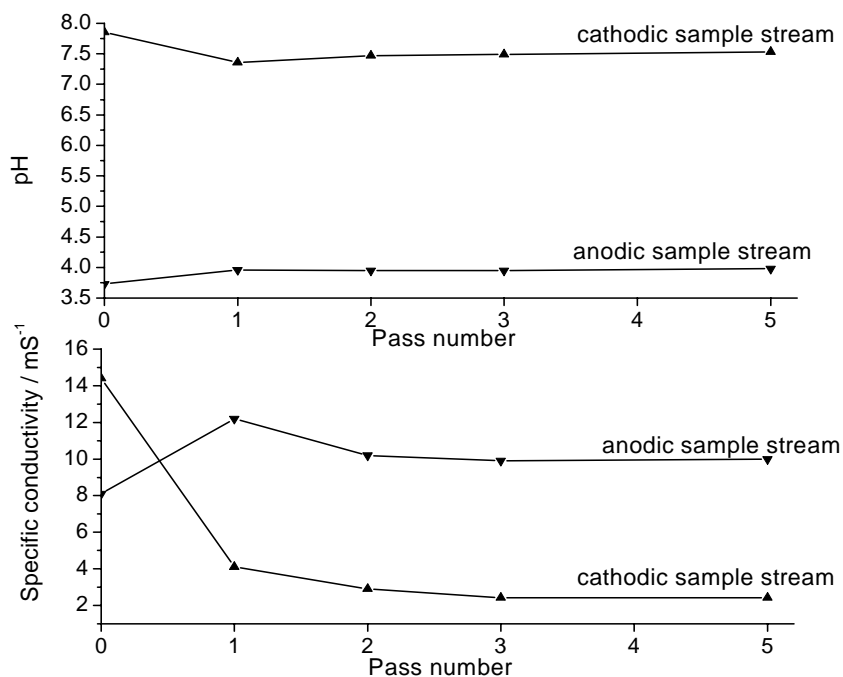


**Figure 38.** pH and conductivity changes in the anodic and cathodic sample streams during pH-biased IET experiment for determining the optimum biaser concentration.

Samples taken from the outlet of the cathodic and anodic separation compartments when 2 mM CAR was used as the pH-biaser in the feed, were analyzed by CIEF (Figure 39 and 40). In each figure, panel 1 shows the results for the feed stream, panel 2 for the 1<sup>st</sup> pass, panel 3 for the 3<sup>rd</sup> pass, while the bottom panel shows the results for the 5<sup>th</sup> pass. The horizontal axis represents the focusing positions (expressed in pixels) in the separation capillary of the iCE280 (50 mm corresponds to 2050 pixels). Dansyl- $\gamma$ -aminobutyric acid (DNS-GABA), with a pI of 4.4, is a pI marker and can be seen in each sample at around pixel 300. The largest peak around pixel 460 corresponds to ovalbumin (approximate pI 4.8). The second largest peak around pixel 960 corresponds to

ovotransferrin (approximate pI 6.6). The absorbance of the protein bands at 280 nm is recorded on the vertical axis. The bottom panel in Figure 39 shows that the ovalbumin is removed from the cathodic sample stream after 5 passes. Correspondingly, the bottom panel in Figure 40 indicates that after the 5<sup>th</sup> pass, ovalbumin was recovered in the anodic sample stream.

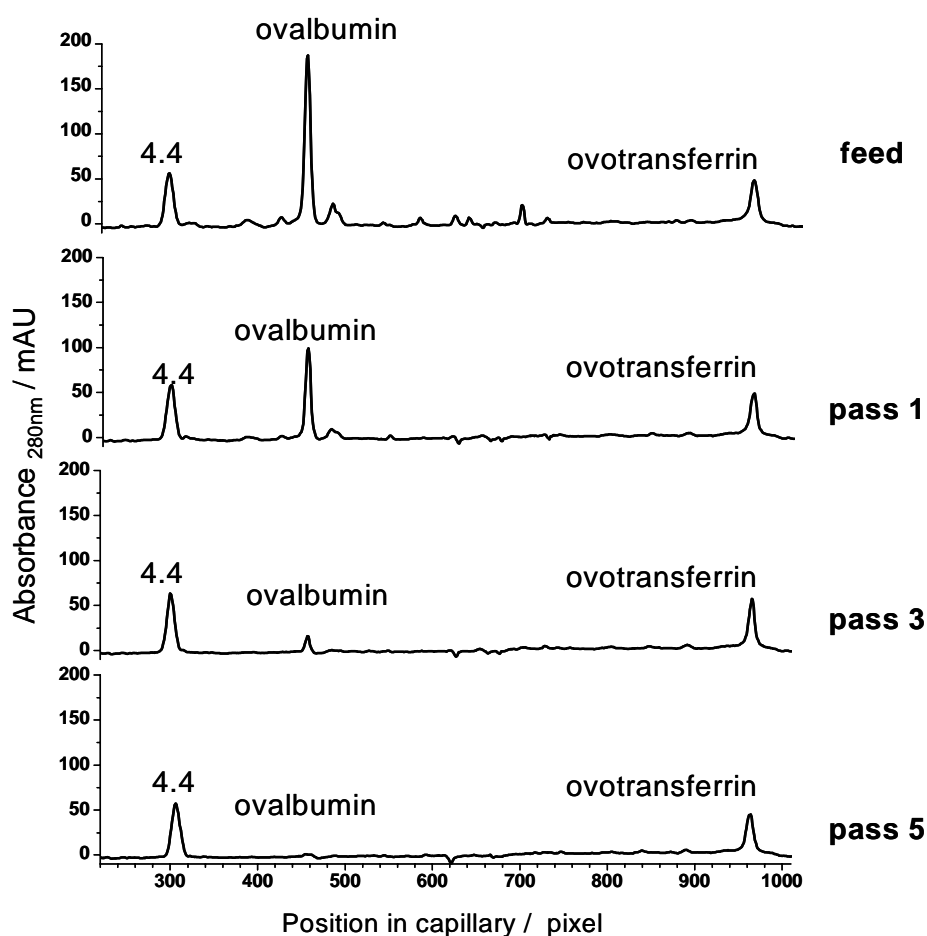


**Figure 39.** CIEF analysis of the cathodic sample stream over 5 passes showing the transfer of ovalbumin when 2 mM CAR is used as biaser.



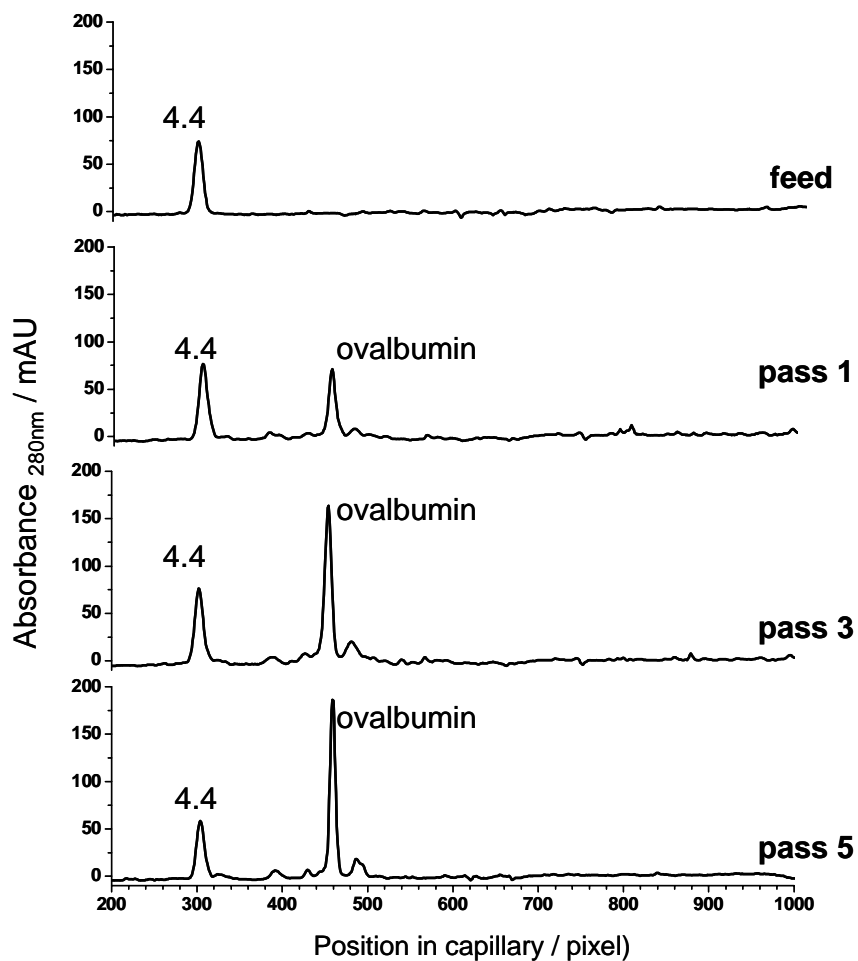


**Figure 40.** CIEF analysis of the anodic sample stream over 5 passes showing the recovery of ovalbumin when 2 mM CAR is used as biaser in the cathodic sample stream.

Table 3 shows the number of passes required for complete transfer of ovalbumin as a function of the concentration of the pH biaser. With no pH biaser, 15 passes are needed to move all ovalbumin (24 mg) from the solution reservoir of the cathodic separation compartment into the solution reservoir of the anodic separation compartment. By having a CAR concentration as low as 0.5 mM, the required number of passes is almost

halved. For the 1 mM, 2 mM and 5 mM CAR concentrations, the required separation time remains constant at 5 passes, then the required number of passes increases back to 15 for 15 mM CAR. The production rates (amount of ovalbumin moved per minute) are shown in the third column in Table 3: it varies from a low of 1.6 mg / min at 0 mM and 15 mM biaser concentrations to a high of 4.8 mg / min (288 mg / h) at a biaser concentration of 2 mM CAR. The last column in Table 3 shows the specific energy consumption required to complete the separation (Wh / mg ovalbumin). Even though the required number of passes is constant for the 1 mM, 2 mM and 5 mM biaser concentrations, energy consumption is at a minimum for the 2 mM CAR. This CAR concentration represents the best compromise between titrating ovalbumin to a sufficiently highly charged state (to increase its mobility and solubility) and reducing the transference number of ovalbumin (i.e., increasing the percentage of the electrophoretic current that CAR carries compared to ovalbumin).

**Table 3.** Summary of the results showing the dependence of the pass number, required to complete the transfer of 24 mg of ovalbumin, on the concentration of CAR. The specific energy consumption (Wh/mg) were calculated for each concentration of CAR.

CAR (mM)	Passes required	Production rate (mg ovalbumin/min)	Specific energy consumption (Wh/mg ovalbumin)
0	15	1.6	0.3
0.5	8	3	0.26
1	5	4.8	0.26
2	5	4.8	0.22
5	5	4.8	0.24
15	15	1.6	0.43

In the next set of experiments, the feed concentration of egg white was increased fourfold (total of 96 mg ovalbumin), while the biaser-to-ovalbumin concentration ratio was kept the same as for the best case in Table 3, 2 mM CAR. 18 passes were needed to move all 96 mg of ovalbumin, corresponding to a production rate of 5.3 mg ovalbumin / min (318 mg / h) and specific energy consumption of 0.15 Wh / mg ovalbumin. These figures of merit are very close to what were found for the best case at the 1 mg / ml egg white feed concentration indicating that the system behaved linearly under the conditions used.

Lastly, to see if an increased conductance in the anodic sample stream would allow for a higher transfer rate of ovalbumin out of the cathodic separation compartment, the

concentration of glutamic acid in the anodic sample stream was increased to 20 mM. The biaseer concentration in the cathodic separation compartment was kept at 2 mM CAR. In this way, the number of charge carriers in the anodic separation compartment increased, leading to higher solution conductivity, and less potential being used across this distance. After four passes the binary IET separation was complete, representing an increased production rate of 6 mg ovalbumin / min (360 mg / h) and a practically unchanged specific energy consumption of 0.226 Wh / mg ovalbumin. Thus, it appears that when the binary IET system is operated in an asymmetric feed mode (feed in the cathodic or anodic separation compartment, but not both), it is advantageous to use a high biaseer concentration in the receiving stream and an optimum biaseer concentration in the feed stream. The optimum concentration has to be sufficiently high to titrate the target proteins away from their isoelectric points, but low enough to minimize the reduction of their transference numbers.

In summary, a first approximation model of the charge vs. solution pH curve of a hypothetical protein resembling ovalbumin indicated that the addition of an isoelectric auxiliary agent (with a pI of 2 units or so removed from that of the target protein) to the protein mixture in relatively low concentrations (approximately 100 moles of isoelectric biaseer for each mole of target protein) should insure a sufficiently high electric charge on the target protein. If this is achieved, then the protein will maintain a relatively high electrophoretic velocity and have adequate solubility throughout the separation, while reducing the specific energy consumption required for the complete transfer.

## Concentration and fractionation of bovine serum proteins

### 6.2.1.4 Background and objective

The successful proteomic profiling of a protein mixture is achieved by isolating and identifying all the proteins present. The large dynamic range of protein concentration found in most biologically interesting samples means that the species with low abundance are often not identified. Serum is a particularly challenging sample, where two proteins can differ in abundance by as much as a factor of  $10^{10}$ . For example, the most abundant protein in serum is albumin, with a typical concentration of about 50 mg/ml, compared to one of the least abundant proteins, interleukin-6, with a typical concentration of a 5 pg/ml [78]. Another challenging aspect to serum is the presence of post-translational modifications, such as glycosylation or phosphorylation, which can occur on most proteins, further increasing the heterogeneity of the sample. To make a protein sample more manageable for proteomic research, prefractionation techniques are often used to reduce the sample complexity, before an attempt is made to separate and characterize the individual proteins. Some of the most successful pre-fractionation techniques have included IET separations [39, 50, 79, 80]. After pre-fractionation, the most popular method used to separate a protein population is two dimensional gel electrophoresis (2DGE), followed by protein identification using mass spectrometry. The first dimension in 2DGE is IEF (normally on an immobilized pH gradient strip, IPG), followed by the size-based separation using sodium dodecylsulfate-polyacrylamide gel electrophoresis (SDS-PAGE) in the second dimension. This approach has led to the discovery and characterization of many new proteins. The maximum number of protein

spots that can be detected on a typical 2D gel today, is almost 1000. However, estimates of the number of proteins that should be in serum (from calculations based on the genetic code and estimates based on the expected post-translational modifications) indicate that the number should be closer to 50,000 [78]. There are several possible strategies to increase the number of proteins identified. For example, resolution can be increased and the limit of detection can be decreased in the separation and identification steps, respectively. To help achieve this goal, pre-fractionation steps could be improved so that significant concentration factors can be achieved for the low abundance proteins.

One of the important benefits of the Twinflow, that lends itself to pre-fractionation, is its ability to concentrate a particular subset of proteins during a separation. In this Twinflow application, pH-biased isoelectric trapping was used to simultaneously fractionate and concentrate proteins from bovine serum with low ( $< 4.0$ ) and high ( $> 8.4$ ) pI values. In addition, the low pI fraction was sub-fractionated further, by repeating the binary IET separations.

#### 6.2.1.5 Instrument set-up, materials, and method

The bovine serum sample was prepared by diluting 150 ml of serum to a volume of 1.5 L with a solution of 30 mM histidine. Before the separation was started, the diluted serum was desalted using a single separation-compartment configuration, where the anodic membrane had a pH of 2 and the cathodic membrane had a pH of 11. The sample was desalted until its conductivity leveled off at about 100  $\mu\text{S}/\text{cm}$ , which required three

passes through the Twinflow with a constant current of 500 mA. The separation cartridge for the first fractionation step had an anodic membrane with a pH of 2.0, a separation membrane with a pH of 8.4, and a cathodic membrane with a pH of 11. The desalted sample was filled into the reservoir attached to the anodic separation compartment. The reservoir attached to the cathodic separation compartment was filled with 15 ml of a 10 mM lysine solution (the collection stream for the proteins with pI values higher than 8.4). For the second fractionation step, the pH 8.4 separation membrane was changed to a membrane that had a pH of 4.0. The 1.5 L diluted serum sample, collected from the anodic sample reservoir at the end of the first fractionation, was used as the feed in the cathodic separation compartment for the second fractionation step. The reservoir attached to the anodic sample compartment was filled with a 10 mM glutamic acid solution and was used as the collection stream for proteins with pI values below 4.0. The large feed volume, used for each of the two fractionation steps, was passed through the Twinflow in pass-by-pass mode at 20 ml/min, while the small volume collection stream was pumped through in recirculation mode. For all the Twinflow experiments described in this section, the anolyte was a 30mM methanesulfonic acid solution and the catholyte was a 100 mM sodium hydroxide solution. The protein compositions of the fractions were analyzed using a variety of techniques including, SDS-PAGE, polyacrylamide gel IEF, and two-dimensional gel electrophoresis (2DGE).

The low pI fraction from the last step was sub-fractionated by three successive pH-biased IET separations. 10 mM histidine was added to the low pI fraction, this solution was used as the feed in the cathodic separation compartment. 10 mM aspartic acid was used as the collection stream for the anodic separation compartment in each of the three sub-fractionation steps. The first fraction was obtained by using a separation membrane which had a pH value of 3.0. At the end of the separation, the sample in the anodic sample reservoir was removed, and replaced with a fresh solution of 10 mM aspartic acid. The feed sample in the cathodic sample reservoir was retained for use in the next step. The separation membrane was changed to one with a pH value of 3.5, and the separation was performed again. This process was repeated for the last fraction, using a separation membrane with a pH value of 3.9. In each of the three separations the anodic membrane had a pH of 2.0 and the cathodic membrane had a pH of 11.0. The sub-fractions were analyzed by reversed-phase HPLC.

#### 6.2.1.6 Results and discussion

The schematic of the Twinflow, set-up for the high pI fractionation step, is displayed in Figure 41. The aliquots taken from the sample streams were analyzed by SDS-PAGE, under non-reducing conditions and stained using Coomassie blue (Figure 42). Lane 1 shows the feed sample before any separation has occurred. The major proteins from serum can be identified from this lane, based on their relative molecular mass. The major band just below the 66 000 marker is albumin. The dark band just above the albumin is serum transferrin, with an approximate relative molecular mass of 70 000, and the band



at around 120 000, is polyclonal immunoglobulin G (IgG). The entire 1.5 L volume of feed was passed through the Twinflow four times, the samples taken at the end of each pass were loaded into lanes 2 -5. Corresponding samples were also taken from the collection stream, from the cathodic separation compartment, over the four passes and loaded into lanes 6 – 9. The last lane on the gel contains the relative molecular mass markers. The first 5 lanes appear very similar, suggesting that the feed protein composition was not visibly changing over the four passes. However, there was certainly protein moving from the anodic feed stream into the cathodic collection stream, because the intensity of the band at 120 000 is clearly increasing in lanes 6 – 9. The 120 000 molecular weight band in the collection stream most likely corresponds to high pI isoforms of polyclonal IgG.

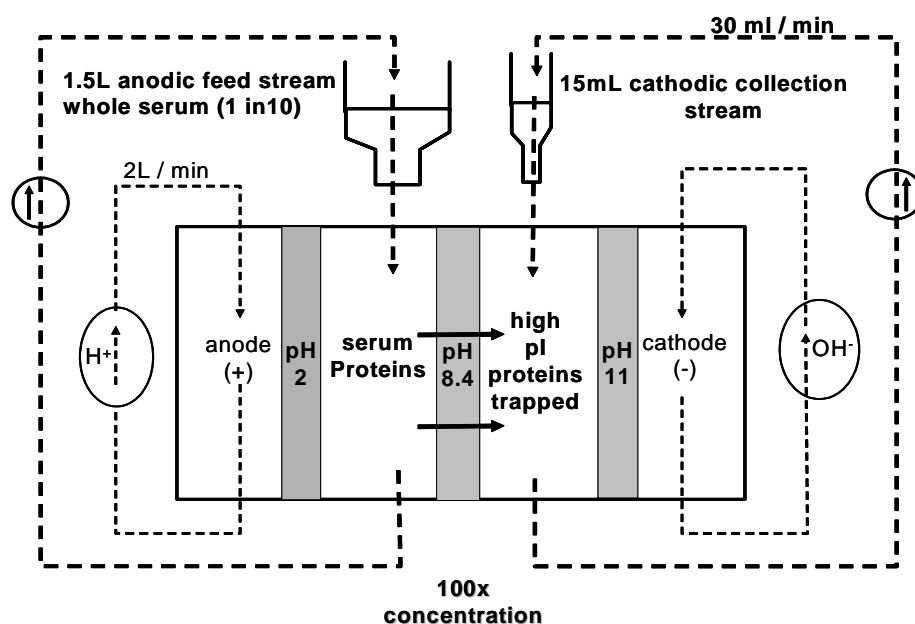


**Figure 41.** Schematic of the Twinflow set-up for fractionation of proteins in bovine serum with pI values higher than 8.4

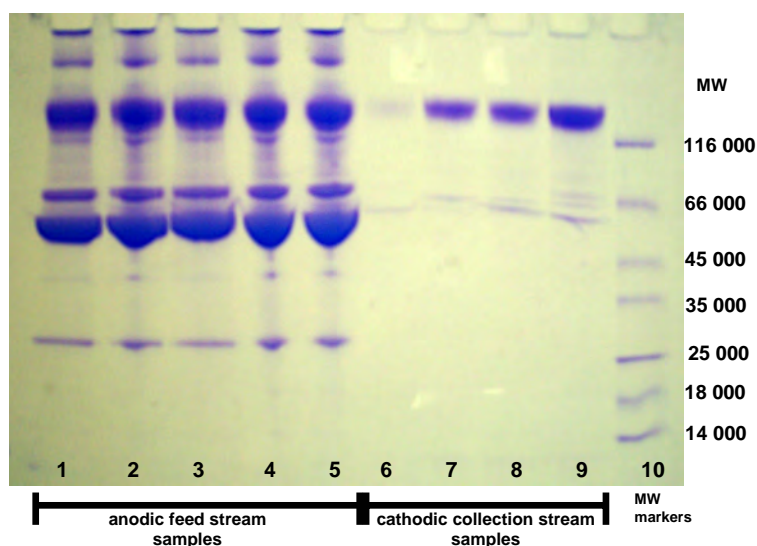


**Figure 42.** SDS-PAGE image of the samples analyzed from the anodic feed stream and the cathodic collection stream over passes 4 through the Twinflow during the high pI fractionation of bovine serum.

For the second fractionation step, the objective was to move the low pI proteins from the cathodic feed stream into the anodic collection stream (Twinflow set-up shown in Figure 43). The starting composition of the feed stream was analyzed by SDS-PAGE gel, and is shown in lane 1 of Figure 44. Lanes 2 – 5 contain the samples collected from the feed stream at the end of each pass. Again, very little change could be seen in the feed samples over the four passes. However, as the pass number increases, multiple bands can be seen in the collection streams (lanes 6 - 9). The major band in the collection stream is at approximately 40 000, and does not correspond to any of the visible proteins in the feed stream. This is a good visual example of the effects of the hundred-fold concentration factor that can be achieved with the Twinflow and demonstrates the power of pre-fractionation. The high abundance proteins in the 1.5 L volume of feed prevent

the use of a high enough protein load during analysis to see the low abundance proteins. In the 15 mL volume of the collection stream, free of the albumin, the low abundance proteins are more concentrated and are more readily detected.

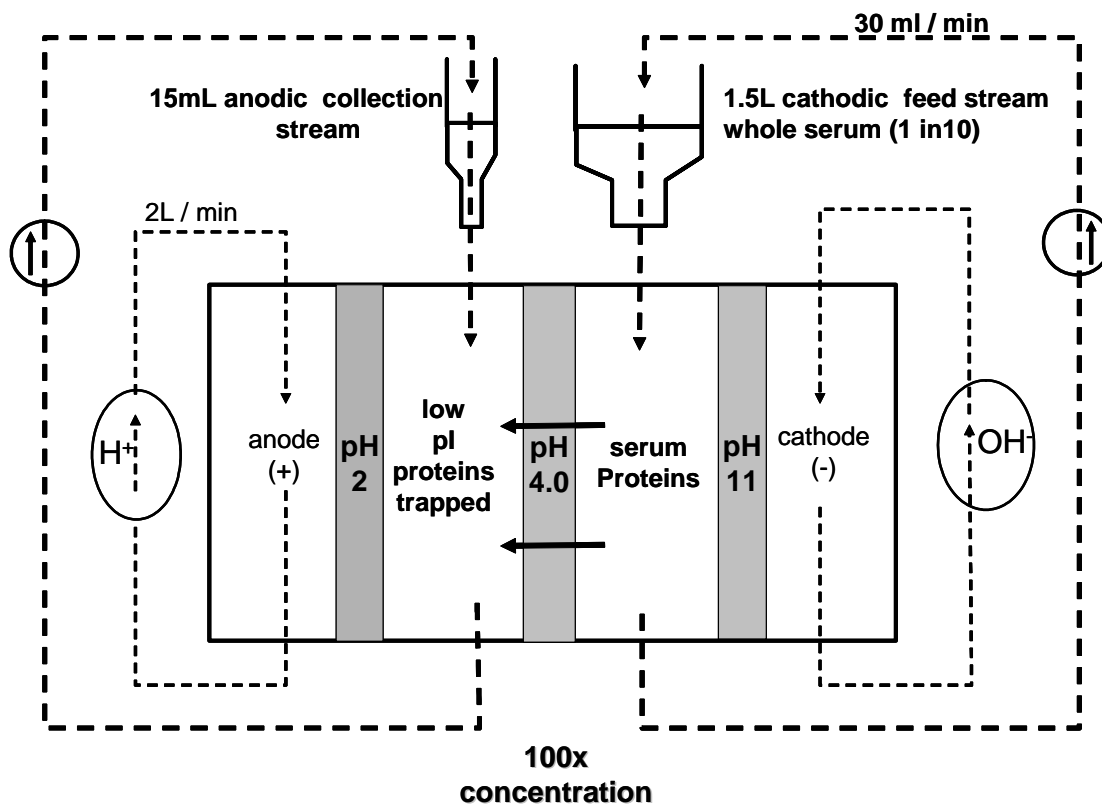


**Figure 43.** Schematic of the Twinflow set-up for fractionation of proteins in bovine serum with pI values lower than 4.0.

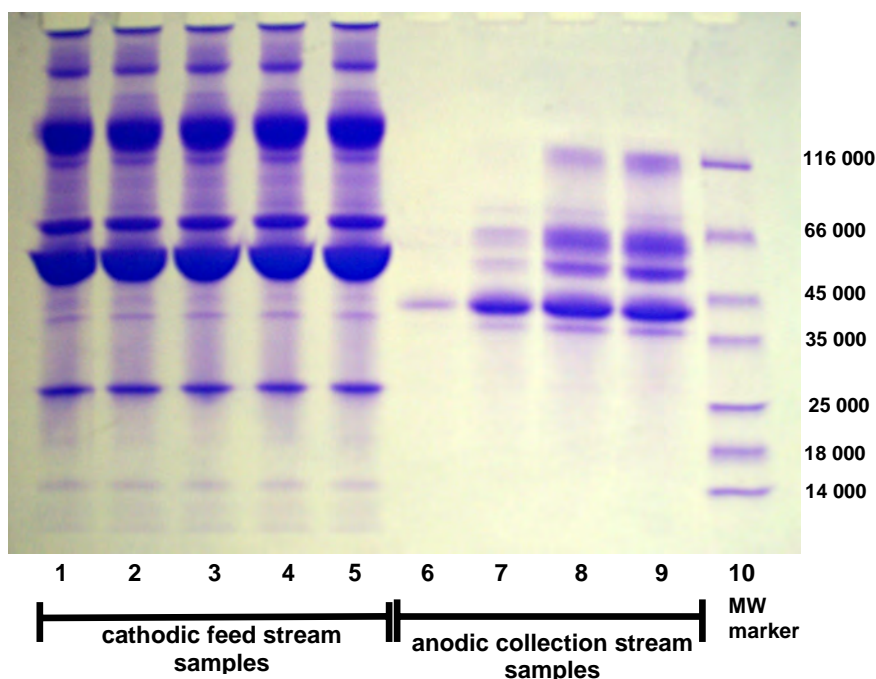


**Figure 44.** SDS-PAGE image of the samples analyzed from the cathodic feed stream and the anodic collection stream over passes 4 through the Twinflow during the low pI fractionation of bovine serum.

By performing these two separations the high pI fraction should contain proteins which have pI values in the  $8.4 < \text{pI} < 11.0$  range, and the low pI fraction should have proteins with pI values in the  $2.0 < \text{pI} < 4.0$  range. To confirm that the proteins in the high and low pI fractions actually did have high and low pI values, the fractions were analyzed on an IEF polyacrylamide gel (Novex, pH 3-10). Lane 4, in Figure 45, contains only pI markers, showing that the pH gradient in the IEF gel runs from high to low from the top to the bottom of the gel. Lane 1 contains an aliquot of the unfractionated serum, the stained streak along the length of the gel is the result of the wide distribution of the pI values for the proteins in serum. The darkest band at about pI 4.8, is albumin. The second lane contains the proteins from the low pI fraction and the third lane contains

proteins from the high pI fraction. Although the resolution and sensitivity in these gels are not very good, the gel does provide reasonable evidence that the pI cuts were accurate.

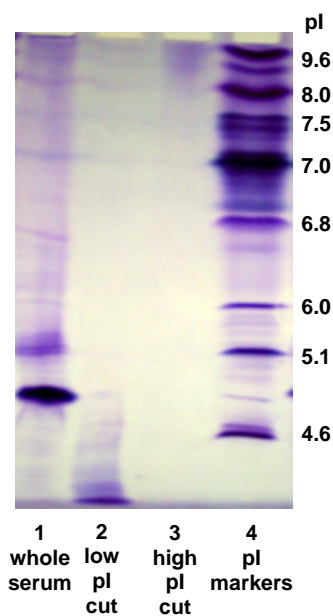


**Figure 45.** IEF gel image showing the low pI fraction (lane 2) and the high pI fraction (lane 3) from whole bovine serum (lane 1).

For further comparison, unfractionated bovine serum and the low pI fraction ( $2.0 > pI > 4.0$ ) were analyzed by two-dimensional gel electrophoresis (2DGE). 400  $\mu\text{g}$  of unfractionated serum protein was reduced and alkylated and then loaded onto an 11 cm, pH 3-10 IPG strip. After rehydrating the strip for 7 hours, it was focused for a total of 100 kVhrs. For the second dimension, the proteins on the strip were run off and separated according to size, on a 4-20% polyacrylamide gradient gel and stained using

Coomassie blue. The same protocol was used for the low pI fraction, but only 100  $\mu\text{g}$  of protein was used. Figure 46 shows a comparison of the two stained gel images: the top gel is for the unfractionated serum and the bottom gel is for the low pI fraction. Along the horizontal axis a grid has been made to estimate the pH gradient of the IPG strip. The relative molecular mass standards are on the left hand side of the gel. Therefore, from each coordinate on the gel, both pI value and relative molecular mass information can be obtained. This analysis shows the increased protein spot intensity for the proteins in the concentrated low pI fraction, compared to the fainter protein spots in the same region from the unfractionated sample. Notice that the low pI fraction appears to contain proteins with pI values all the way up to 4.8, even though the separation membrane had a pH of 4.0. The reason for this discrepancy is that the fraction was obtained on the Twinflow under native conditions (no detergents, reducing or alkylating agents were used). During sample preparation for the 2DGE, the proteins were denatured, reduced, and alkylated to decrease protein precipitation and protein artifacts (e.g., disulfide bond formation) during the separation. After this treatment, a protein would no longer be in its three-dimensional native conformation and thus, its apparent pI value can shift. In addition, some of the proteins in native conditions would almost certainly be present as protein complexes. Under denaturing conditions, these complexes would break apart into individual proteins, and could have different pI values compared to the whole complex. Nonetheless, this analysis clearly demonstrated the fractionation and concentration abilities of the Twinflow.

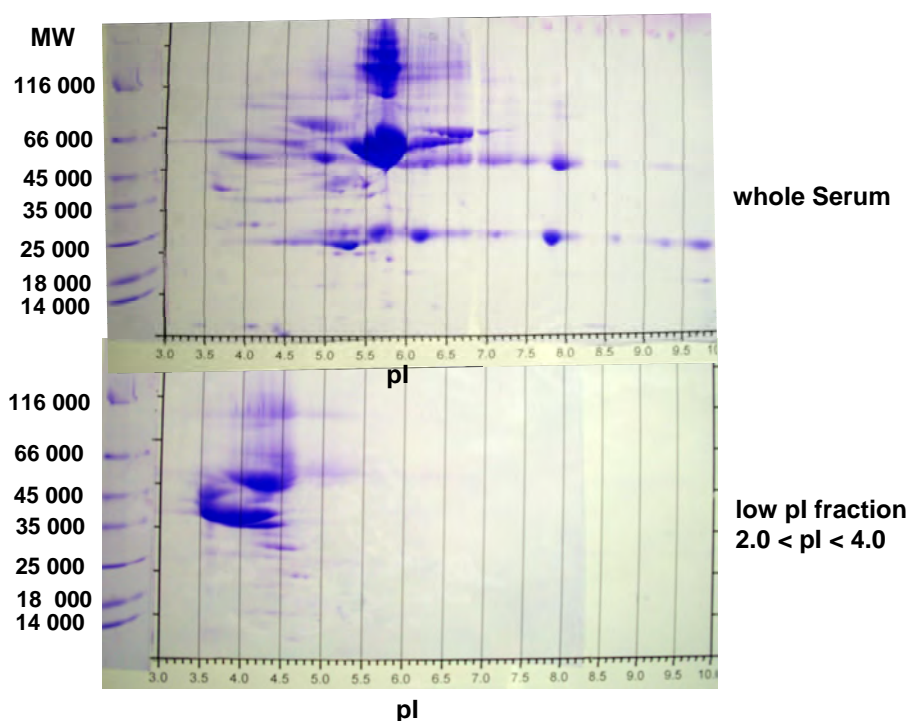


**Figure 46.** 2D gels of whole serum (top) and the low pI fraction separated by the Twinflow (bottom).

Since several proteins were detected in the low pI fraction ( $2.0 < pI < 4.0$ ), the fraction was further separated into four narrower pI fractions using pH-biased IET, and then these sub-fractions were analyzed by reversed phase HPLC. The column dimensions were 33 x 4.6 mm i.d., it was packed with non-porous 1.5  $\mu\text{m}$  silica beads that had a polymer pellicle with bonded C-18 groups as the stationary phase. A 0 – 100% linear solvent gradient was run in 30 minutes from 0.08% trifluoroacetic acid (TFA)-water to 0.1% TFA-acetonitrile. The eluted proteins were detected by a flow-through UV-absorbance detector at 214 nm. Figure 47 shows the chromatograms of the whole  $2.0 < pI < 4.0$  fraction. The chromatograms of the four narrow, low pI fractions are displayed

in Figure 48. The first fraction should contain proteins with pI values in the  $2.0 < \text{pI} < 3.0$  range (panel 1). Only a very small absorbance signal at 11.7 minutes was detected, indicating that no proteins of very significant concentration were present in this fraction. The next sub-fraction contained proteins with pI values in the  $3.0 < \text{pI} < 3.5$  range (panel 2). The peaks detected in this fraction correspond to the early eluting peaks (between 7 – 12 minutes) in the feed sample (possibly low molecular weight peptides). The major peak from the whole fraction, eluting at around 16.5 minutes, was almost entirely found in the protein sub-fraction representing proteins with pI values in the  $3.5 < \text{pI} < 3.9$  range (panel 3). Lastly, the  $3.9 < \text{pI} < 4.0$  fraction (panel 4) contained the proteins that were retained the longest by the HPLC column. Thus, by performing a series of binary IET separations, the complexity of a protein sample can be significantly reduced.

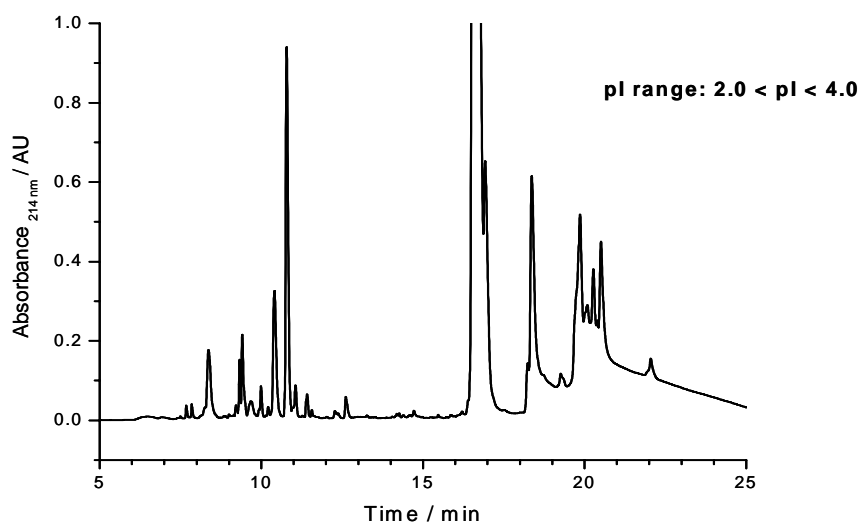


**Figure 47.** Chromatogram of the whole low pI fraction ( $2.0 < \text{pI} < 4.0$ ) from bovine serum analyzed by reversed phase HPLC.



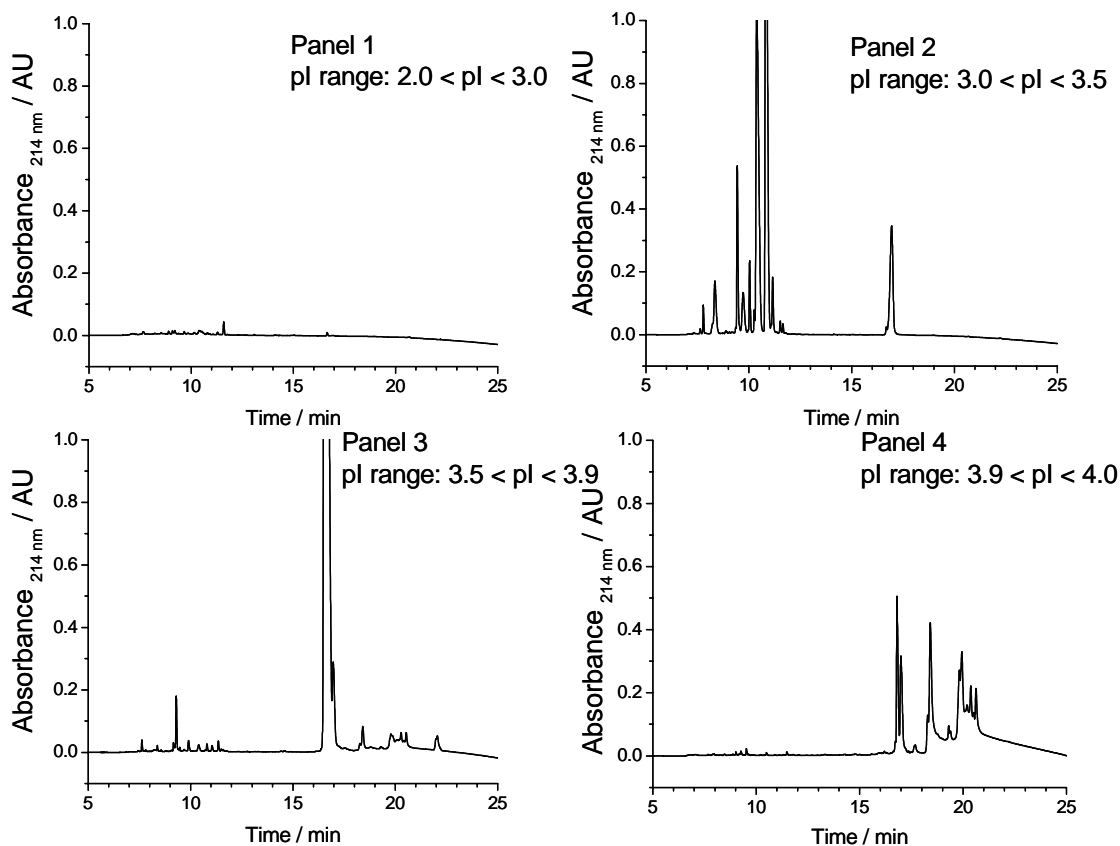


**Figure 48.** Chromatograms of the samples from each of the four sub-fractionations made on the low pI fraction, analyzed by reversed phase HPLC.

To conclude, this series of experiments demonstrated the utility of the Twinflow for pH-biased IET fractionation and concentration of complex protein samples. The ability of the Twinflow to accommodate liters of sample feed, and achieve high concentration factors, make it particularly useful for proteomics applications that focus on the identification of low abundance proteins within a specific pI range.

## 6.2.2 A comparison between two fractionation techniques: chromatofocusing versus pH-biased isoelectric trapping

### 6.2.2.1 Background and objective

Chromatofocusing uses an ion exchange column and a pH gradient in the mobile phase to separate proteins on the basis of their pI values. A protein with an opposite charge compared to the charge of the bound functional group on the ion exchange resin will bind to the resin. The elution of the bound proteins is then dependent on the pH of the mobile phase. When the pH of the mobile phase is at a value equal to the pI of a protein, the net charge on the protein is zero, the protein is no longer bound strongly to the column and is eluted. In practice, separation is achieved by creating a pH gradient along the length of the column over the course of the separation. The wider the range of the pH gradient, and the more shallow its slope, the wider the pI range of proteins that can be resolved. For a detailed review of chromatofocusing, see references [81, 82]. A chromatofocusing column was used to separate bovine serum over a pH gradient between 8.4 and 4.0. However, as part of the ion exchange process, the proteins with pI values outside the pH gradient range (i.e., proteins with pI values less than 4.0 or greater than 8.3) will also be collected in two separate fractions. The protein composition of these low and high pI fractions were analyzed and compared to the low and high pI fractions of the same range obtained by pH-biased IET.

#### 6.2.2.2 Instrument set-up, materials, and method

The chromatofocusing column used in this experiment is part of a two-dimensional liquid separation system called the PF 2D (Beckman Coulter) [83]. The first dimension separates proteins according to their pI on a chromatofocusing column. Directly after the column, there is an online flow-through pH meter and UV-absorbance detector. This allows for the fraction collector to collect fractions based on the pH of the effluent (normally every 0.3 pH units), and the major protein peaks are detected at 280 nm. Each fraction is then analyzed again by a reversed-phase HPLC column, with an online UV-absorbance detector at 214 nm. Thus, the sample has been separated in two dimensions, first by pI and then by hydrophobicity. For this experiment, only the first dimension, the chromatofocusing column, was used.

Firstly, the chromatofocusing column was equilibrated with a pH 8.4 buffer for 210 minutes. The bovine serum sample (total protein load 4.5 mg) was then injected onto the column, and the elution was started by introducing a pH 4 buffer (forming the pH gradient). If there are proteins in the sample with pI values higher than pH 8.4, they will not bind to the column, and will be collected in the first few fractions. After the effluent pH has reached a value of 4.0, the column was washed with 1 M sodium chloride to remove the proteins still bound. If there are any proteins in the sample with pI values lower than 4.0, they will stay bound to the column for the entire time of the pH gradient, and will only be eluted during the 1 M salt wash.

pI fractions, in the same range as the ones collected from the chromatofocusing column, were obtained using pH-biased IET on the Twinflow. The instrument set-up, solution preparation, and method are described in Section 6.2.2.2. The unfractionated serum and the fractions obtained from the chromatofocusing column and from the Twinflow, were analyzed by reversed phase HPLC and SDS-PAGE to compare the protein compositions.

#### 6.2.2.3 Results and discussion

The pH and UV-absorbance trace obtained from separating bovine serum on the chromatofocusing column are shown in Figure 49. Over the first 15 minutes, when the pH of the mobile phase eluting from the column was still about 8.4, a broad peak was detected. The fractions corresponding to this peak were pooled and designated as the fractions containing proteins with pI values greater than 8.4. Between 45 and 100 minutes, the gradient formed, and numerous peaks were detected for the proteins eluting from the column with pI values between 8.4 and 4.0. At 120 minutes, after the 1 M salt wash was started, a large peak was detected. The fractions under the peak were collected, pooled, and designated as the low pI fraction (i.e., proteins with pI values lower than 4.0).

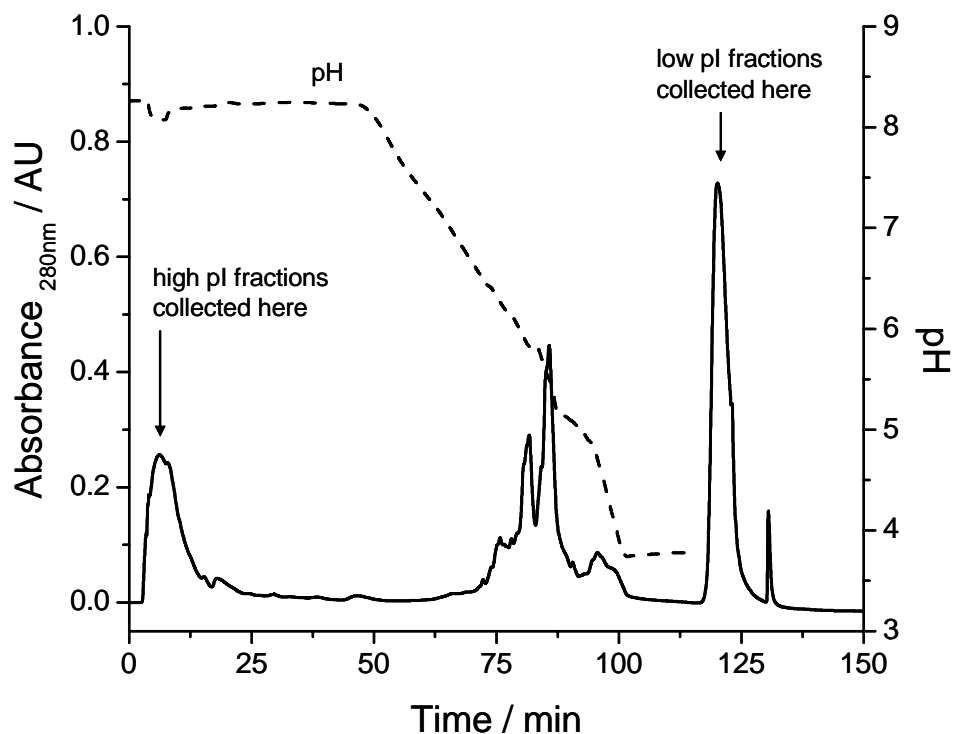


**Figure 49.** pH and UV-absorbance trace of bovine serum separated by the chromatofocusing column.

The protein composition of each high and low pI fraction, from both the PF 2D and the Twinflow, was then analyzed by HPLC. Figure 50 shows the chromatograms from the HPLC analysis for the unfractionated serum (panel 1), the high pI fraction from the chromatofocusing column (panel 2), and the high pI fraction from the Twinflow (panel 3). The corresponding SDS-PAGE image for each of the samples has been included for comparison. Although the high pI fraction from the Twinflow had a lot higher protein concentration than the fraction from the chromatofocusing column, both had very broad peaks, consistent with the elution of large proteins with numerous isoforms, such as anti-

bodies. This assumption is supported by the SDS-PAGE result which shows that the same large relative molecular mass proteins are present in both the high pI fractions from the chromatofocusing column (lane 2) and the Twinflow (lane 3).

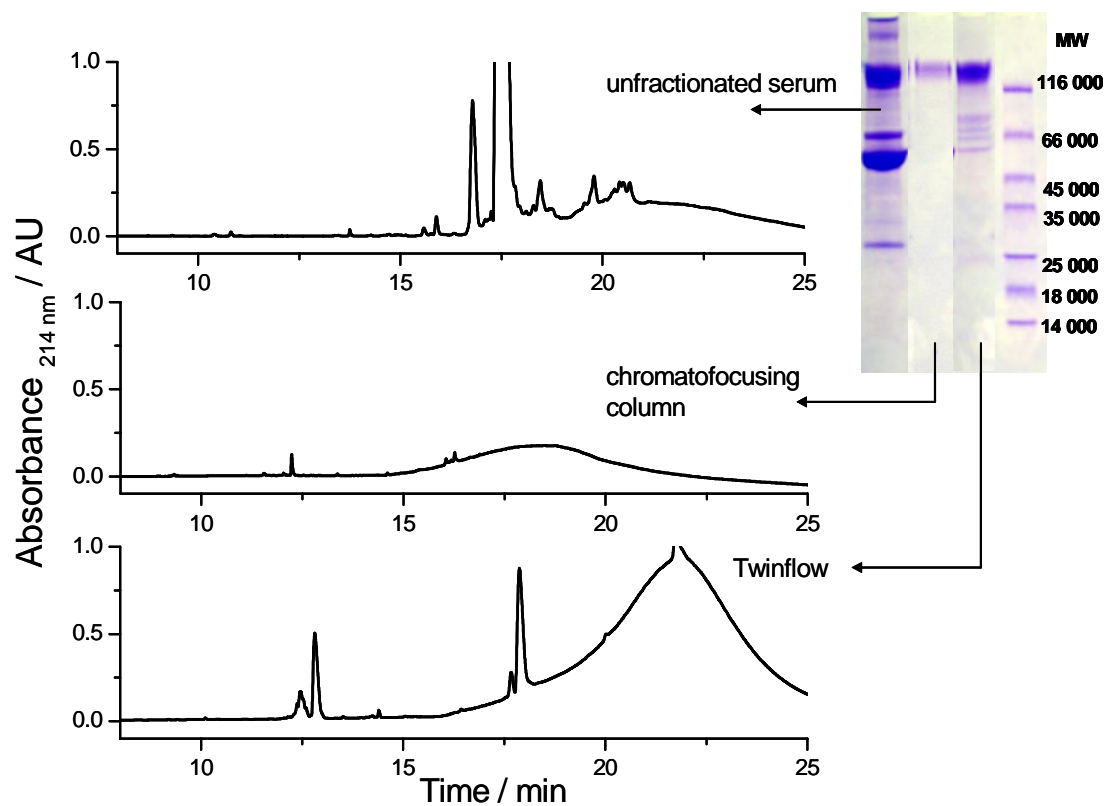


**Figure 50.** Chromatograms for the reversed phase analysis comparing the whole serum (top), chromatofocusing high pI fraction (middle) and the Twinflow high pI fraction (bottom). The corresponding samples are shown analyzed by SDS-PAGE.

On the other hand, there were many differences when the low pI fractions were compared (Figure 51). The HPLC analysis of the low pI fraction from the chromatofocusing step (panel 2), and the low pI fraction from the Twinflow separation (panel 3), are clearly very different. A similar difference in bands was seen in the corresponding SDS-PAGE analysis, suggesting that the two fractionation techniques are separating different subsets of proteins. Furthermore, if the analysis of the low pI fraction from the chromatofocusing column is compared to the analysis of the unfractionated serum, either by the HPLC chromatogram or by SDS-PAGE, several similarities are observed. It appears that the 1 M salt wash, used to elute the proteins with pI values lower than 4.0 from the chromatofocusing column, is also eluting a lot of other proteins. Therefore, this suggests that there is a considerable amount of non-specific retention of the serum proteins onto the stationary phase. This retention is not caused by simple electrostatic attraction, because the proteins are not eluted during the pH gradient. They were only removed under the more aggressive ion-exchange conditions of the 1 M salt wash.

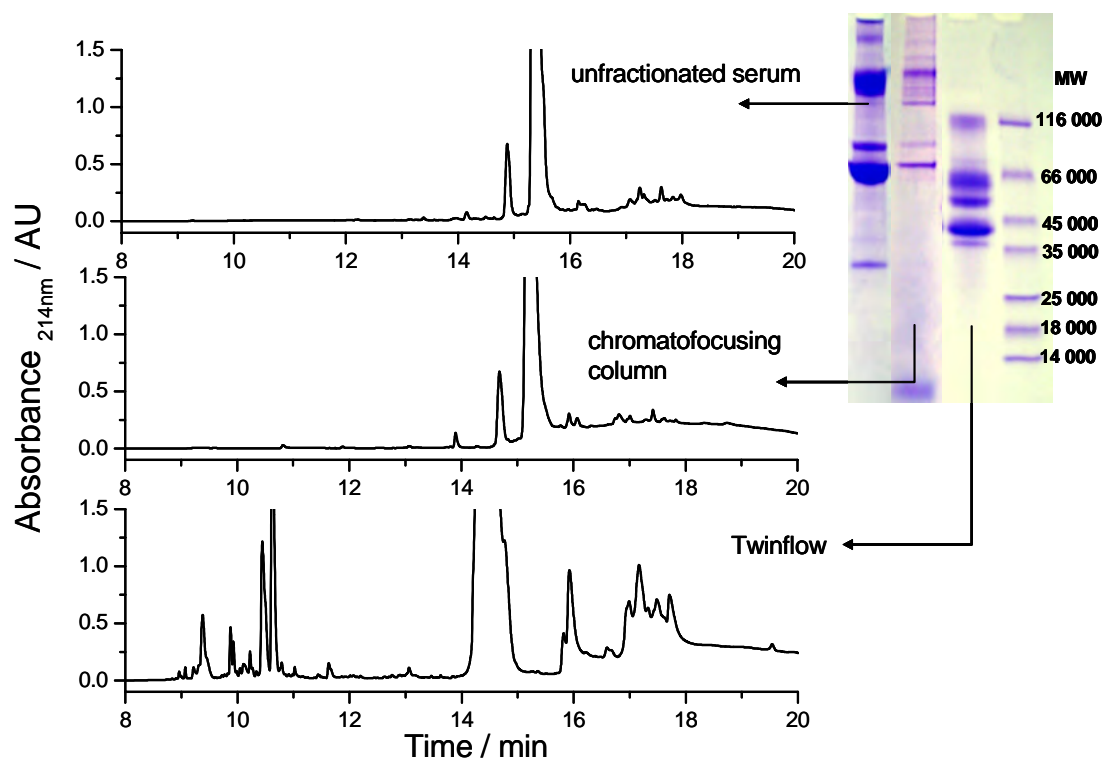


**Figure 51.** Chromatograms for the reversed phase analysis comparing the whole serum (top), chromatofocusing low pI fraction (middle) and the Twinflow low pI fraction (bottom). The corresponding samples are shown analyzed by SDS-PAGE.

In summary, chromatofocusing and pH-biased IET separated a similar population of proteins in the high pI fraction, but very different populations of proteins in the low pI fraction. The chromatofocusing column used under the conditions described here, does not seem to be a good approach if the aim is to obtain a fraction containing only low pI proteins, as the 1 M salt wash removed proteins still bound to the stationary phase, regardless of their pI value.



### 6.2.3 Fractionation of recombinant thyroid stimulating hormone

#### 6.2.3.1 Background and objective

Thyroid stimulating hormone (TSH) plays an important role in the regulation of thyroid gland activity [84]. The diagnosis of thyroid gland dysfunction can be achieved by stimulating the gland with a dose of TSH and then measuring the gland's response. For the most meaningful and accurate diagnosis, the TSH used must be of high purity and homogenous [85]. Thyroid dysfunction is a particular problem for canines. Currently, TSH used for diagnosing canine thyroid dysfunction is obtained from bovine pituitary glands. This is a problem, because there can be extreme batch-to-batch variations in the composition of the TSH preparation. To eliminate the variability, there is interest in developing a recombinant form of TSH (rTSH) that could be used instead [85]. rTSH is grown in a cell culture medium, but must be purified before activity studies can be conducted. Due to the particular expression system used, rTSH is believed to have a highly variable extent of glycosylation. This results in the expression of a wide range of rTSH isoforms with different pI values. In addition, because glycosylation differences result in variable biological activity [86], it would be of interest to characterize the different isoform populations. Utilizing the Twinflow, pH-biased IET was used to separate the rTSH isoforms into several broad pI fractions.

#### 6.2.3.2 Instrument set-up, materials, and method

The cell culture media typically used for the expression of recombinant proteins, generally contain very high concentrations of salt and albumin, and may contain a large

concentration of cell growth nutrients, such as amino-acids. Therefore, before protein separation can be attempted, various strategies were needed to reduce the complexity of the medium. To perform an initial clean up on a 1 L batch of cell culture medium, a precipitation step was used to remove a significant amount of what is believed to be peptide complexes. 1 M sodium hydroxide was used to increase the pH of the medium to 12, at which point it had become very cloudy due to precipitation. The medium was spun centrifuged for 20 minutes at 2000 rpm. The clear supernatants were pooled, and the pellet was discarded. To create the pH-biased conditions, 30 mM lysine was added to the supernatant. Prior to separation of the rTSH isoforms, the sample had to be desalted. The single compartment desalting cartridge contained an anodic membrane which had a pH of 5.0 and a cathodic membrane which had a pH of 13.0. The media was recirculated through the Twinflow and desalted using a current of 1000 mA, until the conductivity of the solution had been reduced to below 1 mS. At the end of each step in this sample preparation process, aliquots were taken so that the concentration of TSH could be measured using an immunoassay specific for TSH. The desalted sample was then filled into the reservoir attached to the cathodic separation compartment of the Twinflow. The reservoir attached to the anodic separation compartment (the collection stream) contained 15 mM glutamic acid. The separation cartridge contained an anodic membrane with a pH of 2.0, the first separation membrane used had a pH of 7.0, and the cathodic membrane had a pH of 13.0. Once the transfer was complete, the collection stream was harvested and the separation membrane was changed to the next highest pH. The other separation membranes used in the subsequent steps included, pH 8.0, 9.0, and 10.0 to

fractionate the sample into broad pI fractions. Each fraction was tested for rTSH concentration using an immunoassay.

#### 6.2.3.3 Results and discussion

The rTSH concentration of the starting medium was 400 ng/mL. In the 1 L volume, this equaled a total of 400 µg of rTSH. After the precipitation and centrifugation steps, approximately 95 % of rTSH was retained (380 µg). During desalting, aliquots were taken from the exit ports of the Twinflow. Figure 52 shows the plot of the change in rTSH concentration and the conductance of the solution. There is some loss of rTSH during the desalting process (~ 15%), probably caused by non-specific adsorption of the protein to the glass reservoirs and tubing in the Twinflow. Once the sample was separated into broad pI fractions, the rTSH amount was measured in each. The results are plotted in Figure 53, showing that the vast majority of rTSH isoforms were present in the  $10 < pI < 13$  fraction. In this study, pH-biased IET on the Twinflow was used to process a large volume (1 L) of cell culture feedstock for the fractionation of a recombinant protein. In addition, sample desalting and separation were achieved, while maintaining reasonably high target recoveries, even though the expression level for rTSH was only in the ng/ml range.

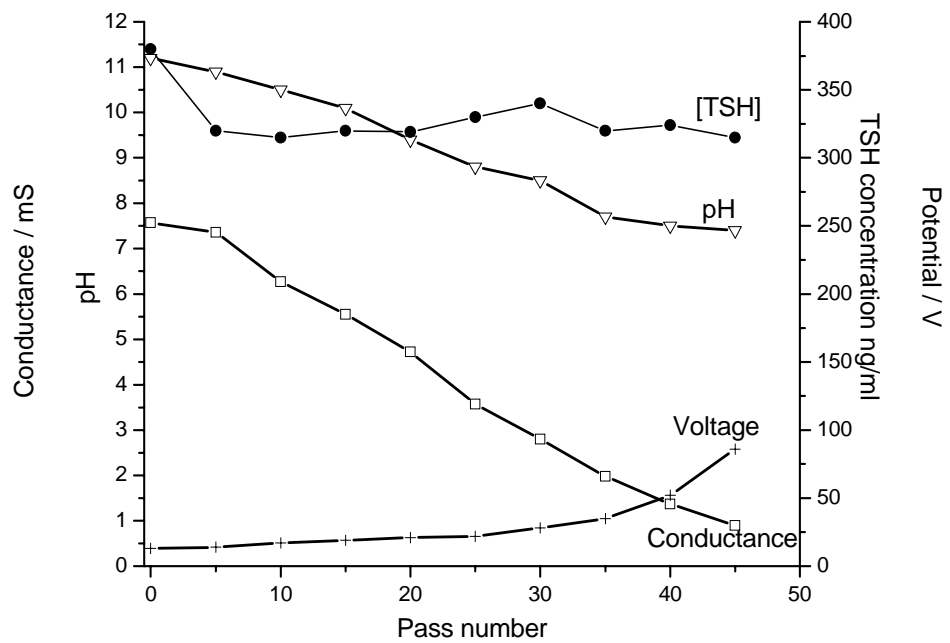


**Figure 52.** Plot of the TSH concentration, pH, and conductivity changes in the sample, and the corresponding voltage change during desalting on the Twinflow.

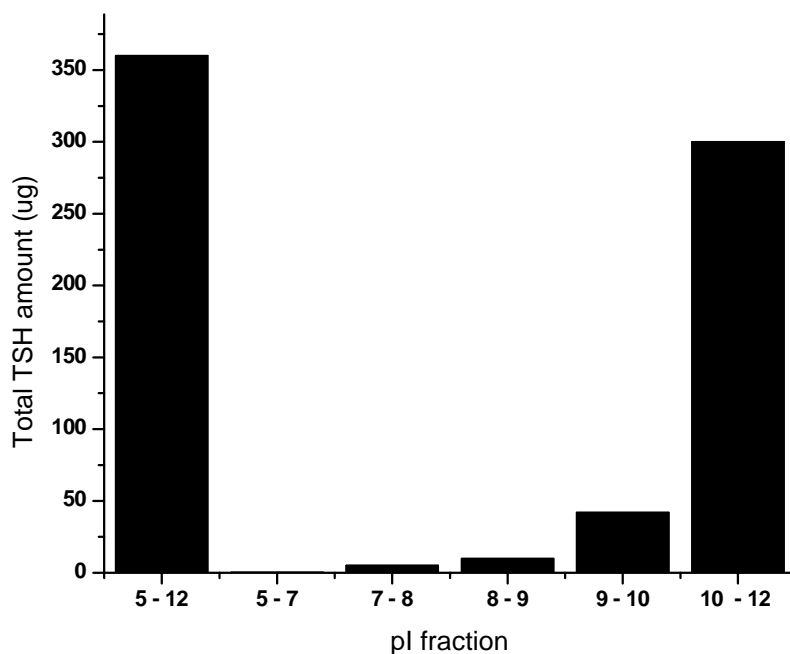


**Figure 53.** Bar graph showing the amounts of TSH in each pI fraction.

#### 6.2.4 Concluding remarks

pH-biased IET alleviates two of the most troublesome characteristics of IET protein separations. Firstly, by maintaining the protein in a charged state, the phenomenon of isoelectric precipitation is alleviated. Secondly, the long separation times of classical IET have been decreased by maintaining a high charge on the protein, and a high electrophoretic velocity. An optimum auxiliary isoelectric agent concentration can be found to fine tune any pH-biased IET separation to improve the energy consumption and the protein transfer rate. The pH-biased IET process was tested as a prefractionation step for the analysis of bovine serum proteins, and for the fractionation of a recombinant glycoprotein from a cell culture feedstock.

### **6.3 pH-biased isoelectric trapping separations on the Biflow**

#### 6.3.1 Fractionation of egg white proteins

##### 6.3.1.1 Background and objective

In Section 6.1, the Twinflow was used to perform two successive binary IET separations on egg white in order to obtain a narrow pI fraction of protein. To eliminate the need for running a separation twice, the Biflow can be used to accomplish fractionation in a single step. In this set of experiments, the Biflow was used to obtain narrow and also, broad pI fractions of chicken egg white proteins. In each case, there are proteins present in the feed with pI values both higher and lower than the target proteins pI values.

Before the fractionation experiments were performed, the composition of the egg white sample was analyzed by CIEF on the iCE280. By using five pI markers, a very good approximation of the pI values of all the detectable egg white proteins was obtained (Figure 54). This helped in the selection of the correct separation membrane for each fractionation step.

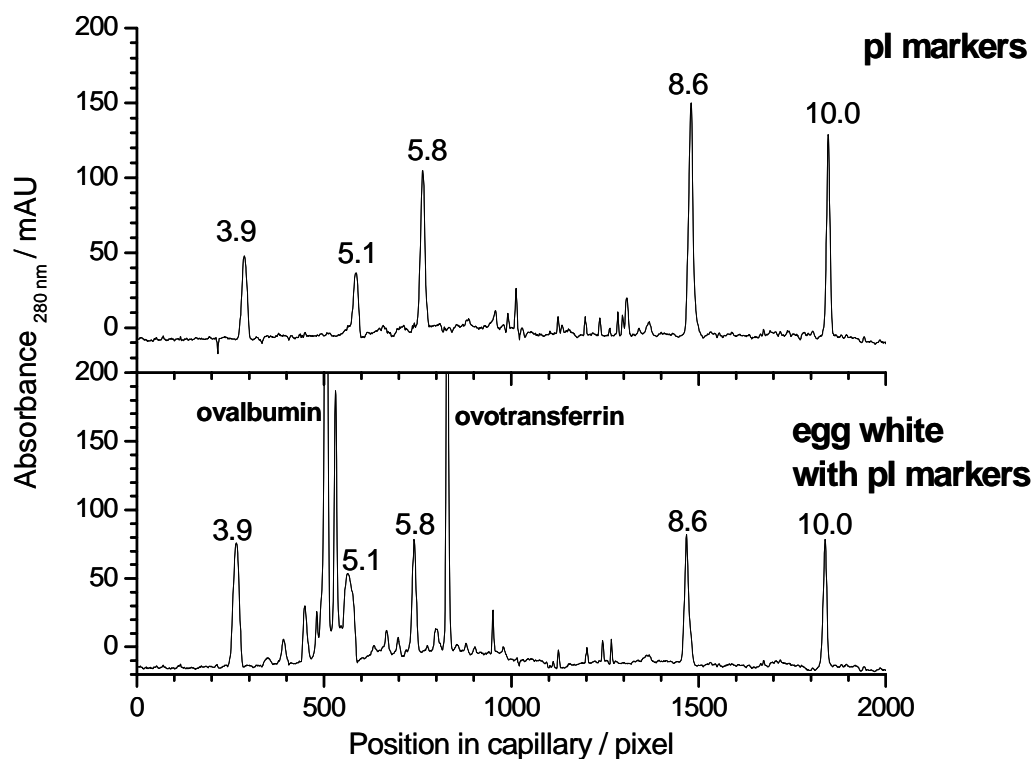


**Figure 54.** CIEF analysis of six pI markers (top) and six pI markers with the egg white sample (bottom).

### 6.3.1.2 Instrument set-up, materials, and method

There were three individual Biflow fractionation experiments. For each one, two separation compartments were configured. In the first experiment, the pH of the separation membrane in the first unit was 5.4, the second unit had a separation membrane with a pH of 4.7. In the second experiment, a pH 4.5 separation membrane was used in the first unit, and a pH 4.4 separation membrane was used in the second unit. For the third experiment, the separation membrane in the first unit had a pH of 5.5,

and the separation membrane in the second unit had a pH of 5.4. The same pH 2.0 anodic membrane and pH 11 cathodic membrane was used for every separation cartridge. In all three experiments, the feed was egg white diluted 1 in 25 with a solution of 5 mM histidine (HIS) and 5 mM lysine (LYS). 80 ml of the feed was filled into the reservoir attached to the cathodic separation compartment of the first unit. The transfer loop contained 40 ml of 10 mM glutamic acid (GLU) and was pumped into the anodic separation compartments of both units. The product collection stream contained 20 ml of 5 mM HIS, and was recirculated around the cathodic separation compartment of the second unit. Each separation was run in recirculation mode for 100 minutes. The power supply connected to the first separation unit delivered a current ranging from 110 mA to 200 mA, and the current delivered to the second unit ranged from 70 – 80 mA. At the end of each separation, the fractions from the feed, transfer loop, and product collection streams were analyzed by CIEF using the iCE280, and also by SDS-PAGE using a 4-20% gradient gel stained by Coomassie blue.

#### 6.3.1.3 Results and discussion

The schematic in Figure 55 shows the Biflow and the membrane configurations for the first experiment. The aim of the first separation was to fractionate a broad range of mid-pI proteins from egg white, including the most abundant protein, albumin.



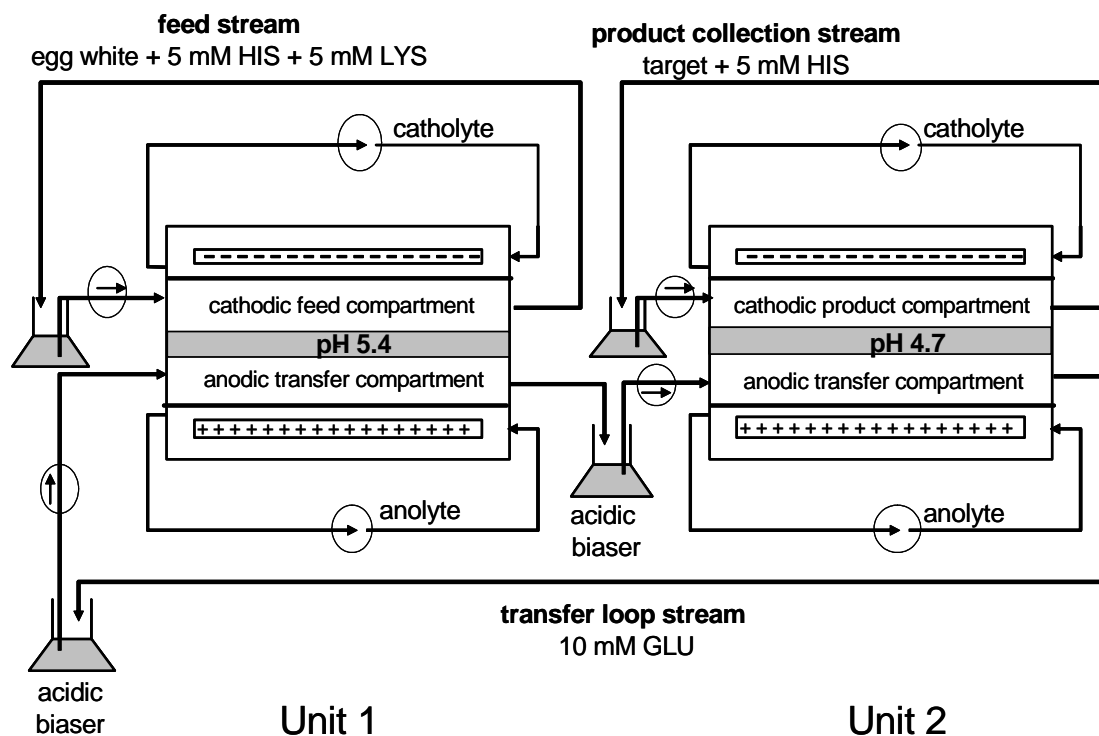


**Figure 55.** Schematic of the Biflow set-up for the isolation of egg white proteins with pI values between 4.7 and 5.4.

Figure 56 shows the electropherograms obtained on the iCE280 for the starting feed sample (panel 1), the final feed sample (panel 2), the final transfer loop sample (panel 3), and the final product sample (panel 4). Dotted lines indicate the pH points where the membranes are cutting the sample. The pI marker meta-aminobenzoic acid (MABA), with a pI value of 3.9, was added to each fraction, just before the fraction was analyzed by the iCE280. All the proteins with pI values below the pH of the first separation membrane (pH 5.4) transferred into the anodic transfer loop stream of the first compartment, which shuttled them across to the second unit. In the second unit, all the proteins with pI values above pH 4.7 were transferred into the product collection stream.

This left only proteins with pI values higher than 5.4 in the final feed (panel 2), and only proteins with pI values between 2.0 and 4.7 in the final transfer loop stream (panel 3).

The final product collection stream (panel 4) contained all of the albumin isoforms, plus any other protein with a pI between 4.7 and 5.4.

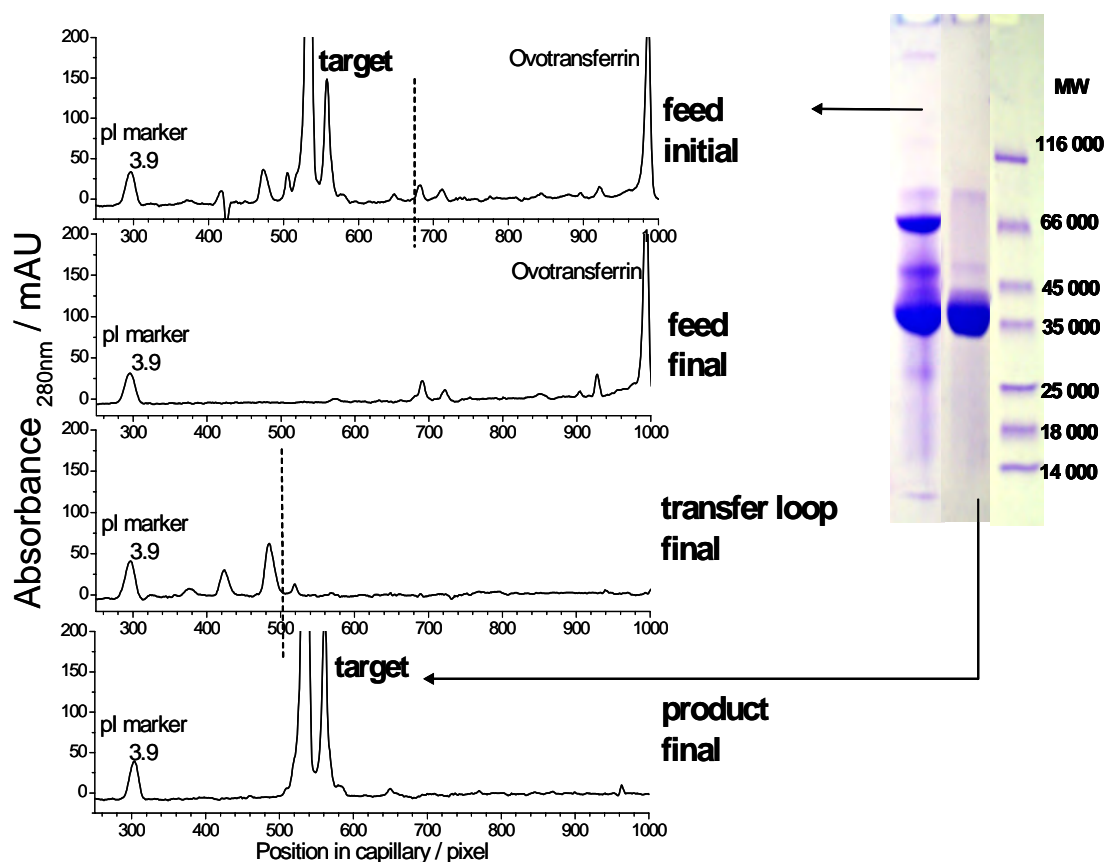


**Figure 56.** CIEF analysis showing the protein composition of the sample streams in the Biflow during the separation of egg white proteins with pI values between 4.7 and 5.4. The SDS-PAGE of the initial feed and final product samples are shown for the sake of comparison.

To further analyze this fraction, the unfractionated egg white and the sample from the final product stream were separated by two dimensional gel electrophoresis (2DGE) (Figure 57). The top gel image is that of the unfractionated egg white sample. The bottom gel image is that of the sample from the product collection stream, showing the focused ovalbumin isoforms in the middle.

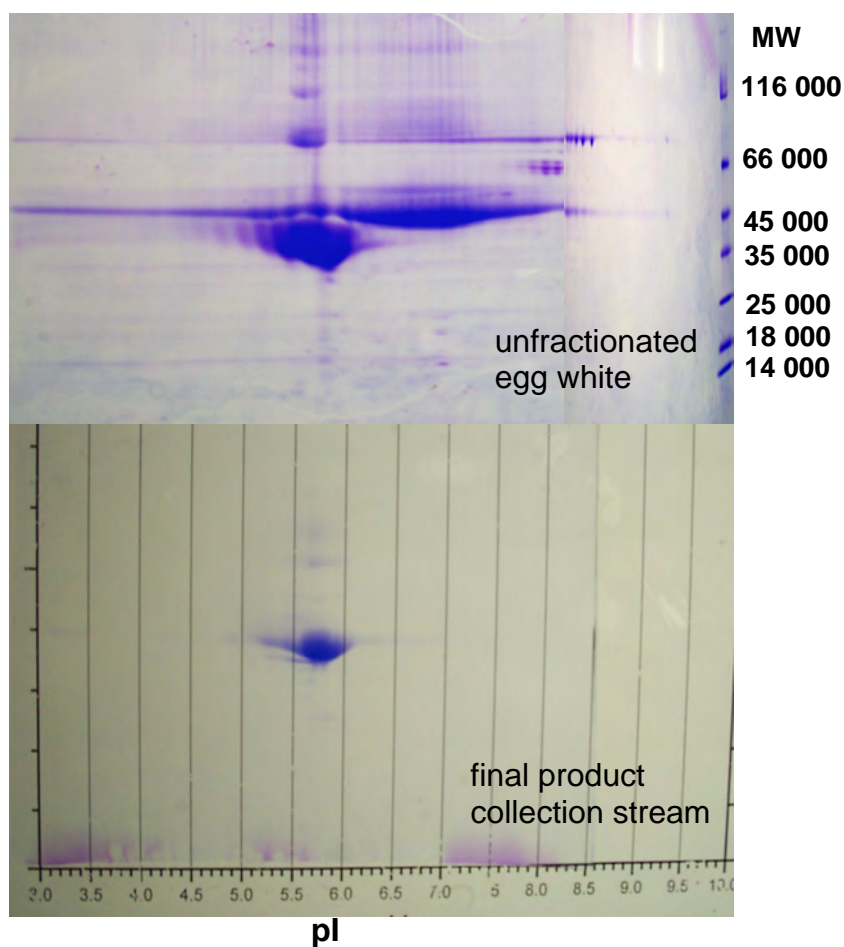


**Figure 57.** 2D gel images of unfractionated chicken egg white (top) and the sample from the Biflow final product collection stream (bottom).

This result again illustrates the issue of the pI value of a protein changing after being reduced and alkylated during the sample preparation steps for 2DGE. The stained protein spot for the major albumin isoforms has a pI range of 5.5 – 6.0. The use of detergents together with reducing and alkylating agents in 2DGE, cause proteins to be unfolded and protein complexes to be broken, which can alter the apparent pI value of the protein. On the other hand, when the same sample was analyzed by CIEF on the iCE280, under non-reduced and non-alkylated conditions, the resulting signal for the major albumin isoforms isolated in the Biflow product stream were in the pI 4.7 - 5.4 range (Figure 56). This indicated that the buffering membranes (with pH values of 4.7 and 5.4) did indeed fractionate the intended proteins, and the discrepancy on the 2D gel is related to sample preparation.

The aim of the second and third separations was to fractionate and also concentrate two minor proteins from egg white. A concentration factor of four was achieved for the proteins in the product stream compared to the feed stream by having four times less volume in the product stream. Figure 58 shows the trace from the iCE280 instrument for the whole egg white. The two minor protein targets are circled by a dotted line on the electropherogram.

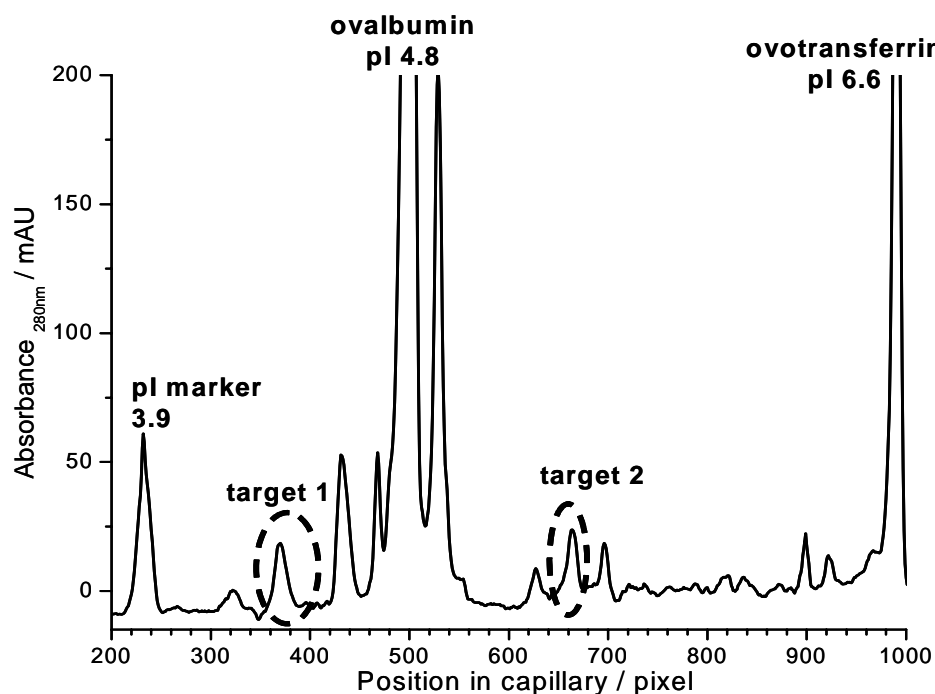


**Figure 58.** CIEF analysis of egg white showing the two minor proteins that will be separated by pH-biased IET on the Biflow.

The pI range of the first minor target was between 4.4 and 4.5. The results of this separation are displayed in Figure 59. The approximate points where the separation membranes cut the sample are shown by a dotted line. Most of the egg white proteins remained in the feed stream (panel 2). The proteins with pI values between 2.0 and 4.4 remain trapped in the transfer loop stream (panel 3), while the product stream contained the proteins with pI values between 4.4 and 4.5 (panel 4). Most of the target protein was successfully transferred through the transfer loop stream and into the product collection stream (a small amount remained in the feed, due to incomplete transfer), where it was concentrated approximately four times compared to the feed stream concentration.

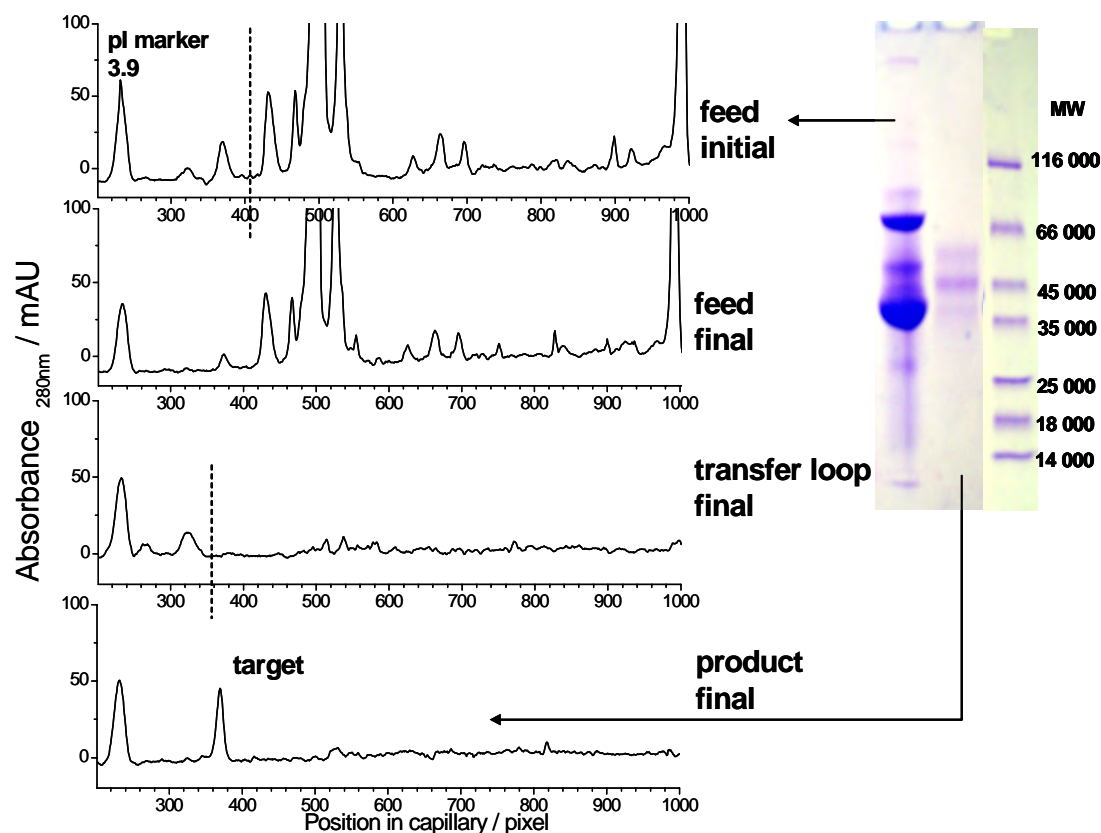


**Figure 59.** CIEF analysis of the Biflow separation of the low pI minor protein target from egg white. The initial feed and final product samples are also shown analyzed by SDS-PAGE for comparison.

The other minor protein target was in the pI range of 5.4 and 5.5. The protein composition of each sample stream can be seen in the traces in Figure 60. Again, the minor target is trapped and concentrated over the course of the experiment in the product stream. This Biflow application demonstrates the utility of pH-biased IET for fractionating a narrow pI range of proteins in one step. It should also be emphasized here, that the success of a given fractionation relies on the operator knowing the

operating pH value of the buffering membranes used for the separation and the pI of the protein of interest.

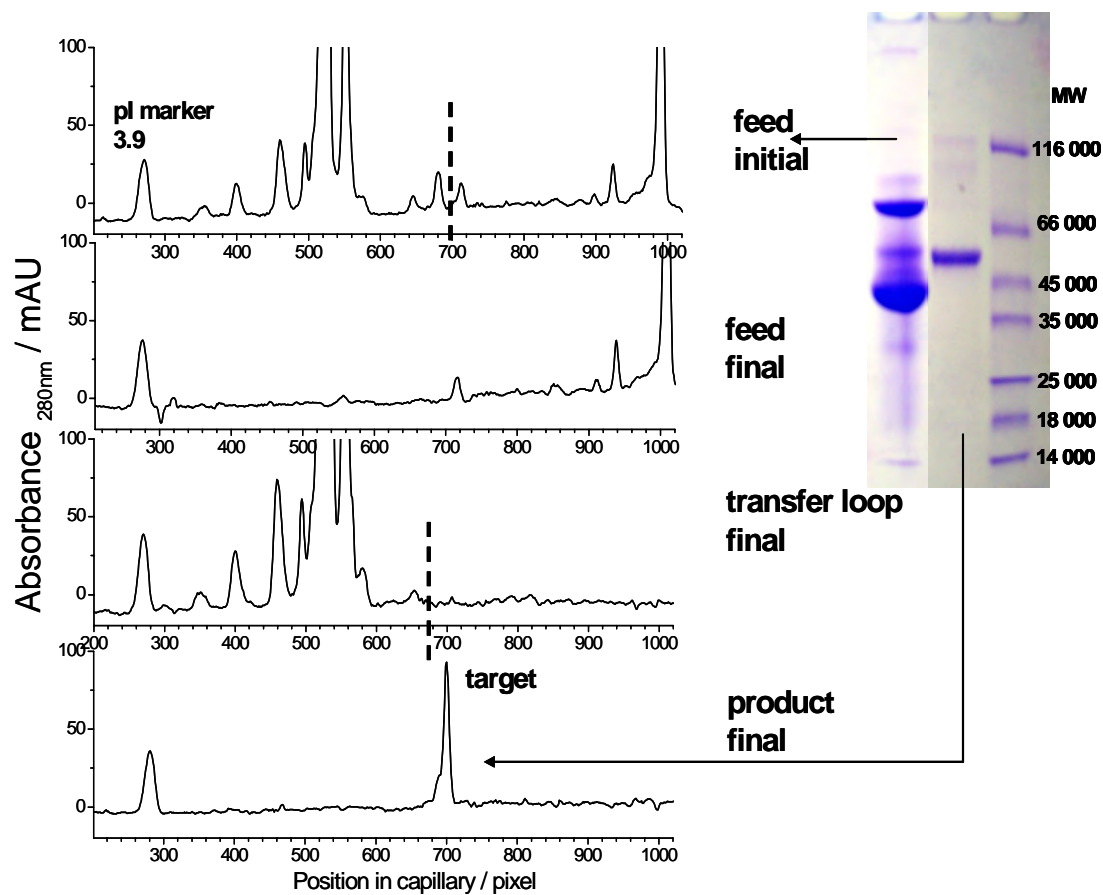


**Figure 60.** CIEF analysis of the Biflow separation of the mid pI minor protein target from egg white. The initial feed and final product samples are also shown analyzed by SDS-PAGE for comparison.

## 6.3.2 Fractionation of bovine serum proteins

### 6.3.2.1 Background and objective

As discussed in Section 6.2.2, the power of IET prefractionation can be applied to studies in proteomics, to help detect low abundance proteins. The narrow fractions made in Section 6.2.2, can only be obtained on the Twinflow by successively “cutting” into the sample from either the low or high pH side. If, however, the region of interest was in the mid-pI range, at least two separate fractionation steps would have to be done on the Twinflow. The objective of this study was two-fold. Firstly, to demonstrate how the Biflow can be used to obtain a mid-pI fraction in a single step and then to demonstrate how the prefractionation / concentration step can be used to increase the limit of detection for other protein separation techniques. For example, if there was interest in characterizing a sub-population of proteins of a specific pI range from a complex sample, the Biflow could be used to fractionate and concentrate this sub-population. This would allow for a higher load of the proteins of interest to be used for the characterization step, compared to what could be applied if the whole complex sample was used without prefractionation. Two different protein characterization techniques were used to test this hypothesis. The first one was two dimensional gel electrophoresis (2DGE), the second one was two dimensional liquid chromatography on an instrument called the PF 2D. 2DGE is a gel based technique that separates proteins according to their pI value, and then according to their relative molecular mass. The PF 2D separates proteins according to their pI value, and then by hydrophobicity (see Section 6.2.3.2 for a more detailed description of the PF 2D). Proteins in bovine serum with pI values



between 4.5 and 4.8 were arbitrarily designated as the sub-population of interest.

Therefore, after fractionating this range on the Biflow, it was analyzed by 2DGE and by the PF 2D to see if there were extra proteins detected compared to if the whole serum sample was analyzed without prefractionation.

#### 6.3.2.2 Instrument set-up, materials, and method

To obtain the mid-pI fraction from bovine serum, the Biflow was configured as shown in the schematic in Figure 61. The first separation unit had a separation membrane with a pH value of 4.8, the second unit had a separation membrane with a pH value of 4.5. Both cartridges had anodic membranes which had pH values of 2.0, and cathodic membranes with pH values of 11.0. The 1000 ml feed was prepared by diluting 100 ml of desalted bovine serum 1 in 10 with a 30 mM histidine (HIS) solution. The 50 ml transfer loop stream contained 5 mM glutamic acid (GLU). The product stream, connected to the cathodic separation compartment of the second unit, was a 10 ml mixture of 30 mM HIS and 30 mM lysine (LYS). Aliquots taken from the starting feed, and final product streams at the end of the separation were analyzed by 2DGE and by the PF 2D. For the 2DGE an 11cm pH 3-10 IPG strip was used for the first dimension, and a 4-20% gradient gel was used for the second dimension, which was stained with Coomassie blue. 400  $\mu$ g of total protein was loaded on the first dimension for the whole serum, and 100  $\mu$ g for the sample from the final product collection stream. For the PF 2D, the same samples were analyzed on the chromatofocusing column (the first dimension) using the conditions described in Section 6.2.3.2, and the relevant fractions (from the 4.5-4.8 pI

range) from the first dimension were analyzed on the second dimension using the reversed phase HPLC column (see Section 6.2.2.3 for conditions).

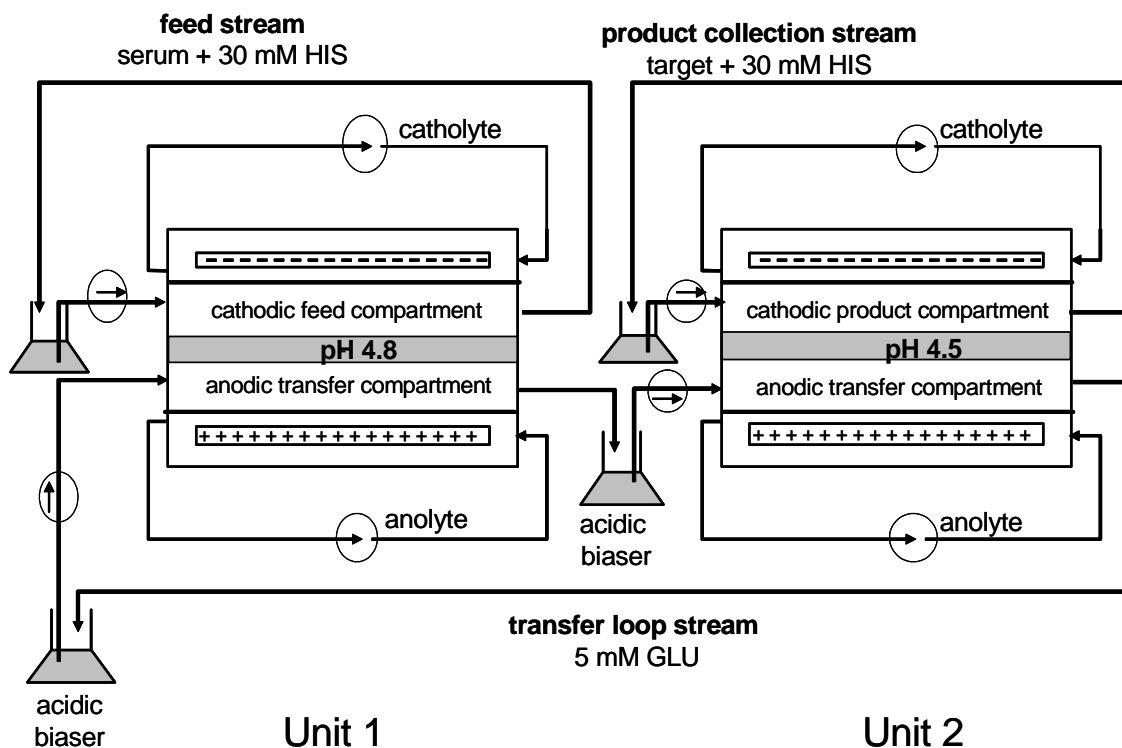


**Figure 61.** Schematic of the Biflow set-up for the separation of bovine serum proteins with pI values between 4.5 and 4.8.

### 6.3.2.3 Results and discussion

The top image in Figure 62 shows the whole bovine serum sample after it was analyzed by two-dimensional gel electrophoresis (2DGE). The major protein, albumin, is the overloaded protein spot in the middle of the gel, corresponding to approximately pI 5.8. The sample from the product stream was also analyzed by 2DGE and is shown on the

bottom image in Figure 62. Comparing the same regions of the feed sample 2DGE map, with the product sample 2DGE map, there is clearly an enrichment of the proteins. The volume difference of the product stream versus the feed stream was 100 fold, resulting in an approximately 100-fold increase in concentration.

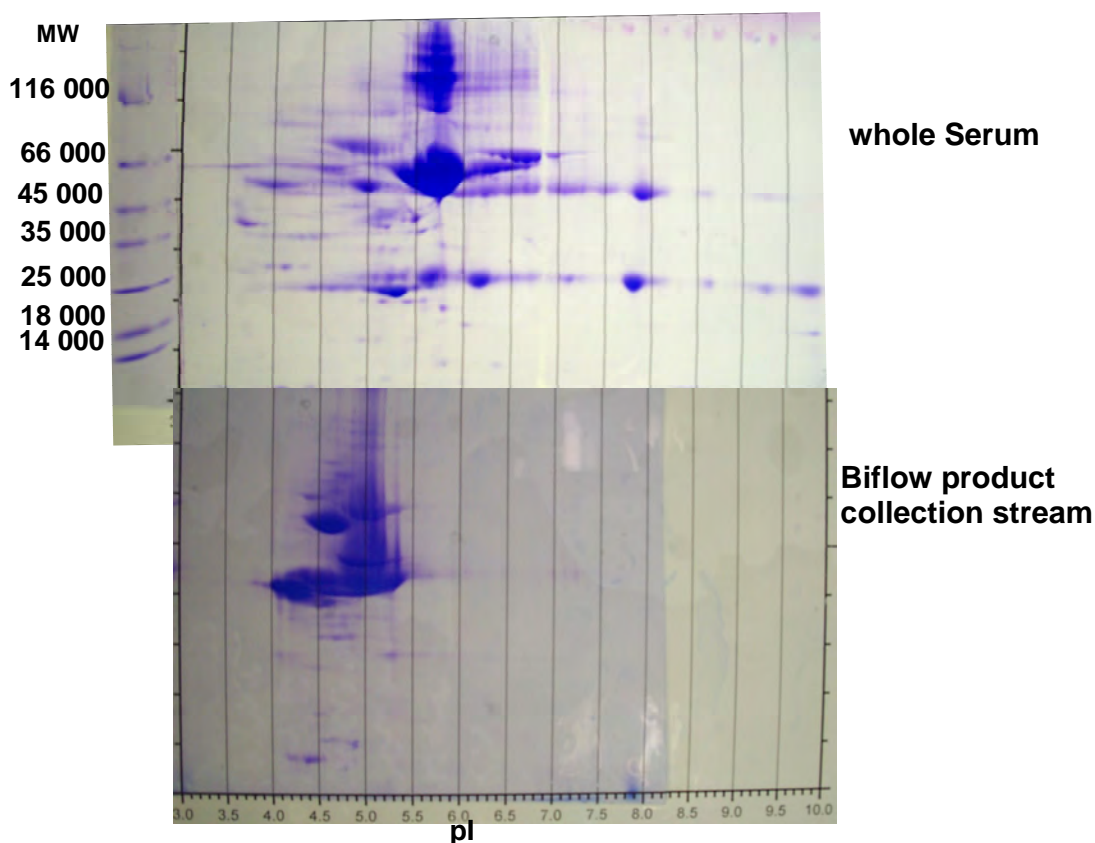


**Figure 62.** 2D gels of whole bovine serum (top) and the sample from the Biflow product collection stream.

The pH and UV-absorbance traces from the first dimension chromatofocusing of the unfractionated serum are shown in Figure 63. The first dimension method was programmed to collect fractions every 0.3 pH units. The fraction corresponding to the

region of interest (pH 4.5 – 4.8,) is shown in more detail in the inset box in Figure 63.

This fraction was then analyzed by the second dimension HPLC column.

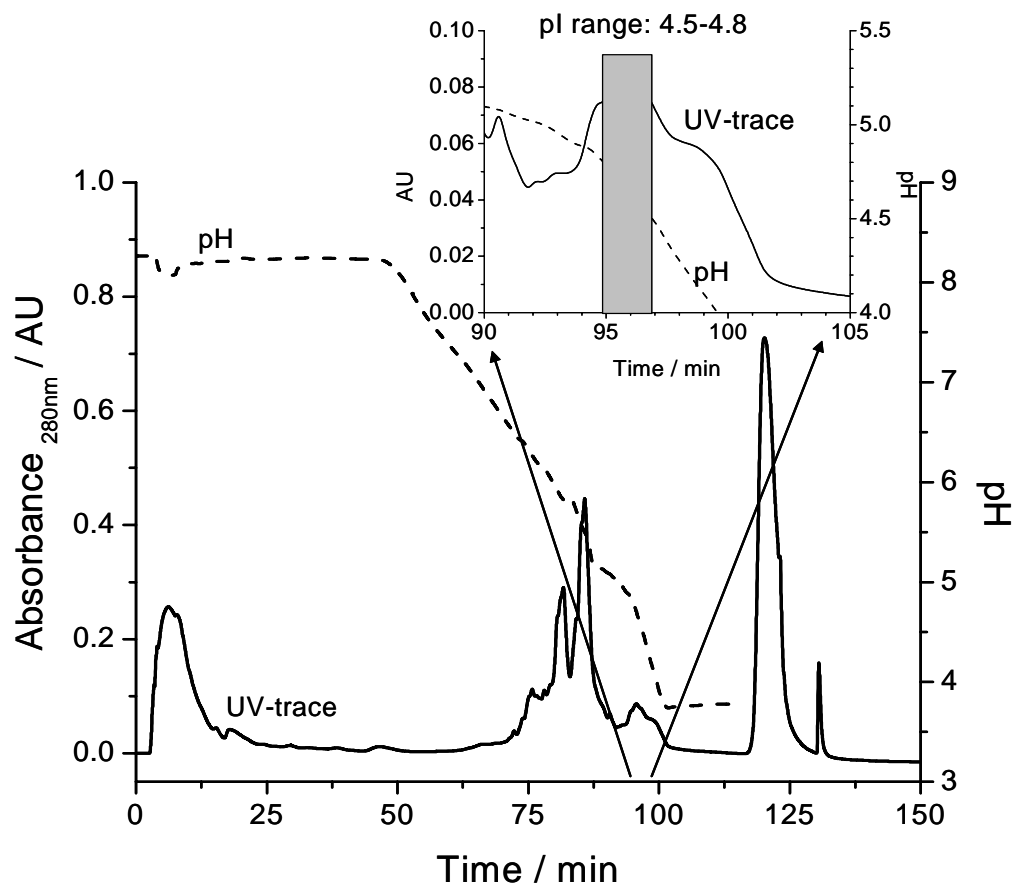


**Figure 63.** pH and UV-absorbance trace of bovine serum separated by the chromatofocusing column with extra detail of the pH 4.0 – 5.5 region.

The sample taken from the product collection stream of the Biflow (representing the concentrated proteins in the pI range of 4.5 – 4.8) was also analyzed on the first

dimension of the PF 2D (Figure 64). As expected, the major peak eluted from the chromatofocusing column around the pH 4 – 5 region. The fraction under this peak was then analyzed in the second dimension by reversed phase HPLC.

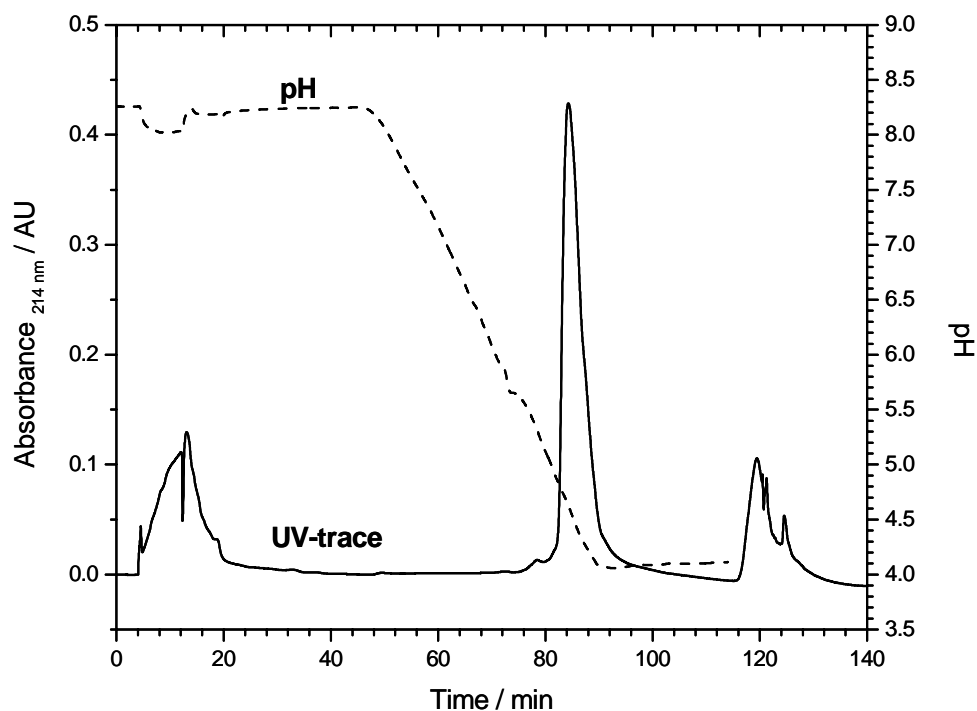


**Figure 64.** pH and UV-absorbance trace of the sample taken from the Biflow product collection stream during the fractionation and concentration of proteins with pI values in the 4.5-4.8 range.

Figure 65 compares the chromatograms for the HPLC analysis of the sample prefractionated by the Biflow (top panel) and the protein sample not-prefractionated (bottom panel) from the pI 4.5 – 4.8 range. The protein composition is similar in each,

however, there is a large increase, particularly in the signal for the proteins eluting between 18 and 20 minutes in the sample prefractionated and concentrated by the Biflow. In summary, the fractionation and concentration steps carried out on the Biflow were able to enrich a region of proteins and increase the limits of detection for both the 2DGE and PF 2D.

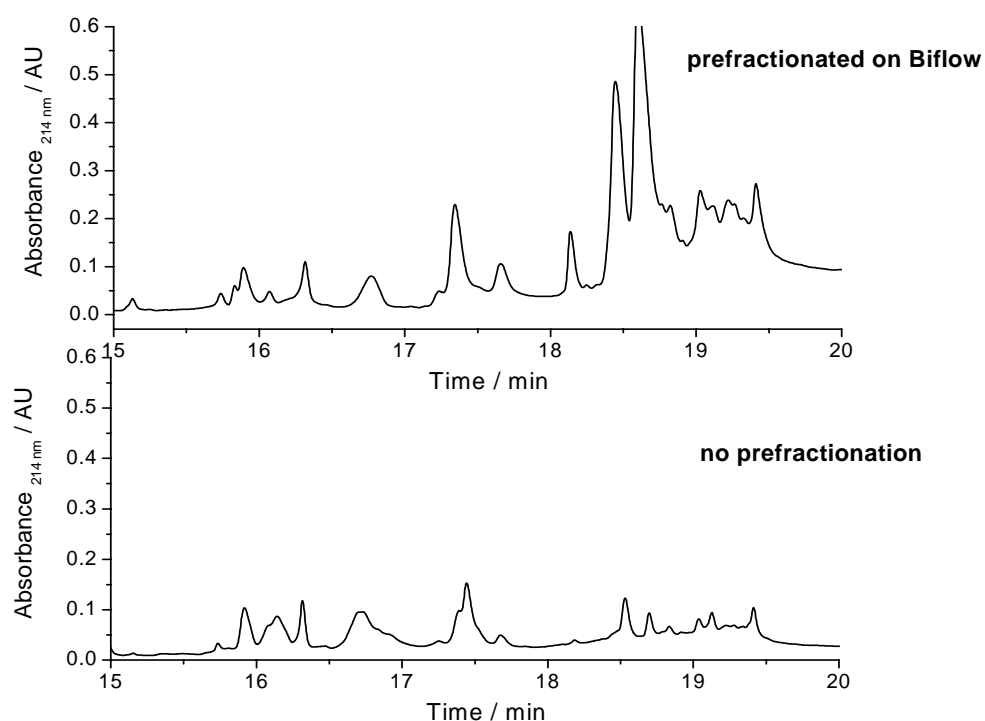


**Figure 65.** Chromatograms of the reversed phase HPLC analysis comparing the samples containing proteins with pI values in the 4.5-4.8 range prefractionated on the Biflow (top) and the serum sample that was not prefractionated (bottom).

### 6.3.3 Concluding remarks

pH-biased IET has been carried out for a variety of protein samples using the Biflow. When a specific protein fraction is desired from a complex mixture, containing other proteins with pI values both above and below the pI value of the target, the Biflow provides a one step process for obtaining the fraction. The ability of the Biflow to also concentrate the desired fraction, during the separation, makes it particularly useful for proteomic applications. The applications tested on the Biflow have demonstrated the ruggedness of the system as it was able to process large volume protein samples containing salt and highly abundant contaminating proteins.

## 7. CONCLUSIONS

### 7.1 Improved isoelectric trapping instrumentation

Isoelectric trapping (IET) has enjoyed many successes in the separation of proteins for obtaining pure fractions and more recently, for prefractionation of samples for proteomics. Several IET devices have been commercialized, but the technology never gained widespread acceptance. In addition, no significant advances in instrumentation have been made since the Isoprime became available in the late 1980's.

A technology was developed for the binary separation of proteins based on their differences in charge-sign or charge-size, using an instrument called the Gradiflow. The Gradiflow had several design features which made it particularly attractive for electrophoretic separations. The inter-membrane distance and the total anode-to-cathode distance were minimized, providing a short migration path and the ability to generate high field strengths. This resulted in a small sample compartment, of only 1.5 mL in volume, but large sample volumes could still be processed by recirculating the solutions from external reservoirs. Using this instrument as a template, the Twinflow was designed. The Twinflow has the same two sample compartment configuration, but has been modified so that IET separations can be performed (independent anode and cathode reservoirs and the elimination of transmembrane pressure gradients). In addition, the more efficient sample cooling developed for the Twinflow enables higher power loads to be applied, and thus faster separations. The Twinflow is capable of making a binary



separation on mixtures of ampholytes, which can be either small molecules or proteins. The major drawback for the Twinflow is that to fractionate a target ampholyte, where there are contaminating ampholytes with higher and lower pI values, two independent and successive separations have to be performed. The next generation in IET equipment addresses this shortcoming by connecting two Twinflow units in series. This instrument is called the Biflow. Once the pI value of the target protein or other ampholyte is known, separation membranes are chosen such that their pH values bracket the pI value of the target. One separation membrane is used in each of the two units, and after the separation, only proteins with pI values between the pH values of the two separation membranes, will be in the product collection stream. Therefore, membrane selection is based on how wide or narrow a pI range is required for the fraction in the product stream. The difference between a successful, and a failed IET separation, often comes down to the quality of the buffering membranes. Not only do the operating pH values of the membranes have to be known, but the mechanical and chemical stability of the membranes must be high. The new instrumentation introduced in this study, have proven to be rugged and user friendly. In addition, the improvements in separation speed (up to 500 mg of protein / hour) and energy efficiency demonstrate the advantages of the Twinflow and Biflow over other IET devices.

## 7.2 pH-biased isoelectric trapping

Another reason, contributing to the lack of widespread use of IET as a common separations method, is that the process itself suffers from several limitations. As an IET separation nears completion, the proteins trapped in each compartment get closer and closer to their isoelectric points. This means that the surface charge density on these proteins gets closer to zero, causing a slower electrophoretic velocity and thus, long separation times. Furthermore, a protein in its isoelectric state has a high tendency to precipitate. To alleviate these problems, pH-biased IET was developed. To control the pH, an isoelectric buffer (called an auxiliary isoelectric agent or pH biaser), is added to the sample solution. The pH biaser is chosen such that it has a high solubility and has a pI value such that it will be trapped in the separation compartment by the buffering membranes, along with the proteins of interest. In addition, the pH-biaser ideally has a pI value at least two pH units from the pI values of the sample proteins. With the pH-biaser controlling the solution pH, the protein never reaches its isoelectric point, but still is trapped between the buffering membranes. By maintaining the protein in a charged state, the solubility and the electrophoretic velocity remain high.

Separations using the pH-biased IET principle were performed for several different types of samples, on both the Twinflow and Biflow. Proteins from complex mixtures such as egg white, serum, and cell culture media have been successfully purified or fractionated using pH-biased IET. In addition, the desalting process during IET has been investigated, and it proved to be a convenient method for removing non-ampholytic

components from a sample. This could be achieved either as a separate desalting step before separation, or combined into one step with the separation. There are several areas which would particularly benefit from pH-biased IET separations. Firstly, prefractionation for proteomics could benefit from the combined fractionation and concentration that can be achieved on the Twinflow or Biflow. This combination can allow the detection of many more of the low abundance proteins than previously possible, and it can be easily carried out prior to most protein characterization methods. Secondly, separations of protein isoforms, such as glycoproteins in serum or recombinant proteins from a cell culture, could benefit by taking advantage of the high resolution in pI discrimination that can be achieved using pH-biased IET. With the majority of the operating conditions for a successful pH-biased IET separation now understood, together with the advances in IET instrumentation, the technique should certainly be considered an important separations tool for protein chemists.

## REFERENCES

- [1] Righetti, P. G., *Isoelectric Focusing: Theory, Methodology and Applications*, Elsevier Biomedical Press, Amsterdam 1983, pp. 1-147.
- [2] Kolin, A., *J. Chem. Phys.* 1954, 22, 1628-1629.
- [3] Martin, A. J. P., Hampson, F., *J. Chromatogr.* 1979, 159, 101-110.
- [4] Bier, M., Long, T., *J. Chromatogr.* 1992, 604, 73-83.
- [5] Rilbe, H., *J. Chromatogr.* 1978, 159, 193-205.
- [6] Svensson, H., *Acta. Chem. Scand.* 1962, 15, 325-341.
- [7] Vesterberg, O., *Acta. Chem. Scand.* 1969, 23, 2653-2666.
- [8] Rilbe, H., in: Catsimpoolas, N., (Ed.), *Isoelectric Focusing*, Academic Press, New York 1976, pp. 14-51.
- [9] Vingradov, S. N., Lowenkron, S., Andonian, H. R., Bagashaw, J., Felegenhauer, K., Pak, S. J., *Biochem. Biophys. Res. Commun.* 1973, 54, 501-506.
- [10] Righetti, P. G., Pagani, M., Gianazza, E., *J. Chromatogr.* 1975, 109, 341-356.
- [11] Charlionet, R., Martin, J. P., Sesboue, R., Madec, P. J., Lefebvre, F., *J. Chromatogr.* 1979, 176, 89-101.
- [12] Just, W. W., *Anal. Biochem.* 1980, 102, 134-144.
- [13] Righetti, P. G., Hjerten, S., *J. Biochem. Biophys. Methods* 1981, 5, 259-272.
- [14] Mosher, R. A., Thormann, W., Bier, M., *J. Chromatogr.* 1986, 351, 31-38.
- [15] Nguyen, N. Y., Chrambach, A., *Anal. Biochem.* 1976, 74, 145-153.
- [16] Mosher, R. A., Thormann, W., Graham, A., Bier, M., *Electrophoresis* 1985, 6, 545-551.
- [17] Bier, M., Ostrem, J., Marquez, R. B., *Electrophoresis* 1993, 14, 1011-1018

- [18] Righetti, P. G., *Immobilized pH Gradients: Theory and Methodology*, Elsevier Biomedical Press, Amsterdam 1990, pp. 10-12.
- [19] Bjellqvist, B., Ek, K., Righetti, P. G., Gianazza, E., Gorg, A., Westermeier, R., Postel, W., *J. Biochem. Biophys. Methods* 1982, 6, 317-339.
- [20] Jonsson, M., Stahlberg, J., Fredrickson, S., *Electrophoresis* 1980, 1, 113-118.
- [21] Radola, B. J., *Biochim. Biophys. Acta.* 1969, 194, 335-338.
- [22] Radola, B. J., *Biochim. Biophys. Acta.* 1974, 386, 181-195.
- [23] Chapius-Cellier, C., Francina, A., Arnaud, P., *Anal Biochem.* 1981, 113, 325-331.
- [24] Bours, J., in: Catsimpoolas, N., (Ed.), *Isoelectric Focusing*, Academic Press, New York 1976, pp. 209-227.
- [25] Hjerten, S., *Chromatogr. Rev.* 1967, 9, 122-219.
- [26] Lundahl, P., Hjerten, S., *Ann. N. Y. Acad. Sci.* 1973, 209, 94-111.
- [27] Jonsson, M., Rilbe, H., *Electrophoresis* 1980, 1, 3-14.
- [28] Bier, M., *Electrophoresis* 1998, 19, 1057-1063.
- [29] Ivory, C. F., *Electrophoresis*, 2004, 25, 360-374.
- [30] Hannig, K., *J. Chromatogr.* 1978, 159, 183-191.
- [31] Kasicka, V., Prusik, Z., Pospisek, J., *J. Chromatogr.* 1992, 608, 13-22.
- [32] Burggraf, D., Weber, G., Lottspeich F., *Electrophoresis* 1995, 16, 1010-1015.
- [33] Binion, S. B., Rodkey, L. S., Egen, N. B., Bier, M., *Electrophoresis* 1982, 3, 284-288.
- [34] Martin, A. J. P., Hampson, F., US Patent 4, 243, 507, 1981.
- [35] Wenger, P., de Zuanni, M., Javet, P., Gelfi, C., Righetti, P. G., *J. Biochem. Biophys. Methods*, 1987, 14, 29-43.
- [36] *Doctor pH Manual*, Amersham Pharmacia Biotech, 1993, San Francisco, CA.
- [37] Righetti, P. G., Wenisch, E., Faupel, M., *J. Chromatogr.* 1989, 475, 293-309.

- [38] *IsoPrime Manual*, Amersham Pharmacia Biotech, 1999, San Francisco, CA.
- [39] Zuo, X., Speicher, D. W., *Anal. Biochem.* 2000, 284, 266-278.
- [40] *Isoelectric<sup>Q</sup> Manual*, Proteome Systems Ltd., 2003, Woburn, MA.
- [41] Chiari, M., Nesi, M., Roncada, P., Righetti, P. G., *Electrophoresis* 1994, 15, 953-959.
- [42] Fortis, F., Girot, P., Brieu, O., Boschetti, E., *Proteomics* 2005, 5, 620-628.
- [43] Fortis, F., Girot, P., Brieu, O., Castagna, A., *Proteomics* 2005, 5, 629-638.
- [44] McMurry, J., *Organic Chemistry*, Brooks/Cole, Pacific Grove, CA, 2000.
- [45] Lalwani, S., Shave, E., Fleisher, H. C., Nzeadibe, K., Busby, M. B., Vigh, G., *Electrophoresis* 2004, 25, 2128-2138.
- [46] Lalwani, S., Shave, E., Vigh, G., *Electrophoresis* 2004, 25, 3323-3330.
- [47] Fleisher, H. C., Vigh, G., *Electrophoresis* 2005, 26, in press.
- [48] Righetti, P. G., Bossi, A., Wenisch, E., Orsini, G., *J. Chromatogr.* 1997, 699, 105-115.
- [49] Righetti, P. G., Wenisch, E., Jungbauer, A., Katinger, H., Faupel, M., *J. Chromatogr.* 1990, 500, 681-696.
- [50] Righetti, P. G., Castagna, A., Herbert, B., Reymond, F., Rossier, J.S., *Proteomics* 2003, 3, 1397-1407.
- [51] Shave, E., Vigh, G., *Electrophoresis* 2004, 25, 381-387.
- [52] Nisbet, A. D., Saundry, R. H., Moir, A. J. G., Fothergill, L. A., Fothergill, J. E., *Eur. J. Biochem.* 1981, 115, 335-345.
- [53] Peters, T., *All About Albumin: Biochemistry, Genetics, and Medical Applications*, Academic Press, San Diego, CA 1996, pp. 24-54.
- [54] Horvath, Z. S., Corthals, G L., Wrigley, C. W., Margolis, J., *Electrophoresis* 1994, 15, 968-971.
- [55] Margolis, J., Corthals, G., Horvath, Z. S., *Electrophoresis* 1995, 16, 98-100.

- [56] Horvath, Z. S., Gooley, A. A., Wrigley, C. W., Margolis, J., Williams, K. L., *Electrophoresis* 1996, *17*, 224-230.
- [57] Corthals, G., Margolis, J., Williams, K. L., Gooley, A. A., *Electrophoresis* 1996, *17*, 771-775.
- [58] Corthals, G. L., Molloy, M. P., Herbert, B. R., Williams, K. L., Gooley, A. A., *Electrophoresis* 1997, *18*, 317-323.
- [59] Corthals, G., Collins, B. M., Mabbutt, B. C., Williams, K. L., Gooley, A. A., *J. Chromatogr. A* 1997, *773*, 299-309.
- [60] Lim, S., Manus, H. P., Gooley, A. A., Williams, K. L., Rylatt, D. B., *J. Chromatogr. A* 1998, *827*, 329-333.
- [61] Rylatt, D. B., Napoli, M., Ogle, D., Gilbert, A., Lim, S., Nair, C. H., *J. Chromatogr. A* 1999, *865*, 133-145.
- [62] Thomas, T. M., Shave, E., Bate, I. M., Gee, S. C., Franklin, S., Rylatt, D. B., *J. Chromatogr. A* 2002, *964*, 161-168.
- [63] Rothemund, D. L., Thomas, T. M., Rylatt, D. B., *Protein Expression and Purification* 2002, *26*, 149-152.
- [64] Rothemund, D. L., Locke, V. L., Liew, A., Thomas, T. M., Wasinger, V., Rylatt, D. B., *Proteomics* 2003, *3*, 279-287.
- [65] Moller, C. C., Thomas, D., Van Dyk, D., Rylatt, D., Sheehan, M., *Electrophoresis* 2005, *26*, 35-46.
- [66] Ogle, D., Ho, A., Gibson, T., Rylatt, D., Shave, E., Lim, P., Vigh, G., *J. Chromatogr. A* 2002, *979*, 155-161.
- [67] Righetti, P. G., Barzaghi, B., Faupel, M., *J. Biochem. Biophys. Methods* 1987, *15*, 163-176.
- [68] Wu, J., Pawliszyn, J., *J. Chromatogr. B* 1995, *669*, 39-43.
- [69] Righetti, P. G., Etori, C., Chafely, P., Wahrmann, J. P., *Electrophoresis* 1990, *11*, 1-4.
- [70] Glukhovskiy, P., Vigh, G., *Anal. Chem.* 1999, *71*, 3814-3820.

- [71] Rizzi, A. M., Kremser, L., *Electrophoresis* 1999, 20, 2715-2722.
- [72] Spanik, I., Lim, P., Vigh, G., *J. Chromatogr. A* 2002, 960, 241- 246.
- [73] Glukhovskiy, P., Landers, T. A., Vigh, G., *Eletrophoresis* 2000, 21, 762-766.
- [74] Gaveby, B. M., Pettersson, P., Andrasko, J., Flygare, L. I., Johannesson, U., Gorg, A., Postel, W., Domscheit, A., Mauri, P. L., Pietta, P., Gianazza, E., Roghetti, P. G., *J. Biochim. Biophys. Methods* 1988, 16, 141-164.
- [75] Stevens, L., *Comp. Biochem. Physio.*, 1991, 100B, 1-9.
- [76] Desert, C., Guerin-Dubiard, C., Nau, F., Jan. G., Val, F., Mallard, J., *J. Agric. Food. Chem.* 2001, 49, 4553-4561.
- [77] Croguennec, T., Nau, F., Pezenec, S., Piot, M., Brule, G., *Eur. Food. Res. Technol.* 2001, 212, 296-301.
- [78] Anderson, N. L., Anderson, N. G., *Mol. Cell. Proteomics* 2002, 1, 845-867.
- [79] Pederson, S. K., Harry, J. L., Sebastian, L., Baker, J., Traini, M. D., McCarthy, J., Manoharan, A., Wilkins, M R., Gooley, A. A., Righetti, P. G., Packer, N. H., Williams, K. L., Herbert, B. R., *J. Proteome Res.* 2003, 2, 303-311.
- [80] Stasyk, T., Huber, L. A., *Proteomics* 2004, 4, 3704-3716.
- [81] Sluyterman, L. A., Elgersma, O., *J. Chromatogr.* 1978, 150, 17-30.
- [82] Sluyterman, L. A., Kooistra, C. *J. Chromatogr.* 1989, 470, 317-326.
- [83] *ProteomeLab PF 2D Operator's Manual*, Beckman Coulter, 2003, Fullerton, CA.
- [84] Pickles, A. J., Peers, N., Robertson, W. R., Lambert, A., *J. Mol. Endocrinol.* 1992, 9, 245-250.
- [85] Yang, X., McGraw, R. A., Ferguson, D. C., *Domestic Animal Endocrinology* 2000, 18, 379-393.
- [86] Pickles, A. J., Peers, N., Robertson, W. R., Lambert, A., *J. Mol. Endocrinol.* 1992, 9, 251-256.



## VITA

Evan Eric Shave received his bachelors of Medical Science degree from The University of Sydney in 1998. After working at an Australian biotechnology company for two years, he moved to the USA and entered the graduate chemistry program at Texas A&M University in June 2001. Working in the Separations Science Group, under the direction of Professor Gyula Vigh, his research interests included preparative and analytical-scale electrophoretic protein separations and development of the associated instrumentation.

Evan may be reached at the following address: 60 Byng St. Orange, NSW 2800 Australia, or by email: [ev\\_sta@yahoo.com](mailto:ev_sta@yahoo.com).